ANNUAL PROGRAM REVIEW

CHEMICAL RECOVERY AND CORROSION

March 25-26, 1998

ANNUAL PROGRAM REVIEW

CHEMICAL RECOVERY AND CORROSION

March 25-26, 1998

Institute of Paper Science and Technology
500 10th Street, N.W.
Atlanta, Georgia 30318
(404) 894-5700
(404) 894-4778 FAX

Table of Contents

Table of Contents (continued)

CHEMICAL RECOVERY
PROJECT ADVISORY COMMITTEE

IPST Liaison: Dr. Jim Frederick (404) 894-5303; FAX (404) 894-4778
RAC Liaison: Dr. John Glomb (212) 318-5000; FAX (212) 318-5090

Mr. John Andrews *(1999)
Utility Improvement Manager
Westvaco Corporation
5600 Virginia Avenue
Post Office Box 118005
Charleston, SC 29423-8005
(803) 745-3212
(803) 745-3229 FAX

Mr. Michael G. Fremont *(1999) (Vice Chairman)
Special Projects Engineer - Process Design
P.H. Glatfelter Co.
228 South Main Street
Spring Grove, PA 17362
(717) 225-4711
(717) 225-7124 FAX

Dr. Robert R. Horton *(1999)
Radian International LLC
1979 Lakeside Parkway
Suite 800
Tucker, GA 30084
(770) 724-1053
(770) 414-4919 FAX

Dr. Ted Mao *(2001)
Product Development Engineering
Asea Brown Boveri Inc.
1410 Blair Place - Suite 600
Gloucester, ON, CANADA K1J 9B9
(613) 747-5746
(613) 747-5875 FAX

Dr. George W. McDonald *(2001)
Pulping Group Leader
Union Camp Corporation
Research and Development Division
Post Office Box 3301
Princeton, NJ 08543
(609) 844-7271
(609) 844-7323 FAX
george_mcdonald@ucamp.com

Mr. Bob Roscoe *(2001)
Senior Engineering Specialist
Weyerhaeuser Company
WTC 2H22
Tacoma, WA 98477-0001
(253) 924-2345
(253) 924-6324 FAX

Mr. David E. Fletcher *(Alternate)
Manager, Technical Marketing
EKA Chemicals Inc.
1519 Johnson Ferry Road
Suite 200
Marietta, GA 30062
(770) 509-2014
(770) 937-9688 FAX

Mr. Gopal C. Goyal *(2000)
Sr. Research and Development Engineer
Potlatch Corporation
20 North 22nd Street
Post Office Box 503
Cloquet, MN 55720-0503
(218) 879-0690
(218) 897-2375 FAX
gcgoyal@potlatchcorp.com

Mr. Robert C. Larson *(1999)
Director, Fiber Engineering & Manufacturing Services
Fort James Corporation
Post Office Box 899
Neenah, WI 54957-0899
(920) 729-8050
(920) 729-8597 FAX
Bob_Larson@Email.JRC.COM

Mr. Gerald Maples *(1998)
Functional Team Leader
Champion International Corporation
Post Office Box 87
375 Muscogee Road
Cantonment, FL 32533
(904) 937-4863
(904) 968-3077 FAX
maplej@champint.com

Mr. Karl T. Morency *(2001) (Chairman)
Senior Utility Systems Engineer
Georgia-Pacific Corporation
Engineering & Technology
133 Peachtree Street, NE
Atlanta, GA 30303
(404) 652-4629
(404) 584-1466 FAX
ktmorenc@gapac.com

Mr. Denis Roy *(1998)
St. Laurent Paperboard Inc.
1000 Chemin de l'Usine
C.P. 914
La Tuque, Quebec G9X 3P8, CANADA
(819) 676-8100 (690)
(819) 676-8120 FAX

* The dates in ( ) indicate the final year of the appointment.

Revised 03/20/98:at

Chemical Recovery (cont.)

Mr. Robert Sasser *(1998)
Chief Engineer
Temple-Inland Inc.
Post Office Box 816
Silsbee, TX 77656
(409) 276-1411
(409) 276-3108 FAX

Mr. John C. Sokol *(2001)
Manager, Technology Development
EKA Chemicals Inc.
1519 Johnson Ferry Road
Suite 200
Marietta, GA 30062-6438
(770) 578-0858
(770) 578-1359 FAX

Mr. W. Chris Suggs *(2001)
Manager, Power & Utilities
The Mead Corporation
3131 Newmark Drive
Miamisburg, OH 45342
(937) 495-5276
(937) 495-5333 FAX

* The dates in ( ) indicate the final year of the appointment.
** Indicates external advisor

DUES-FUNDED PROJECT SUMMARY

Project Title:	Control of Evaporator Fouling
Project Code:	
Project Number:	F016-01
PAC:	Chemical Recovery
Division:	Chemical Recovery and Corrosion
Project Staff	
Faculty/Senior Staff:	J. Frederick, W. Schmidl, N. DeMartini
Staff:	G. Dent
FY 98-99 Budget:	TBA
Allocated as Matching Funds:	None
Time Allocation	
Faculty/Senior Staff:	J. Frederick (10%), W. Schmidl (50%); N. DeMartini (62%)
Support:	G. Dent (25%)
Supporting Research	
M.S. Students:	G. Lansdell (MS candidate)
Ph.D. Students:	None
External:	J. Smith (PhD candidate, GIT)

RESEARCH LINE/ROADMAP: Improved Capital Effectiveness. 8. Develop technologies (compatible with present pulp-mill assets) to allow cost-effective expansion of kraft-pulp-equivalent fiber capacity (hardwood and softwood) by 30% without adding Tomlinson recovery boilers.

PROJECT OBJECTIVES:
The first objective is to obtain data on the current state of black liquor evaporator fouling through a survey of the industry's evaporators. The second objective is to understand the causes of scale formation in black liquor evaporators and high solids concentrators. The third is to provide design data and guidance tools to reduce fouling (and thereby increase evaporator capacity) through improved design and operation.

PROJECT BACKGROUND:
This project was begun this fiscal year, in response to industry demand for improved capacity in black liquor evaporators and high solids concentrators. At an IPST organized meeting of industry representatives in May, 1997, it was decided that the most critical issue was soluble scales in high solids black liquor concentrators, and that this problem needed to be solved first. $CaCO_3$ scaling of black liquor evaporators, especially in mills where modified kraft pulping technologies are used, was also recognized as a critical problem.

A three-pronged approach has been taken in the initial six months of this work. First, a survey of black liquor evaporator fouling problems in North American kraft pulp mills was undertaken. Second, advanced chemical equilibrium modeling methods were employed to predict the solubility behavior of sodium salts in black liquor as it is concentrated to high dry solids contents. Third, an experimental program was begun to obtain experimental data on the solubility of sodium salts in black liquor at high dry solids contents.

SUMMARY OF RESULTS:

1. Evaporator Fouling Survey
A second IPST survey of evaporator fouling in the North American kraft pulping industry was conducted in 1997. This survey has identified both similarities and differences in the nature and extent of the problem since the first survey conducted by Grace in 1974-75. These characteristics are a reflection of the changes in pulping technology and evaporation technology, and changes in mill wide processes such as mill closure, and are manifested in the types and distribution of scales, evaporator performance parameters, and the composition of the processed black liquors.

A questionnaire and a request for black liquor and scale samples were distributed to 40 kraft pulp mills. This questionnaire requested detailed information on the nature of the wood supply, the pulping process and conditions; liquor processing; a description of the evaporator equipment configuration, performance characteristics, and scaling conditions of the evaporator system; and the liquor and scale composition. To date, 26 mills returned a completed questionnaire, 20 submitted liquor samples, and 9 submitted scale samples. The following companies participated in the survey:

Boise Cascade	P.H. Glatfelter	Union Camp
Fort James	Mead	Weyerhaeuser
Georgia-Pacific	Potlatch	Willamette Industries

The black liquor samples were analyzed for total solids content, total carbon, hydrogen, oxygen, sulfur, metals content, anions, residual active alkali, fiber, and residual soap content. The scale samples were analyzed for inorganic phase composition by X-ray diffraction.

The key results of the survey are that the average product solids content from evaporator trains is higher today, 58% versus 49%, a result of the current widespread use of falling film technology with liquor recirculation, and the fact that a number of evaporator sets now have integrated concentrators. More mills process hardwood liquors than in the 1970's. The black liquors processed contain more potassium, carbonate, and sulfate than they did in the 1970's, and probably more chloride. They contain the same amount of sodium, residual active alkali, and soap; and despite the impact of mill closure, the black liquors contain less of all other metals.

The average overall heat flux, average overall heat transfer coefficient, and average temperature difference per effect are down by 10%, 8%, and 3% respectively, compared to two decades ago. However, this is based on data from only a limited number of mills. This is also the result of the increase in falling film concentrators that operate at lower heat fluxes and lower temperature differences. The frequency of soluble scales and of fiber, soap, organic scales have increased. Fewer mills report $CaCO_3$ scale problems, but fewer report no scale problems. Overall, the cleaning frequency is lower today than two decades ago. Boil-out frequency is down by 20%, and acid cleaning by 63%, but the frequency of hydroblasting is up by 130%.

2. Prediction of the Solubility of Sodium salts in Black Liquor at at High Dry Solids Content

The Environmental Simulation Program (ESP) software by OLI Systems, Inc. was used to simulate the composition of model green and white liquors containing NPE's: Ba, Ca, Mg, and Mn. Predicted saturated solution concentrations for Ba agreed very well with measured values for suspended solids-free liquor, but for Ca, Mg, and Mn, the predicted values were at least a factor of ten lower than the measured values. However, ESP did correctly predict the expected solid phases: $BaSO_4$, $CaCO_3$, $Mg(OH)_2$, and $Mn(OH)_2$. Simulations of the solubility behavior as a function of temperature for aqueous Na_2CO_3 and Na_2SO_4 were also performed. The predicted saturated solution curves matched the experimental data extremely well over the temperature range of 0-200°C for Na_2CO_3, and 0-220°C for Na_2SO_4.

Simulations of Na_2CO_3 and Na_2SO_4 solubility in black liquor at high dry solids content were performed for actual evaporator operating conditions and black liquor composition. Saturated solution and solid phase compositions were calculated as a function of total dry solids from 40 to 75 wt. %. The predicted solubility curves are presented in Figure 1. The simulations predicted realistic values for the soluble Na_2CO_3, and Na_2SO_4 concentrations, and the expected solid phases--burkeite ($2Na_2SO_4.Na_2CO_3$), and Na_2CO_3. Perhaps most significantly, the simulations predicted the presence of two "critical solids" levels: (1) the well known critical solids point where burkeite begins to precipitate, and (2) a second point where Na_2CO_3 precipitates as a separate phase.

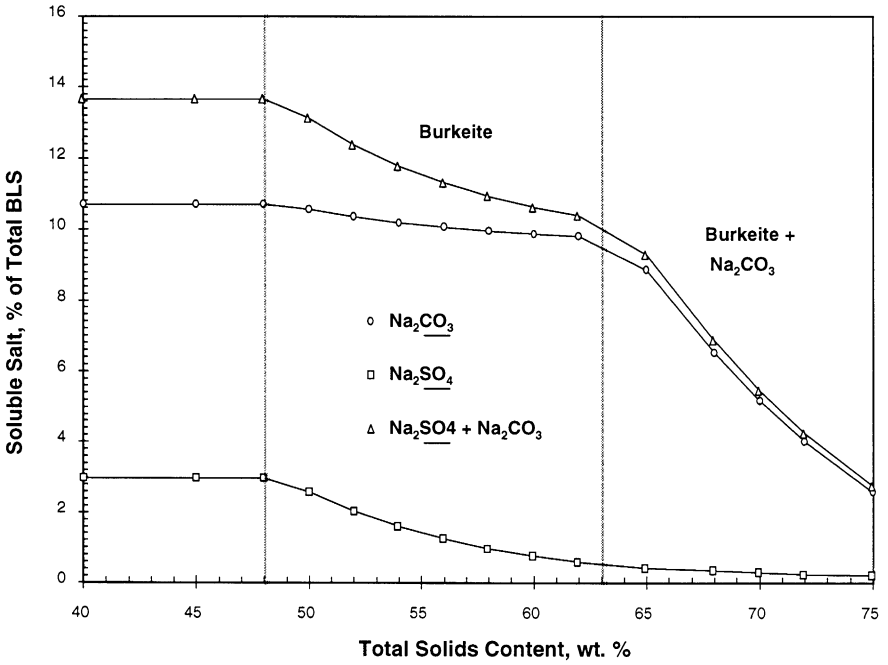

Figure 1. Simulated Solubility of Na_2SO_4 and Na_2CO_3 in Black Liquor at 116°C.

For these particular simulation conditions, the predicted burkeite precipitation point is 48-50% solids which agrees very well with a critical solids of 51% calculated by Grace's method. From Figure 1, the Na_2CO_3 precipitation point is 62-65% solids, although this has not yet been verified experimentally. This simulated solubility behavior is important for understanding the scaling behavior of concentrators which typically operate in the range of 50-70+% solids. The Na_2CO_3 precipitation is much more strongly dependent on the solids content than is burkeite precipitation. It may therefore be desirable to promote burkeite precipitation over Na_2CO_3 precipitation by extending the burkeite precipitation range and thus push the second critical solids point to a higher level.

3. **Summary of Sodium Salt Solubility Data**

Initial experiments have been run which determine the solubility of sodium compounds in aqueous solutions. The mixtures tested had sodium salt/water ratios slightly above the solubility limits of the sodium salts tested. These duplicate experiments run by Tom Grace[1] and have been used to establish good technique before work with black liquor begins. All initial solutions were within 0.5 weight percent of those done by Tom Grace. The compositions of the samples, drawn from these solutions after reaching equilibrium, are given in Tables 1-4.

[1] Grace, T. M. "Solubility Limits in Black Liquor", Institute of Paper Chemistry Project 3136, Report 1, February 22, 1974.

Table 1. Na_2CO_3-NaOH-H_2O system (30% Na_2CO_3 by weight)

System	%Na_2CO_3	%NaOH
Na_2CO_3-H_2O – this study	28.0	
Grace, 1974	29.5	
Na_2CO_3-2.5% NaOH-H_2O – this study	25.0	2.4
Grace, 1974	26.6	2.7
Na_2CO_3-5% NaOH-H_2O – this study	18.0	8.1
Grace, 1974	18.9	8.3

Table 2. Na_2SO_4-H_2O system (30% Na_2SO_4 by weight)

System	%Na_2SO_4
Na_2SO_4-H_2O - – this study	27.1
Grace, 1974	28.5

Table 3. NaCl-H_2O system (30% NaCl by weight)

System	%NaCl
NaCl-H_2O – this study	26.8
Grace, 1974	26.0

Table 4. Na_2CO_3-Na_2SO_4-NaCl-H_2O system (10% Na_2CO_3, 10% Na_2SO_4, 10% NaCl by weight)

System	%Na_2CO_3	%Na_2SO_4	%NaCl
Na_2CO_3-Na_2SO_4-NaCl-H_2O	5.8	9.0	10.9
Grace, 1974	6.3	8.1	10.7

One liter, stirred and heated pressure vessels are being used for the sodium salt solubility studies. Both have sampling tubes that sit in solution with a Nupro sintered filter on the end. Filter sizes from 2 to 15 microns have been used successfully. The temperatures are controlled with PID controllers that receive the temperature input from a thermocouple that sits in a thermowell.

The operating temperature for the aqueous solutions has been 100^{O}C. Pressure within the vessel has been between 8 and 15 psig depending on the vapor pressure of the particular solution. Samples were drawn between 20 and 24 hours after the solutions had reached operating temperature. In several instances, multiple samples were taken to insure that equilibrium had been reached.

Sodium carbonate and sodium hydroxide concentrations are determined by potentiometric titration with 0.05N HCl. Sodium chloride and sodium sulfate concentrations are determined by capillary ion electrophoresis (CIE) and a metals analysis (ICP) is used to determine sodium and sulfur composition. The metals analysis provides a check for the results from the other two test methods.

A couple of modifications are being made to the two pressure vessels to improve mixing. Several more tests are going to be run with aqueous solutions to confirm the quality of the results after the modifications have been made. Some experiments will also be run with black liquor to bring about familiarity with its characteristics until arrival of two more Parr reactors that will allow studies with high solids black liquor. These new Parr reactors are designed to work with high solids solutions that act like polymers.

GOALS FOR FY 98-99:

A. Experimental Scaling Studies

1. Set up of the annular flow, fouling test cell that will be used initially by Grant Lansdell in studying calcium carbonate scaling.
2. Construct a single tube pilot evaporator, initially capable of falling film and forced circulation studies.

B. Survey of Evaporator Fouling

1. Complete generating and filling the database with the process data and liquor composition data.
2. Complete evaporator heat balance calculations to determine thermal performance parameters.
3. Perform the statistical analyses of the data to identify the most influential variables that can be correlated to liquor composition and evaporator operating parameters.
4. Present available results at the International Chemical Recovery Conference.
5. Publish the results as a report to the membership, and as technical paper in TAPPI Journal.

C. Modeling of Sodium Salt Solubility in Black Liquor

1. Repeat simulations of Na_2CO_3 and Na_2SO_4 solubility in black liquor for a range of Na_2CO_3 , Na_2SO_4, and total Na concentrations in order to determine reasonable ranges for the burkeite and Na_2CO_3 precipitation points
2. Evaluate ESP performance for common aqueous inorganic systems using a modified Kraft database recently supplied by OLI.
3. Install and learn to use Weyerhaeuser's NAELS program.
4. Work with OLI and NAELS to expand the database for relevant compounds.
5. Apply the software to simulate mill problems.

DELIVERABLES:
A technical paper that contains a preliminary analysis of the results from the evaporator fouling survey is included as an attachment to this report.

Expected deliverables in the next twelve months include 1) a final report on the evaporator survey, 2) solubility data for sodium salts at high dry solids content; 3) a validated chemical equilibrium model for predicting the onset of rapid precipitation of Na_2CO_3 at high dry solids content, and guidelines for optimizing high solids concentrator operation and other recovery cycle parameters to minimize fouling in high solids concentrators.

SCHEDULE

ID	Task Name
1	**Experimental Scaling Studies**
2	**A. Annular flow test cell:**
3	1. Heating elements arrive
4	2. Piping/set up complete
5	3. Successfully hydro-tested
6	**B. Pilot Evaporator:**
7	1. Main equipment/vendors identified
8	2. Equipment arrives
9	3. Pilot Evaporator erected
10	4. Successfully hydro-tested
11	**Survey of Evaporator Fouling**
12	1. Complete the process and liquor database
13	2. Complete evaporator heat balance calculations
14	3. Statistical analyses of the data
15	4. Present Intl Chem Recov Conf paper
16	5. Write a report to the membership
17	6. Write a technical paper for Tappi J.
18	**Modeling of Sodium Salt Solubility in Black Liquor**
19	1. Evaluate solubility vs. Na, CO3, SO4, OH conc's.
20	2. Evaluate ESP with OLI modified Kraft database
21	3. Install and learn to use Weyco NAELS program
22	4. Expand OLI and NAELS databases
23	5. Apply the software to simulate mill problems.

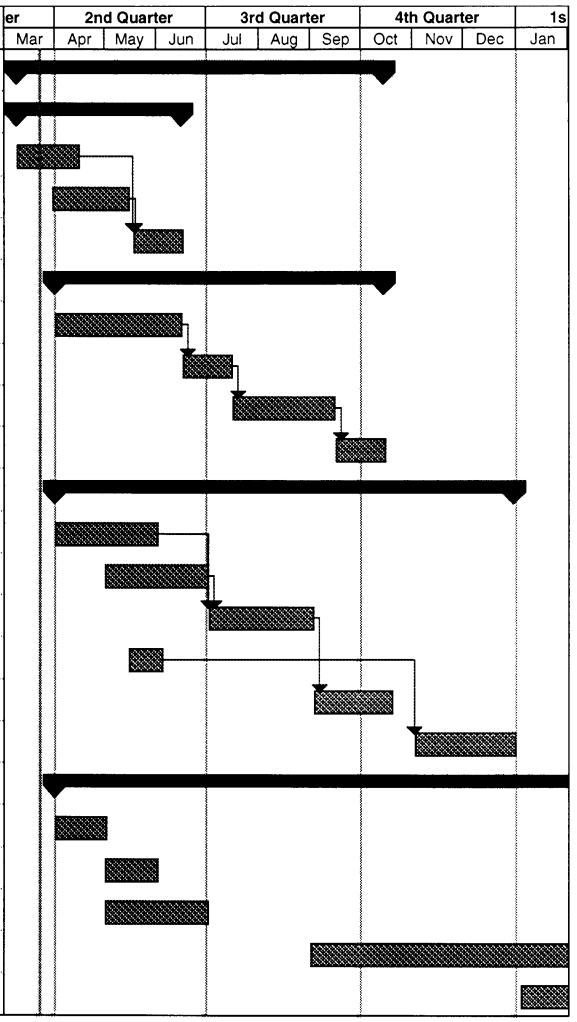

CURRENT TRENDS IN EVAPORATOR FOULING

Wolfgang Schmidl
Wm. James Frederick
The Institute of Paper Science & Technology
Atlanta, Georgia, 30318
USA

ABSTRACT

A second IPST survey of evaporator fouling in the North American kraft pulping industry was conducted in 1997. The objective was to assess the nature and extent of these fouling problems, and the changes since the first survey conducted by Grace in 1974-75. A questionnaire and a request for black liquor and scale samples were distributed to 40 kraft pulp mills. This questionnaire requested detailed information on the nature of the wood supply, the pulping process and conditions; liquor processing; a description of the evaporator equipment configuration, performance characteristics, and scaling conditions of the evaporator system; and the liquor and scale composition. 25 mills returned a completed questionnaire, and 19 submitted liquor samples. The black liquor samples were analyzed for total solids content, total carbon, hydrogen, oxygen, sulfur, metals content, anions, residual active alkali, fiber, and residual soap content. The scale samples were analyzed for inorganic phase composition by X-ray diffraction.

The key results of the survey are that the average product solids content from evaporator trains is higher today, 58% versus 49%, a result of the current widespread use of falling film technology with liquor recirculation. More mills process hardwood liquors than in the 1970's. The black liquors processed contain more potassium, carbonate, and sulfate than they did in the 1970's, and probably more chloride. They contain the same amount of sodium, residual active alkali, and soap; and despite the impact of mill closure, the black liquors contain less of all other metals.

The average overall heat flux, average overall heat transfer coefficient, and average temperature difference per effect are down by 10%, 8%, and 3% respectively, compared to two decades ago. This is also the result of the increase in falling film concentrators that operate at lower heat fluxes and lower temperature differences. The frequency of soluble scales and of fiber, soap, organic scales have increased. Fewer mills report $CaCO_3$ scale problems, but fewer report no scale problems. Overall, the cleaning frequency is lower today than two decades ago. Boil-out frequency is down by 20%, and acid cleaning by 63%, but the frequency of hydroblasting is up by 130%.

INTRODUCTION

This project is the outgrowth of a workshop held at IPST in May, 1997 to discuss the state of evaporator fouling in the context of current operating conditions, changes in the characteristics of the feed black liquor due to pulping process changes, and throughput demands dictated by pulp production targets. The consensus among the attendees from the pulp and paper industry and evaporator manufacturers was that the severity of the problem has increased in recent years, and that there is a significant lack of scientific understanding of the inorganic chemistry involved when concentrating kraft black liquors to the high dry solids content (typically > 70%) that has become the current practice.

The workshop group identified an urgent need to generate experimental data on the solubility of various inorganic species, such as sodium carbonate, sodium sulfate, soluble calcium, and aluminosilicates, in black liquors concentrated to high solids. In addition, a parallel need was identified, and a plan of action was agreed upon, to survey the industry on the nature and extent of evaporator fouling problems and to identify the most influential variables.

This survey has five primary objectives: (1) to define the nature and extent of the fouling problem with hard data instead of with a collection of anecdotal experiential information, (2) to identify the most influential variables, both main factors and interactions, that can be correlated to liquor composition and evaporator operating parameters, (3)

to compile a database of liquor chemical composition and evaporator operating and performance parameters so that normal or typical ranges for these variables can be established, (4) to evaluate the evaporator variables within the context of the overall mill and chemical recovery operations, and (5) to compare this survey's findings with those from a similar one conducted by Grace in 1974-75 [1].

BACKGROUND

Grace's Evaporator Fouling Survey

The fouling of black liquor evaporators is certainly not a recent phenomenon. A comprehensive survey of evaporator fouling problems was conducted by Grace [1] in conjunction with an experimental study of sodium sulfate and sodium carbonate solubility behavior in black liquors. He analyzed information obtained by questionnaire and by chemical analysis of the composition of liquor samples that were also submitted.

The major findings of his survey were that calculated values of the average heat fluxes for the evaporator sets of the reporting mills spanned a wide range, from 7,900 - 22,000 W/m^2 (2,500-6,900 Btu/ft^2hr). Similarly, the average overall heat transfer coefficients for these evaporator sets ranged from 720 - 1,870 W/m^2K (127-329 $Btu/ft^2hr°F$). These represent a nearly three-to-one range in the effective evaporative capacity per unit of evaporator surface area. Scaling appeared to be the primary factor responsible for this variability in productivity [1].

The most commonly reported scales were soluble (Na_2CO_3--Na_2SO_4) scales and calcium carbonate scales. Calcium carbonate scales appeared to constitute a more serious problem in the industry. In addition to being more difficult to remove, they had a dominant effect on evaporator productivity. Surprisingly, the data obtained in Grace's survey did not support the concept that rapid growing but easily removable soluble scales were responsible for most of the short-term degradation in evaporator performance while residual, insoluble calcium scales caused only a gradual deterioration in base-line performance. They indicate, instead, that substantial amounts of calcium scale can be removed by boiling out the evaporator with water, and that rapid growing calcium scales can govern the short-term performance [1].

The calcium content of the liquor was the most important variable affecting calcium scaling, and there are indications that the amount of calcium in the liquor was influenced more by wood supply than by internal process conditions. Parameters controlling the formation of soluble scale could not be identified, and no correlation could be established between scaling behavior and those variables associated with the solubility of Na_2CO_3 and Na_2SO_4 in black liquor. This was due, in part, to the dominance of calcium scales [1].

The data also suggested that some soap in the liquor is beneficial and that there may exist an optimum degree of soap removal. A beneficial effect of residual active alkali in the liquor was also indicated, but no correlation was established between the measured fiber content of the liquor and scaling [1].

Changes in Pulping and Evaporation Technology

In the early 1970's, almost all kraft pulping was by the conventional batch process, and evaporator configurations were almost exclusively of the long tube vertical (LTV) type with a rising liquor film flow pattern. These evaporators discharged the product liquor at approximately 50% dry solids content. To reach the firing solids of 60-65%, the liquor was then further concentrated in venturi cyclone or cascade type direct contact evaporators (DCE).

Since that time, several significant process changes have directly and indirectly impacted the operation and performance of evaporator sets. New pulping technologies were developed and commercialized in the 1980's: Kamyr's Modified Continuous Cooking (MCC®) and Extended Modified Continuous Cooking (EMCC®), Beloit's Rapid Displacement Heating (RDH®), and Sund's Defibrator's Superbatch® processes have become established as older units have been retrofitted and new capacity has been brought on line [2, 3]. These new processes have fundamentally changed some of the chemistry in the black liquor evaporator feed. For example, black liquor is contacted with fresh wood chips before heading toward the evaporators. This results in an increased calcium load in the liquor in the form of organically bound calcium which is thermally unstable and can decompose in the higher

temperature effects, releasing free calcium which will combine with the abundant carbonate ions to form insoluble calcium carbonates.
Significant changes have also occurred to evaporator systems. New evaporator geometries have been commercialized to mitigate scaling problems, increase capacity, and raise the discharge solids content [4]. Two of these designs are tube type and dimple plate type falling film evaporators. Concurrently, there was a move toward low odor recovery boilers, and a drive to increase the dry solids content of the liquor fired to increase recovery boiler capacity and improve steam production. This resulted in replacement of many DCE's with various types of black liquor concentrators to raise the discharge solids from the usual ~50% exiting the multi-effect evaporator train to a dry solids content at firing of at least 65-70%, and in some cases as high as 80%.

Some of these concentrators are forced circulation type evaporators, which can either stand alone and receive 45-50% solids from an LTV train or be integrated as the final effect of a falling film set. Two commercialized units are the PFR® Concentrator by Unitech Corporation, and the High Solids Crystallizer by US Filter/HPD which is a forced circulation evaporator/crystallizer. Finally, additional units, so called "superconcentrators", have been added at a small number of mills to reach ~80% solids. These are falling film crystallizer/concentrators with high liquor recirculation rates and introduced seed crystals to promote sodium carbonate crystal growth in the bulk solution rather than on heating surfaces, or tube type falling film evaporators or crystallizer type concentrators operating at high temperatures and pressures. These units are followed by one or more flash tanks to incrementally gain additional evaporation [4].

Mill Closure

A further development has been mill closure, or the drive to reduce overall mill water consumption through recycling and multiple water uses. One adverse side effect of this effort has been the increase in the concentrations of non-process elements (NPE's) in the chemical recovery cycle. These are metal ions such as aluminum, barium, calcium, magnesium, manganese, and silicon, to name the more critical ones. To avoid precipitation of these compounds, in characteristically undesirable locations, effective purging of these elements is necessary in current operating practices. It would be interesting to compare the concentrations of these NPE's in today's black liquors with the results of Grace's study.

PROCEDURES

Survey

An updated evaporator fouling survey questionnaire was developed by Grace based on his original survey, and was distributed to individual mills at a number of North American pulp and paper companies. No attempt was made to blanket the entire industry with this questionnaire, but rather, selected companies were contacted based on their participation in the evaporator fouling workshop mentioned above. This original set of participants was later expanded as the authors interacted with additional mills, some of whom were not experiencing any serious scaling problems, but were eager to participate nonetheless. All told, approximately 40 mills were contacted.

The questionnaire targeted numerous aspects of the entire mill's operation, and a complete description of the design and operation of the evaporator and concentrator systems. The information requested included the nature of the wood supply, the type of pulping process and conditions, white liquor composition, mill water composition, black liquor processing operations such as oxidation and soap removal, a description of the evaporator set(s) and separate concentrator(s) (where appropriate), evaporator operating parameters under various conditions, types and frequencies of cleaning procedures, and types of reported scales and related scaling conditions. Black liquor samples from just upstream of the fouling effect and any available scale samples were also requested.

In order to perform energy balances around the evaporator sets, so that average heat fluxes and heat transfer coefficients could be calculated, additional follow up requests for information were made for data on boiling point rises in the individual effects, and various feed and product liquor and vapor temperatures.

Analytical Procedures

Black liquor samples were analyzed for total solids, and metals by acid digestion followed by Inductively Coupled Plasma (ICP) spectroscopy. Anions (chloride, sulfate, thiosulfate, and oxalate) were analyzed by Capillary Ion Electrophoresis (CIE). Total carbon, oxygen, hydrogen, and sulfur were determined from combustion analyses, carbonate was determined coulometrically by measuring the amount of evolved carbon dioxide from acidified samples, and total organic carbon was determined as the difference between total carbon and total inorganic (carbonate) carbon. Residual active alkali (RAA) was measured by acid titration after precipitation of the inorganic matter and carbonate with barium chloride. The fiber content of the liquor was measured by filtration, and the residual soap content by organic solvent extraction. The scale samples were analyzed for inorganic phase composition by X-Ray Diffraction (XRD).

Data Reduction

The data was entered into a Microsoft Access database. To estimate the evaporator performance, an energy balance calculation was performed for every evaporator set where sufficient data were available. Average values for the operating heat transfer coefficients, thermal driving forces, and heat loads were calculated, accounting for both sensible and latent heat changes in the liquor.

When actual data from the mill were not provided, the sum of the boiling point rises (BPR) was estimated by assuming equal masses of water were evaporated in each evaporator body, calculating the corresponding solids contents, and estimating the BPR from an established BPR solids correlation [5]. For evaporator effects with more than one body, the BPR for the effect was taken as the mean BPR for the respective bodies. Comparing actual BPR data with BPR's estimated as described above, the sum of the estimated BPR's is generally within 20% of the actual sum of the BPR's. Also, the corresponding average temperature difference per effect, and the average heat transfer coefficient per effect, based on the estimated BPR's, are within 10% of those values calculated using actual BPR data.

Statistical Analysis of Data

A statistical analysis of the data will be performed for the final version of this paper. This will consist of analysis of variance calculations between pairs of variables to determine if any correlation exists between evaporator operating variables, black liquor composition variables, and the types and extent of reported scaling.

RESULTS AND DISCUSSION

Distribution of Survey Responses

The overall status of the responses to the questionnaire and the geographical distribution of those responses based on mill location and wood supply are presented in Table I. To date, of the 40 mills contacted, 27 have responded: 25 returned a completed questionnaire, 17 of those also submitted liquor samples, and two mills submitted only a liquor sample for analysis.

The distributions of the respondent mills based on type of pulping process employed, geographic location, and nature of the wood supply, highlight some expected trends, and some important differences from Grace's survey. A small, but significant number of mills use a modified kraft cooking process: MCC®, EMCC®, RDH®, or Superbatch®. These processes can alter the traditional chemistry of the weak black liquor fed to the evaporators. Although these processes still represent a minority of the respondents, their installed capacity will likely increase as old units are retrofitted and new ones are installed. In Grace's survey, none of the mills used a modified kraft process, they were all either conventional kraft, soda, NSSC, or kraft + semi-chemical mills [1].

The geographic distribution of the respondents has been weighted towards the Southeast and Northwest regions. This is an unintended consequence, and may indicate regions where fouling is more prevalent. As may be expected, the nature of the wood supply varies substantially in different regions of the USA and Canada. In the Southeast, two of the ten mills pulp a majority of hardwood, and the remaining eight are majority softwood mills with two pulping

100% softwood. This is more the expected pattern for southeastern mills. The three mid-south mills pulp a majority of hardwood, but less than 80%. In the Northeast, all three mills pulp a majority of hardwood with two pulping 100% hardwood. The lone central mill, and the two north central mills pulp 85-95% hardwood. Finally, in the Northwest, all the mills pulp at least 67% softwood, and three pulp 100% softwood. Overall, for the 25 mills completing the questionnaire, the mean values for softwood, and hardwood production are 55.4%, and 44.6%, respectively. This is substantially different from Grace's survey, where the mean level of hardwood production was 31%.

Table I. Survey responses and geographical distribution of respondents

Pulping Processes Employed	Completed Questionnaires	Liquor Samples[a]	Scale Samples[b]	Wood Supply[c] HW>80%, SW>80%
Conventional Kraft	18	13	4	4, 4
Modified Kraft[d]	5	5	3	1, 2
Kraft + NSSC/Green Liquor[e] (cross recovery)	2	1	1	0, 0
Geographic Region				
Southeast (AL, FL, GA, MS, NC, SC,VA)	10	9	4	0, 2
Midsouth (AR, LA, OK, TX)	3	1		0, 0
Northeast (DE, MD, Mid-Atlantic, New England)	3	2		2, 0
Central (IL, KY, OH, WV)	1	2	2	1, 0
North central (MI, MN, WI)	2	2	2	2, 0
Northwest (ID, OR, WA; Canada: AB, BC)	6	3		0, 4
Total responses	25	19	8	5, 6

[a] The number of mills that submitted black liquor samples. Some mills submitted multiple samples: for multiple evaporator sets and/or multiple samples from one set.
[b] The number of mills that submitted scale samples. Several mills submitted multiple scale samples representing different types of scale.
[c] The number of mills with a wood supply that is, on average, > 80% hardwood, and > 80% softwood.
[d] Modified kraft processes include MCC®, EMCC®, RDH®, and Superbatch®.
[e] NSSC/Green Liquor pulping accounts for 15%, and 33%, respectively, of total pulp production for the two mills reporting. One of the mills employs kraft EMCC® pulping.

Evaporator System Geometries

Most of the mills that participated in this survey have more than one evaporator set: the 25 mills that returned the completed questionnaire operate a total of 49 evaporators, and 25 separate stand alone concentrators. These evaporators and concentrators represent a variety of different types and geometries: LTV rising film, tube type and plate type falling film, blow heat falling film (2 sets), tube type falling film high pressure evaporator, falling film crystallizer/concentrator, and forced circulation evaporator/crystallizers. This is a marked change from Grace's survey of the 1970's when all the evaporators were of the LTV rising film type, although several did have falling film, or forced circulation first effects. Since that time, many mills have integrated one or two falling film concentrator bodies as a new first effect into their existing LTV evaporators, have installed newer tube type or plate type falling film evaporators where the first effect concentrates the liquor to 65-68%, and/or installed additional stand alone high solids concentrator units of the type mentioned above. However, from the information provided by

the mills, the true number of evaporator effects and bodies, and the arrangement of liquor and vapor flows, was not always clear. The mill's effect/body numbering scheme was often inconsistent with the diagrams.

Types and Location of Reported Scale

The distribution of the types of reported scale is presented in Table II, and is a composite of data reported by the mills and compositional analyses of the submitted scale samples. The distribution of the scaling locations based on the approximate liquor solids range is presented in Table III. As one would expect, most mills experiencing scaling reported more than one type of scale.

Table II. Types of scale reported

Type of Scale	Number of Mills Reporting (%)	
	This Survey	Grace's Survey
Burkeite (soluble) scale, Na_2CO_3—Na_2SO_4	17 (35%)	19 (28%)
Calcium carbonate	11 (22%)	20 (30%)
Fiber, soap, and/or other organics	9 (18%)	6 (9%)
Aluminosilicates, and other silicates	4 (8%)	9 (13%)
Pirssonite, $Na_2CO_3.CaCO_3$	1 (2%)	
Sodium oxalate, $Na_2C_2O_4$	1 (2%)	
Other inorganic scale[a]	1 (2%)	
No scale	2 (4%)	10 (15%)
No information	3 (6%)	3 (4%)
Total	49	67

[a] From XRD analysis, the scale sample from this one mill consisted of burkeite, erdite ($NaFeS_2.2H_2O$), and magnetite (α-Fe_3O_4).

Table III. Location of reported scaling

Scaling Location	Liquor Solids Range, %	No. of Mills Reporting
Evaporator Effects	< 30	3
Traditional effects excluding	31 - 40	3
integrated concentrator units.	41 - 50	10
	51 - 60	7
Concentrator Effects	51 - 60	5
Separate unit or integrated 1st	61- 70	10
effect of evaporator train.	71 - 80	2
Total		40

Since the critical solids concentration for burkeite precipitation is generally between 47 and 53% dry solids content, the high percentage of mills reporting scaling in the 41-50% and 51-60% ranges in their traditional evaporator effects and concentrator effects is generally burkeite.

In climbing film LTV evaporators, scaling most frequently occurs in the tubes and liquor distributor plates. Because boiling takes place in the bulk liquor phase as it rises in the tubes, dry spots can develop on the tube walls and provide locations for scale formation. In fact, where mills have reported the data, scaling has primarily occurred in these locations. This points out an inherent design limitation of climbing film LTV evaporators compared to falling

film units. Scaling is less of a problem in falling film units, but tube pluggage can still occur, and is usually caused by poor liquor distribution. In plate type falling film units, pluggage cannot occur. Falling film units are also run at lower steam pressures than LTV systems which minimizes the scaling caused by reverse solubility compounds such as Na_2SO_4, or temperature sensitive calcium complexes [4]. In forced circulation units, if the recirculation rate is not high enough, or the liquor inventory is too low, scales can form in the heat exchanger tubes, or the surfaces of the vapor bodies.

The accepted operating procedure is to run climbing film LTV evaporator effects to produce liquor 1-2% below the critical solids level at which burkeite begins to precipitate, and to run the concentrator effects above this level. For falling film units that are designed for precipitation of sodium salts in suspension, crossing the critical solids level for burkeite precipitation does not require a change in evaporation technology.

Evaporator Performance Parameters

A summary of evaporator performance parameters from this survey, and Grace's survey, are presented in Table IV. The average values for the heat flux, temperature difference per effect (ΔT), heat transfer coefficient, and steam economy, are based on heat balances for only five evaporator systems. A more complete set of data will be presented later. The available results show some interesting trends:

1. Overall, cleaning frequency is lower today than two decades ago. Boil-out frequency is down 20% and acid cleaning by 63%. This suggests a better management of scale deposition in the evaporators. Hydroblasting frequency is up by 130%, however. The increase in hydroblasting frequency suggests that the frequency of more difficult to remove scales--$CaCO_3$ and aluminosilicates--would have increased. This does not agree with the results in Table II. The discrepancy may be due to the small number of scale samples obtained in this study.

2. The average product solids content from evaporator trains is higher today, 57.8% versus 48.6%. This is undoubtedly a result of the widespread use of falling film technology with liquor recirculation. Falling film units can operate above the critical solids content of black liquor (typically 47-53% dry solids content) without experiencing fouling problems.

3. The average overall heat flux, average overall heat transfer coefficient, and average ΔT are down by 10%, 8%, and 3% respectively, compared to two decades ago. This is also the result of the increase in falling film concentrators that operate at lower heat fluxes and lower ΔT's.

Table IV. Averages of evaporator performance parameters

Performance Parameter	This Survey			Grace Survey (1974-75)		
	Mean	Std. Dev.	Range	Mean	Std. Dev.	Range
Boil out frequency, times/mo.	3.25	3.24	.083-12.2	4.09	3.5	0.33 - 15
Acid cleaning freq., times/mo.	0.092	0.049	.042-.167	0.25	0.67	0 - 3.5
Hydroblasting freq., times/mo.	0.107	0.083	.056-.167	0.047	0.059	0 - 0.21
Total cleaning freq., times/mo.	3.16	3.80	.083-12.3	4.39		
Prod. Loss between cleanings, %				15.8	8.6	2.7 - 30.9
Rate of production decline, %/mo.				71.6	55.6	8 - 241
Evaporator product solids, wt. %	57.8	9.9	47 - 80	48.6	3.7	42 - 62
Average heat flux, W/m^2	13,100	2,520	9,810 - 16,000	14,500	3,130	7,880 - 21,800
Average ΔT, °C	12.4	2.2	10.6-15.9	12.8	2.8	9.3 - 23.3
Ave. heat transfer coef., W/m^2K	1,050	89	921-1,130	1,140	295	721-1,870
Saturated steam temp., °C	144	10	129 - 192	141	7.2	127 - 162
Steam economy	5.30	1.78	3.94-7.89			

Cleaning frequencies are generally not a very good measure of the degree of scaling because mills with no, or only minor scaling problems, will often boil out the evaporators once a year prior to vessel inspections. Similarly, boil-outs are often performed on a regularly scheduled basis even if there is insufficient performance loss due to scaling to warrant cleaning. They are used proactively as routine preventative measures to forestall significant performance declines, and not always reactively, to respond to obvious scaling problems.

The cleaning frequencies do not include data for evaporator sets where one body of a multi-body first effect is always in wash mode--this is more of a preventative measure and the data would seriously skew the overall averages. The total cleaning frequency is the sum of the boil-out, acid cleaning, and hydroblasting frequencies, and any other identified cleaning method, such as flushing the effects with warm water or hot condensate. Cleaning frequencies for both surveys are comparable, although the current survey shows lower boil-out and acid cleaning frequencies, and higher hydroblasting frequencies than Grace's survey as discussed above. As one would expect for this type of data, the ranges of values are quite large.

The evaporator product solids content data includes values for traditional evaporators, separate concentrators, and integrated evaporator/concentrators as discussed previously. Most mills also reported the product solids of the liquor exiting the flash tank as compared to exiting the last effect or concentrator. In general, a solids gain of one to two percent can be assumed for the flash tank. In Grace's survey, the reported solids values were for the liquor prior to the flash tank.

The average overall heat flux and the average overall heat transfer coefficient provide an estimate of evaporation capacity when comparing two evaporator trains. They are less useful for troubleshooting, however. Ideally, monitoring the average heat transfer coefficient for each effect as a function of time would be the best way to track the evaporator performance. However, this data was not requested because it was believed to be too difficult to obtain from the mills.

Black Liquor Composition

A summary of the black liquor composition data for the two surveys is presented in Table V. From a comparison of the analytical data, it is apparent that the mean composition of black liquor has changed since the 1970's, in some cases dramatically. Most notably, the Na_2CO_3 and Na_2SO_4 concentrations are both higher now; Na_2CO_3 by 15%, and Na_2SO_4 by 88%.

The sharp increase in sulfate concentration is probably due to the addition of R8 or R10 chlorine dioxide generator effluent rich in saltcake to various points in the liquor system. A number of mills reported adding it to the weak black liquor, and a few to the concentrator feed. In addition, a few mills reported adding tall oil acidulation waste to the weak black liquor, and one liquor sample was analyzed for a mill practicing cross recovery of kraft and NSSC black liquors, although NSSC production accounted for only 15% of total pulp production. The modest increase in carbonate concentration is more problematic and may simply reflect a causticizing conversion that is slightly lower now, and/or an analytical artifact that all of the carbonate was assumed to be sodium carbonate. The increase in potassium concentration noted in Table V may be in the form of potassium carbonate which would account for most of the increase in carbonate.

The black liquors submitted for analysis were also sampled at various locations. Most were first effect or concentrator feed samples, where the scaling primarily occurring, but a number of samples were weak or intermediate liquors. Several mills also sent multiple samples representing different evaporator sets and/or multiple samples from the same set.

Table V. Averages of black liquor composition variables

Analyte	This Survey			Grace's Survey (1974-75)		
	Mean	Std. Dev.	Range	Mean	Std. Dev.	Range
Na_2CO_3, wt. %	10.0	2.6	4.77 - 14.5	8.7	1.45	6.6 - 12.3
Na_2SO_4, wt. %	6.03	4.18	1.94 - 16.1	3.2	1.5	0.9 - 8.3
Na_2CO_3/ Na_2SO_4	2.49	1.67	0.51 - 6.33			
Na_2S, wt. %	0.79	0.92	0.06 - 2.97			
Residual active alkali as Na_2O, wt. %	5.69	1.36	2.81 - 7.66	5.95	1.05	3.9 - 8.6
Sodium, wt. %	18.4	1.65	14.0 - 20.3	18.7	0.88	17.2 - 20.5
Potassium, wt. %	2.02	1.19	0.82 - 5.05	1.36	0.57	0.44 - 2.7
Residual soap, wt. %	0.85	0.48	0.32 - 2.02	0.93	0.42	0.32 - 1.62
Fiber[a], wt. %	0.23	0.24	0.04 - 1.08	0.031	0.031	0.001 - 0.159
Critical solids, wt. %	52.2	2.8	49.0 - 60.3	52.9	2.1	48.4 - 56.3
Carbon, wt. %	34.6	2.32	31.4 - 40.4			
Inorganic carbon, wt. %	1.14	0.30	0.54 - 1.64			
Organic carbon, wt. %	33.5	2.50	30.2 - 39.7			
Hydrogen, wt. %	3.43	0.23	3.05 - 3.96			
Oxygen, wt. %	35.1	2.57	26.4 - 38.4			
Sulfur, wt. %	4.74	0.89	3.34 - 6.65			
Sulfate, wt. %	4.08	2.83	1.31 - 10.9			
Thiosulfate, wt. %	3.98	1.25	2.40 - 6.49			
Chloride, mg/kg	4,810	3,170	1570-12,700			
Oxalate, mg/kg	5,250	3,350	2000-13,400			
Aluminum, mg/kg	49.9	14.8	27.6 - 98.2	139	75	32 - 300
Barium, mg/kg	8.11	5.50	0.94 - 20.2			
Boron, mg/kg	42.0	21.9	24.4 - 132	202	153	49 - 680
Calcium[b], mg/kg	409	278	118 - 1,050	360 450	250 270	90 - 1,080 40 - 1,300
Copper, mg/kg	1.99	1.89	0.72 - 10.2	77	116	7 - 510
Iron, mg/kg	28.9	7.6	18.3 - 49.2	91	16	56 - 120
Magnesium, mg/kg	167	83	29.3 - 309	184	30	140 - 240
Manganese, mg/kg	55.1	24.4	15.1 - 93.1	96	37	42 - 220
Phosphorus, mg/kg	85.0	20.9	53 - 118			
Silicon, mg/kg	676	345	367 - 2,080	1,140	400	240 - 1,800
Strontium, mg/kg	2.93	2.27	0.65 - 8.6			
Vanadium, mg/kg	43.4	50.4	1.39 - 166	111	141	7 - 600
Zinc, mg/kg	8.46	3.91	3.55 - 19.4			

[a] Fiber measurements differed in the pore size of the filters used.

[b] In Grace's survey, two independent calcium determinations were made: by atomic absorption spectroscopy (first entry), and by atomic emission spectroscopy (second entry).

The residual active alkali (NaOH + Na_2S), total sodium, and residual soap, are all comparable to the earlier set of data. The calculated critical solids is also essentially unchanged from the 1970's. This is somewhat surprising given that the Na_2CO_3 and Na_2SO_4 concentrations are both significantly higher now. However, the critical solids calculation is much more sensitive to the total sodium concentration, and that value has not changed appreciably. The potassium level is now 49% higher which is probably an effect of mill closure. The fiber content is almost an order of magnitude greater, probably because a smaller pore size filtering medium was used: ~30 μm pore size instead of the ~60 μm for the previous study.

The trace metals (NPE's), with the exception of calcium, are all significantly lower. This is somewhat surprising considering the expected effects of mill closure on the recovery cycle are to increase concentrations of these elements, but it does indicate that there is adequate purging of these compounds, probably during green liquor clarification.

Overall Mill and Chemical Recovery Operations

It is important to examine evaporator performance in the context of the overall mill and chemical recovery operations because performance problems rarely originate in the evaporator systems themselves, they are almost always "inherited" from somewhere else. The white liquor composition data that is presented in Table VI is mill reported data, and is a valuable barometer for the effectiveness of two important chemical recovery processes. One is causticization of the green liquor to white liquor, as measured by the causticizing efficiency (CE). The other is reduction of the sulfate to sulfide in the recovery boiler, as measured by the reduction efficiency (RE). Causticization and reduction are two important processes that directly affect the burkeite scaling tendencies of the liquor because they determine the residual sodium carbonate, and sodium sulfate, respectively, that are carried through the liquor system as a dead load.

Table VI. Averages of white liquor composition variables

Parameter	This Survey			Grace Survey (1974-75)		
	Mean	Std. Dev.	Range	Mean	Std. Dev.	Range
Tot. Titr. Alkali, as Na_2O g/L	119	7.0	102 - 139			
Active Alkali, as Na_2O g/L	99.2	6.9	85.7 - 119	110.6	43.6	83 - 180
Causticizing Efficiency, %	79.1	3.4	68.0 - 84.0			
Reduction Efficiency, %	92.9	3.1	83.0 - 97.9			
Na_2S, g/L	35.4	5.4	26.4 - 43.3	34.1	11.7	0.3 - 80
Na_2CO_3, g/L	34.1	7.8	23.6 - 52.1	29.6	12.5	1.0 - 49.4
Na_2SO_4, g/L	4.8	2.0	1.1 - 9.9	8.0	6.9	0.1 - 30

The CE values reported by the mills were probably determined directly from the measured white liquor composition without correcting for the NaOH content of the original green liquor. They are therefore slightly higher than the true values obtained if the correction for NaOH in the green liquor is accounted for. Similarly, the RE values were probably reported as sulfide/(sulfide + sulfate), instead of as sulfide/total sulfur, and were probably determined directly from the measured green liquor composition instead of from an analysis of the smelt composition. The mills generally did not specify the basis for the measurements. An exception may be one that was reported as 97.9%.

The causticizing efficiency and sulfur reduction efficiency reported by the mills should be maintained as high as possible subject to chemical equilibrium limitations to minimize the concentrations of sodium carbonate and sodium sulfate, respectively. In Table VI, the mean values for the CE and RE of 79% and 93% are good, but the relatively wide range of values underscores that some mills are operating with a poor CE and/or RE. In fact, one mill had a CE of 68% and a RE of 94%! The corresponding black liquor composition was 14.47 % Na_2CO_3, and 2.97% Na_2SO_4, for a ratio of Na_2CO_3/Na_2SO_4 of 4.87.

Comparing the data for the two surveys, we find that today's white liquors have concentrations of active alkali, and Na_2SO_4, that are 10%, and 40% lower, respectively, than in the 1970's and have a much smaller range of values. The reduction in sulfate concentration is opposite to the black liquor composition. This may due to adequate reduction of the higher sulfate load in the black liquor. The Na_2S concentrations are approximately the same, but the range of values is smaller in today's white liquors. The Na_2CO_3 concentration is 15% higher now which is the same increase in concentration that was reported for the black liquors. As was discussed previously, this increase in Na_2CO_3 concentration may reflect a slightly lower causticizing conversion, and/or an artifact of the analysis. The ranges of reported values in Grace's survey are especially astonishing. This may be partially due to the fact that his survey included data for seven kraft + semi-chemical mills practicing cross recovery, and two soda mills, in addition to the 37 kraft mills.

CONCLUSIONS

This survey of evaporator fouling in the North American kraft pulping industry has identified both similarities and differences in the nature and extent of the problem since Grace's survey in the 1970's. These characteristics are a reflection of the changes in pulping technology and evaporation technology, and changes in mill wide processes such as mill closure, and are manifested in the types and distribution of scales, evaporator performance parameters, and the composition of the processed black liquors.

The key results of the survey are that the average product solids content from evaporator trains is higher today, 58% versus 49%, a result of the current widespread use of falling film technology with liquor recirculation, and the fact that a number of evaporator sets now have integrated concentrators. More mills process hardwood liquors than in the 1970's. The black liquors processed contain more potassium, carbonate, and sulfate than they did in the 1970's, and probably more chloride. They contain the same amount of sodium, residual active alkali, and soap; and despite the impact of mill closure, the black liquors contain less of all other metals.

The average overall heat flux, average overall heat transfer coefficient, and average temperature difference per effect are down by 10%, 8%, and 3% respectively, compared to two decades ago. This is also the result of the increase in falling film concentrators that operate at lower heat fluxes and lower temperature differences. The frequency of soluble scales and of fiber, soap, organic scales have increased. Fewer mills report $CaCO_3$ scale problems, but fewer report no scale problems. Overall, the cleaning frequency is lower today than two decades ago. Boil-out frequency is down by 20%, and acid cleaning by 63%, but the frequency of hydroblasting is up by 130%.

ACKNOWLEDGMENT

The authors wish to thank Tom Grace for assisting us in preparing the evaporator fouling questionnaire; all of the pulp and paper companies that participated in this survey for their cooperation in completing the detailed questionnaire and submitting black liquor and scale samples; the Chemical Analysis Group at IPST for performing the bulk of the analytical work; and the member companies of IPST for their financial support for this project.

REFERENCES

1. Grace, T.M. "A Survey of Evaporator Scaling in the Alkaline Pulp Industry", Institute of Paper Chemistry Project 3234, Report 1 (Sept. 22, 1975).
2. Headley, R.L., "Pulp Cooking Developments Focus on Fiber Yield, Lower Chemical Usage", Pulp & Paper, 70 (10), 49-57 (1996).
3. MacLeod, J.M., "Extended delignification: a status report", Appita, 46 (6), 446-451 (1993).
4. Venkatesh, V., and X.N. Nguyen, "Evaporation and Concentration of Black Liquor", ch. 2 in Chemical Recovery in the Alkaline Pulping Processes, 3rd ed., ed. R.P. Green, and G. Hough. TAPPI Press, Atlanta, 1992, pp. 5-35.
5. Frederick, W.J., "Black Liquor Properties", Ch. 3 in Kraft Recovery Boilers, ed. T.N. Adams. TAPPI Press, Atlanta, 1997, pp. 59-99.

DUES-FUNDED PROJECT SUMMARY

Project Title:	Recovery Boiler Modeling
Project Code:	
Project Number:	F016-02
PAC:	Chemical Recovery
Division:	Chemical Recovery and Corrosion
Project Staff	
Faculty/Senior Staff:	J. Frederick, K. Iisa, S. Lien, T. Grace
Staff:	
FY 98-99 Budget:	
Allocated as Matching Funds:	None
Time Allocation	
Faculty/Senior Staff:	J. Frederick (3%), K. Iisa (8%), S. Lien (25%), T. Grace (3%)
Support:	
Supporting Research	
M.S. Students:	None
Ph.D. Students:	None
External:	None

RESEARCH LINE/ROADMAP: Improved Capital Effectiveness. 8. Develop technologies (compatible with present pulp-mill assets) to allow cost-effective expansion of kraft-pulp-equivalent fiber capacity (hardwood and softwood) by 30% without adding Tomlinson recovery boilers.

PROJECT OBJECTIVES:

The first objective is to complete the analysis of results and reporting of data to satisfy IPST's contract with DOE. The second objective is to evaluate the fume formation, sulfur gas formation and recapture, and NO_X parts of the model when implemented in a detailed computational model. The third is to transfer the detailed combustion model, including the fume, sulfur gas, and NO_X components, to those providers of detailed recovery boiler computational modeling who serve IPST member companies.

PROJECT BACKGROUND:

This recovery boiler project started in October 1990 and was originally scheduled to run for four years. The objective of the project was to develop a computer model of a recovery boiler furnace using a CFD code specifically tailored to the requirements for solving recovery boiler flows and using improved submodels for black liquor combustion based on continued laboratory fundamental studies. There was considerable emphasis on developing accurate predictions of the physical carryover of macroscopic particles of partially burnt black liquor and smelt out of the furnace, since this was seen as the main cause of boiler plugging. This placed strong emphasis on gas flow patterns within the furnace and on mass loss rates and swelling and shrinking rates of burning black liquor drops.

The original project involved three institutions, the Institute of Paper Science & Technology (IPST), the University of British Columbia (UBC), and Oregon State University (OSU). IPST was responsible for overall project leadership, bed modeling, model simplification and application, and overall model validation. UBC was responsible for CFD code development and flow modeling and validation. OSU was responsible for fundamental data on black liquor combustion and formulation of improved black liquor burning models. In addition, T. M. Grace Company, Inc. was involved to provide technical coordination and interpretation.

When the original four-year period was completed, the project was extended for an additional three years. The extension started in September 1994. By this time it had become apparent that many recovery boilers encountered serious plugging problems even when physical carryover was minimal. The objective of the extended project was to improve the utility of the models by including the black liquor chemistry relevant to air emissions predictions and aerosol formation, and by developing the knowledge base and computational tools to relate furnace model outputs to fouling and plugging of the convective sections of the boilers.

Two new members were added to the project team in the extended project. Babcock & Wilcox (B&W) became involved to provide experimentally based information on radiation heat transfer. Tran Industrial Research (TIR) was brought in to provide guidance and information relevant to boiler plugging. In January 1995, as a result of staff changes at IPST, Thomas M. Grace became a part-time employee of IPST in order to serve as principal investigator on the project. As a consequence, T. M. Grace Company, Inc. was no longer involved as subcontractor.

Early in 1995, a critical review of recovery boiler modeling was carried out. As a result of this review and other factors, the extended project was restructured so as to bring it to closure in a manner that would maximize the value of the entire project to the pulp and paper industry. The restructured project was initiated at the end of October 1995 and was completed in June 1997

SUMMARY OF RESULTS:

A new sub-model for conversion of the organic carbon in black liquor to gases was developed. The new carbon sub-model accounts for the kinetics of devolatilization as well as the temperature dependence of the distribution of organic carbon between carbon as gases and fixed carbon as char residue.

A second new sub-model for conversion of the sulfur in black liquor to Na_2S and H_2S was also developed. The new sulfur sub-model accounts for the kinetics of sulfur conversion during devolatilization as well as the temperature dependence of the distribution of sulfur between Na_2S and H_2S.

A detailed model for NO_X formation and destruction was also developed. The NO_X model accounts for the conversion of fuel nitrogen to NO as well as volatile NO_X precursors and N_2, the formation of NO_X from its precursors, simultaneous destruction of both NO and volatile NO_X precursors, and formation of NO_X via the prompt NO_X route.

A rigorous method for accounting for conservation of all chemical elements in black liquor and conservation of energy was developed.

Model validation tests were made by simulating two different kraft recovery boilers and comparing the results with data from field measurements. For each boiler, operating data and measurements of boiler variables that correspond to outputs generated by the model were obtained by the field measurements.

A benchmarking study was made by simulating a physical model of an actual recovery boiler. The physical model was constructed of plexiglass and used water to represent the air flow patterns. Laser doppler velocimetry was used to measure the velocity distribution in the model. The measured velocity was compared to the calculated velocity.

A final report for the project has been prepared and submitted to DOE for final review.

GOALS FOR FY 98-99:

1. Complete a report that describes in detail the current understanding of how to model black liquor burning in a recovery boiler. This report is directed to those involved in recovery boiler model development. It included details of the combustion and chemical species sub-models.
2. Complete a technical monograph on recovery boiler fouling.

3. Evaluate the fume generation, fume enrichment, sulfur gas, and NO_X submodels when included in a detailed computational model for kraft recovery boilers
4. Assist the North American centers for detailed recovery boiler modeling with implementation of the latest version of the combustion and chemical species sub-models.

DELIVERABLES:

1. A report that describes in detail the current understanding of how to model black liquor burning in a recovery boiler, directed to those involved in recovery boiler model development.
2. A technical monograph on recovery boiler fouling.
3. A report that evaluates the fume generation, fume enrichment, sulfur gas, and NO_X submodels when included in a detailed computational model for kraft recovery boilers.
4. Assist the North American centers for detailed recovery boiler modeling with implementation of the latest version of the combustion and chemical species sub-models.

SCHEDULE:

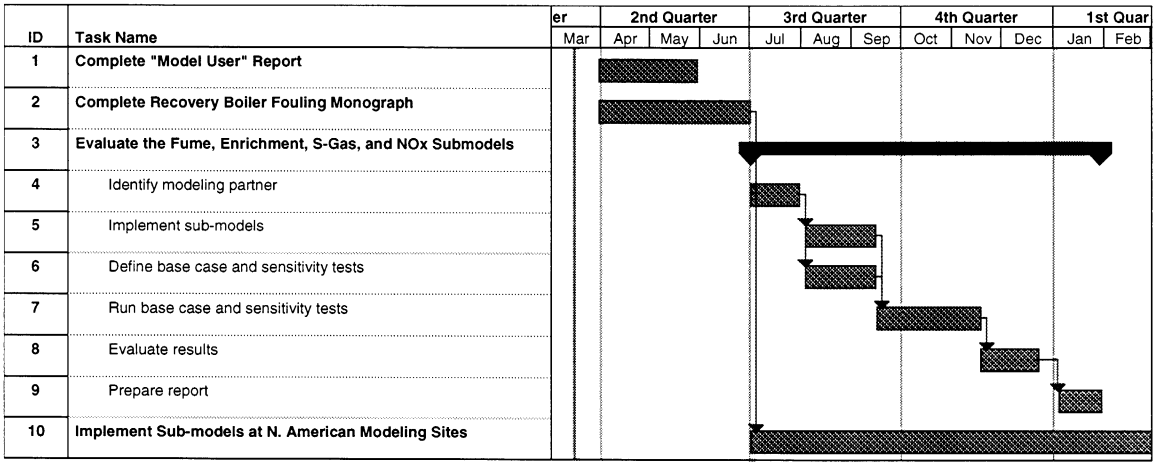

DUES-FUNDED PROJECT SUMMARY

Project Title:	Recovery Boiler Capacity Improvements
Project Code:	
Project Number:	F016-03
PAC:	Chemical Recovery
Division:	Chemical Recovery and Corrosion
Project Staff	
Faculty/Senior Staff:	J. Frederick, S. Lien, K. Iisa
Staff:	Q. Jing
FY 98-99 Budget:	TBA
Allocated as Matching Funds:	$40,000
Time Allocation	
Faculty/Senior Staff:	J. Frederick (10%), S. Lien (34%), K. Iisa (11%)
Support:	Q. Jing (31%)
Supporting Research	
M.S. Students:	None
Ph.D. Students:	None
External:	L. Baxter, Sandia National Labs; S. Sinquefield, OSU (-1/98), R. Wessel, McDermott Technologies, Inc.; H. Tran, U. of Toronto

RESEARCH LINE/ROADMAP: Improved Capital Effectiveness. 8. Develop technologies (compatible with present pulp-mill assets) to allow cost-effective expansion of kraft-pulp-equivalent fiber capacity (hardwood and softwood) by 30% without adding Tomlinson recovery boilers.

PROJECT OBJECTIVES:

The first objective is to complete the analysis of from fume formation experiments conducted at Sandia National Laboratory. The second objective is to obtain new data on the impact of black liquor composition and burning conditions on carry-over and fume particle formation during char bed burning. The third objective is to obtain new data on the impact of fume particle composition and the composition of the surrounding gases on the rate of sintering of recovery boiler deposits.

PROJECT BACKGROUND:

A number of factors can limit the pulp capacity rate supported by a kraft recovery boiler, but the most important of these is normally plugging of gas passages in the superheater, boiler bank, and economizer. Research at Oregon State University, Sandia National Laboratory, and the University of Toronto, in an industry-supported consortium, have investigated deposition of sub-micron fume particles, and completed the first phase in an investigation of how fume composition, gas composition, and temperature impact sintering and hardening of deposits in recovery boilers. As a result of this and earlier work, Key questions were identified regarding the formation, properties, hardening, and removal of recovery boiler deposits. A research project, funded by DOE/Agenda 2020, began in February of this year to address several of these questions. IPST's responsibilities in this project include a) obtaining data on liquor-to-liquor differences in the amounts of fume and larger (10-100 micron) particles generated during burning of black liquor in-flight and on a char bed; b) the impacts of particle composition and gas composition on the rate of sintering and hardening of recovery boiler deposits, and c) radiation properties of entrained particles in kraft recovery boilers.

SUMMARY OF RESULTS:

This is a new project – no results have been obtained to date.

GOALS FOR FY 98-99:

1. Obtain data on the effects of LEFR conditions on fine particle formation.
2. Obtain data on the effect of liquor type and composition on fine particle formation.
3. Obtain data on effect of furnace conditions on fine particle generation during char bed burning.
4. Measure absorption spectra for fume samples from the OSU laminar entrained-flow reactor
5. Determine complex index of refraction of samples of entrained particles from commercial kraft recovery boilers.
6. Analysis of existing U of T data on the effect of fume composition and temperature on sintering rate of recovery boiler deposits
7. Obtain additional data on the effect of fume composition and temperature on sintering rate of recovery boiler deposits

DELIVERABLES:

1. Data on the impact of liquor composition and temperature on fine (0.1-100 micron) particle generation during black liquor burning.
2. Refractive index and absorption coefficient data versus particle composition for fine particles generated during black liquor burning
3. Data on the impact of particle composition on the rate of sintering of recovery boiler dusts.

SCHEDULE:

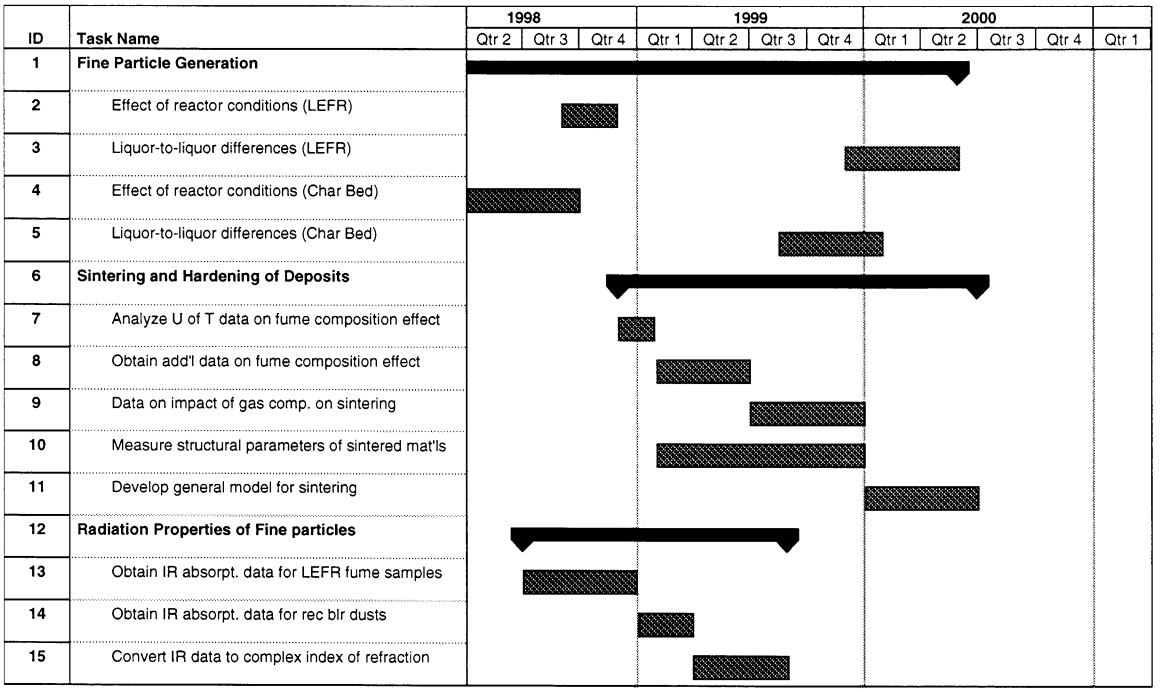

An Experimental Study of the Mechanisms of Fine Particle Deposition in Kraft Recovery Boilers

S. A. Sinquefield, Department of Chemical Engineering, Gleeson 103, Oregon State University, Corvallis, OR 97331, USA

L. L. Baxter, Sandia National Laboratories, 7011 East Avenue, Livermore, CA, 94550, USA

W. J. Frederick, The Institute of Paper Science and Technology, 500 - 10th Street NW, Atlanta, GA 30318, USA

Abstract

Experiments on the deposition of fume (submicron) and intermediate sized (1-100 micron) particles produced during combustion of black liquor have been carried out in Sandiaís Multifuel combustor. Temperature-controlled, cylindrical probes in cross flow were used as the deposition target. Several observations can be made at this point. The fume particles form a deposit structure that is roughly a close packing of spheres while the intermediate sized particles deposit in a dendritic or ëfractalí manor, with very high porosity. Fume particle deposition rates are dependent on the temperature difference between the gas and the surface, indicating a thermophoretic driving force, while deposition rates of intermediate sized particles are surface temperature independent. The particle collection efficiency of fume particles was typically in the 2% range while the larger particles deposited about 4 times more efficiently. Fume particle deposition rates increased only slightly with a three-fold increase in probe diameter.

Introduction

The deposition of carry-over particles[1] is now understood well enough to design recovery boilers to minimize its impact. In contrast, the factors controlling the deposition of finer particles[2] is not well understood. These finer particles consist of two groups: fume (condensation aerosols) mainly in the size range 0.01 ñ 1 micron; and intermediate size, inorganic fragments from larger droplets typically 1-100 micron in diameter. These finer particles can deposit on superheater tubes, but a significant fraction can pass through the superheater and deposit on boiler or economizer tubes.

In 1993, an investigation was begun to determine the mechanism of fine particle deposition in the convective gas passages of kraft recovery boilers, and to identify the factors that control it. This investigation was sponsored by a consortium of six recovery boiler manufacturers and three pulp and paper manufacturers. It was carried out as a collaboration between Sandia

---

[1] Carry-over particles are the smelt residue from black liquor droplets burned in flight. They are typically in the size range 0.5-1 mm.

[2] In this study, fine particles were initially defined as ìfumeî particles - condensation aerosols in the size range 0.01-1 micron. As a result of key findings regarding larger particles, the definition was expanded to include ìintermediate particlesî those in the range 10-100 micron - as well. Deposition of larger particles, typical of burned-out liquor droplet residue (carry-over) particles, were not investigated.

National Laboratories Combustion Research Facility and Oregon State University. The specific objectives of the study were

1. to measure the rate of deposit formation from fine particles under conditions similar to those in recovery boilers,
2. to develop a mechanistic, quantitative model of the deposition of fine particles, and
3. to evaluate the contribution of these particles to fire-side fouling in the superheater, generator bank and economizer sections of recovery boilers.

This document reports some of the results of that investigation.

Fire-side deposition of fume (submicron), and intermediate-sized (1-100 micron), particles on heat transfer surfaces in kraft recovery boilers poses a significant operational problem. These deposits plug gas passages, decrease thermal efficiency, and contribute to corrosion in the convection passes of commercial systems. When soot blowing becomes ineffective, a boiler must be shut down for expensive water washing procedures. An understanding of deposition mechanisms and deposit properties is essential if recovery boiler fouling is to be managed. Further, ash related problems are a major consideration in boiler design and warranty.

Fire-side deposits can be formed by particulate deposition, vapor condensation, or chemical reaction. Each of these will be discussed in turn. Particulate deposition occurs when particles, small enough to be entrained by the flowing hot gas, impinge and adhere to heat transfer surfaces inside of the boiler. There are several mechanisms by which entrained particles can reach a heat-transfer surface in a flow field. Inertial impaction occurs when an entrained particle has sufficient inertia to deviate from the gas streamlines as they change direction in the vicinity of an obstruction in the flow field. Turbulent eddy impaction is similar to inertial impaction except that it involves turbulent fluctuations in gas flows near surfaces. Such fluctuations in both gas flow and boundary layer thickness can lead to the impaction of smaller particles than would normally reach a surface in the absence of turbulence. Thermophoresis refers to small particles moving down a temperature gradient under the influence of gas molecules. The kinetic energy of gas molecules colliding with and leaving the particle is higher on itís hot side than on itís cold side, thereby causing a net driving force toward the cool side.

Vapor condensation occurs in the presence of a surface with a temperature below the dew point. A liquid layer may form on the surface, depending on the thermodynamics of the system. Chemical reactions between the gas and a surface can also lead to deposit growth. The sulphation of carbonate is an important reaction in the smelt bed of recovery boilers. But, since alkali carbonates are a major constituent of superheater deposits (Tran 1986), SO_2 in the flue gas can react with the carbonate in carryover deposits to form CO_2 and a sulphate deposit.

In the classical view of recovery boiler fireside fouling, there are two principal particle sizes responsible for the formation of deposits (Tran 1986, Adams and Frederick, 1988*). Carryover* particles are burned-out liquor droplets, 100 μm to a few mm in size, that become entrained in the upward flowing gases. They deposit primarily on the bullnose and in the superheater sections via inertial impaction. In recent years, recovery boilers have been built with larger cross-sectional areas in the lower furnace and superheater region in order to decrease the gas velocity and thereby decrease the number of entrained particles. *Fume* particles are defined as submicron particles generally formed by vapor condensation. During combustion, a fraction of the alkali chlorides in black liquor vaporizes. As the gases cool, particles nucleate and grow.

Fume particles, in the classical view, deposit in the generator bank and economizer sections of the boiler via thermophoresis.

In recent years some attention (Verrill and Wessel, 1996) has been given to the intermediate particle size range: 1-100μm. Particles of this size could be ejected fragments from the burning droplet, condensation aerosols that grew larger than accepted (Jokiniemi, 1995) growth models predict, or the result of liquid droplets agglomerating and coalescing into a single droplet.

To date, no published measurements have been made of the particle size distribution in the convective sections of recovery boilers. Two published work have been made characterizing the aerosol leaving the economizer section (Kauppinen, 1992 and Bosch, 1971). The results consistently indicate that particles are appoximately 1 μm in size (Figure 1). It is not clear whether these are the only particles present in the convective section, or if the convective pass of the boiler removes larger particles through deposit formation.

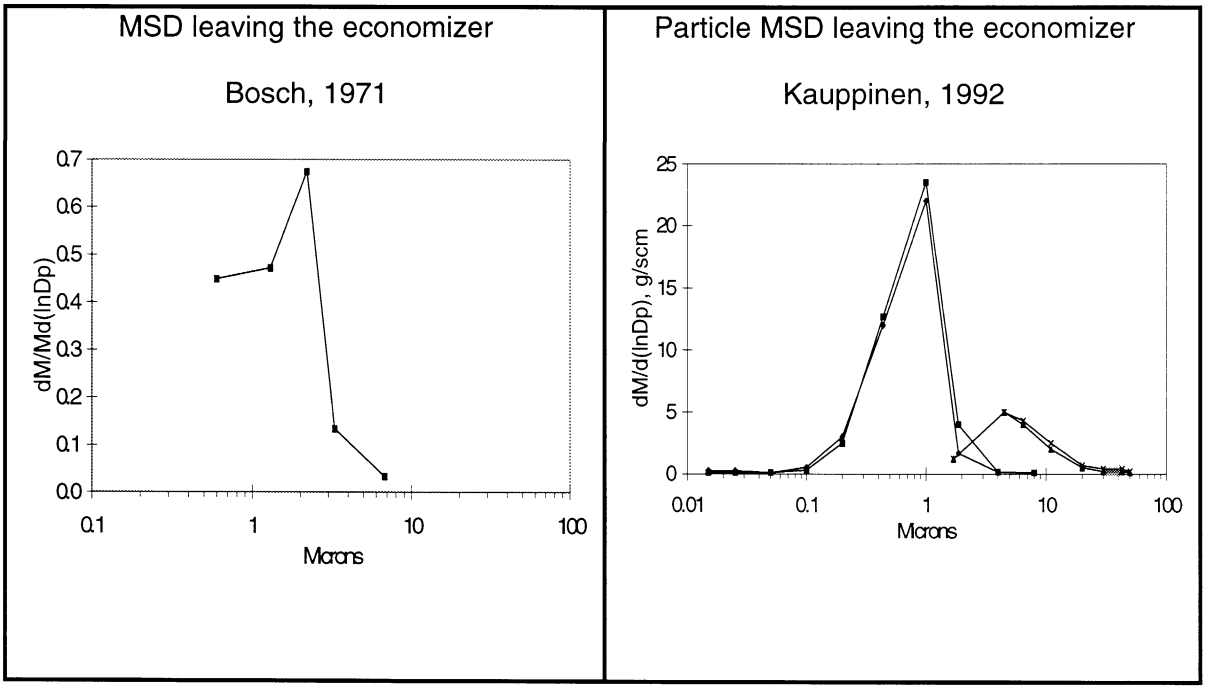

Figure 1. Measured mass size distriubtions leaving the economizer sections of commercial recovery boilers.

Experimental

In this section we review the experimental facilities, probes, diagnostics, and fuels used in this investigation. The experimental facilities include the Multifuel Combustor (MFC) at Sandia National Laboratories' Combustion Research Facility (CRF) and its associated diagnostics and the black liquor fuels. Temperature-controlled probes are used to simulate the heat transfer tubes found in full-scale boilers. The probes are scaled with respect to Reynolds number, Stokes number, or both, depending on the particle deposition mechanisms under investigation.

A variety of *in situ* and *ex situ* diagnostics are used to characterize deposit properties on these surfaces. Those most relevant to this investigations are briefly presented here in the order of: (1) *in situ,* real-time, diagnostics; (2) sampling (*ex situ*), real-time diagnostics; and (3) sampling, *post mordem* diagnostics.

As this investigation represents one of the first uses of black liquor in the MFC, a reasonably complete discussion of the combustor and its diagnostics is presented below.

The Multifuel Combustor

The Multifuel Combustor (MFC) at the Sandia National Laboratories' Combustion Research Facility in Livermore, California (Baxter, 1992) is a down-fired, small pilot-scale, turbulent flow combustor that allows for gas and particle temperature histories to be varied over the range of conditions commonly experienced in commercial combustors (Figure 2). In general, fuel can be injected from any of 11 positions along the length of the combustor (Figure 3), providing variation of fuel residence time in he combustor. The individual modules of the combustor can be independently controlled to vary local conditions of temperature and gas composition, simulating the residence-time dependence of these local variables in commercial-scale equipment. Most of the experimentation is peformed in the open test section at the bottom of the combustor, where optical access and laboratory equipment are available.

In Situ, Real-time Diagnostics

The *in situ*, real-time diagnostics used in this investigation monitor deposit and entrained particle properties. Monitored deposit properties include thickness, surface temperature, mass, and emissivity. Monitored entrained particle properties include concentration, size distribution, and velocity. Deposition targets used in the test section of the combustor provide a surface from which other measurements are made and independently monitors *in situ* properties such as heat flux, probe surface temperature, cooling gas flow rate, and cooling gas temperature. The deposition targets are discussed first, followed by discussions of the other *in situ*, real-time diagnostics relevant to this investigation.

Temperature-controlled probes

Specially designed, temperature-controlled probes were used as targets to collect ash deposits in the test section of the MFC. The surface temperature of the probe is held constant through the use of thermocouples embedded in the surface, internal air-cooling, and a feedback control loop. The probes are capable of axial rotation to generate axisymmetric deposits that are much easier to analyze for purposes of determining thermal conductivities, etc. Most typically, the probes were not rotated during these investigations. Many different probes of similar nominal design are used. Additional details of the designs include removable center sections to allow potting and subsequent microscopic analysis of the samples, screens to promote uniform, turbulent plug flow through the sections used for heat transfer analysis, in-line heaters to allow greater temperature control, and insulation blocks to prevent lateral heat transfer.

Spectroscopic analyses of the surfaces are performed on the shadowed side of the probe or on serpentine tubes used to simulate water walls. The water wall targets are similarly equipped with surface and air temperature thermocouples.

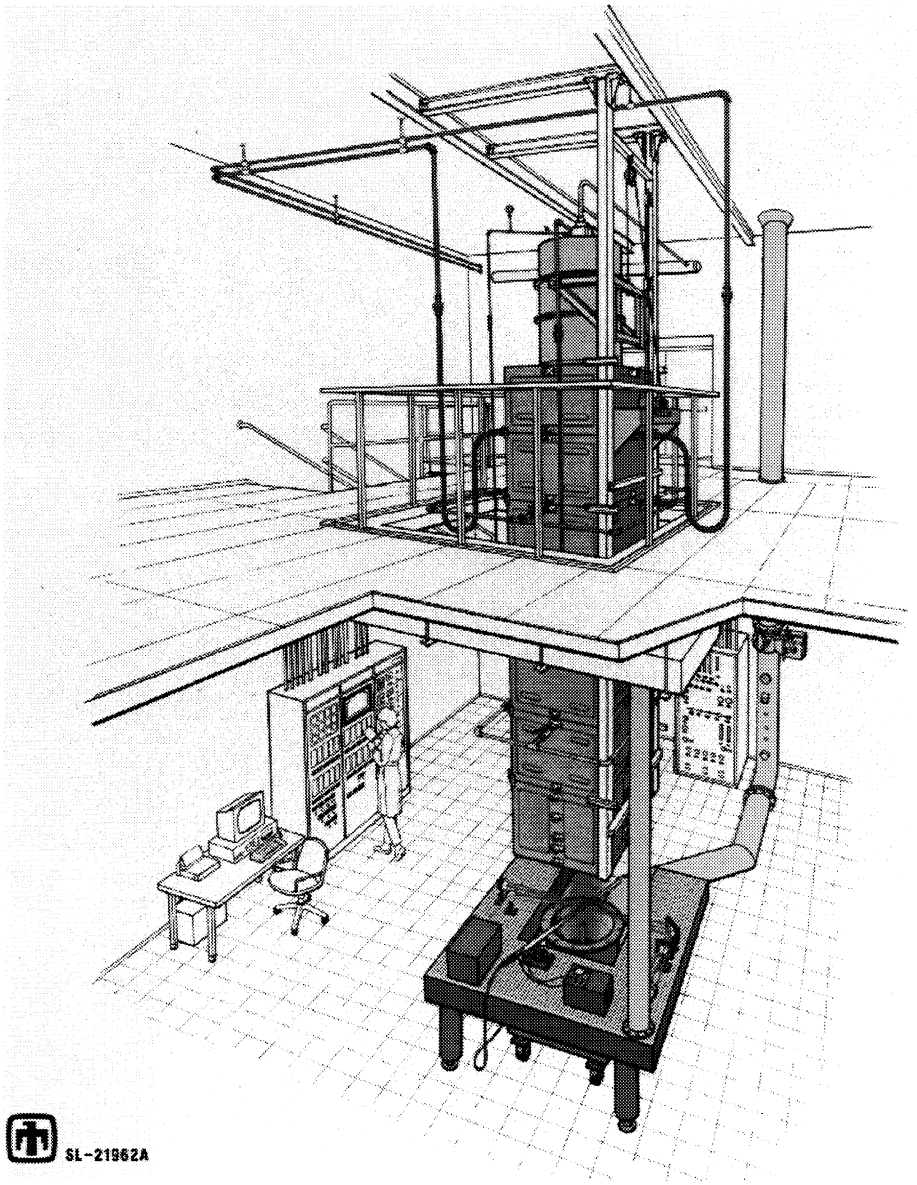

Figure 2. Artistist's sketch of the Multifuel Combustor at Sandia National Laboratories' Combustion Research Facility.

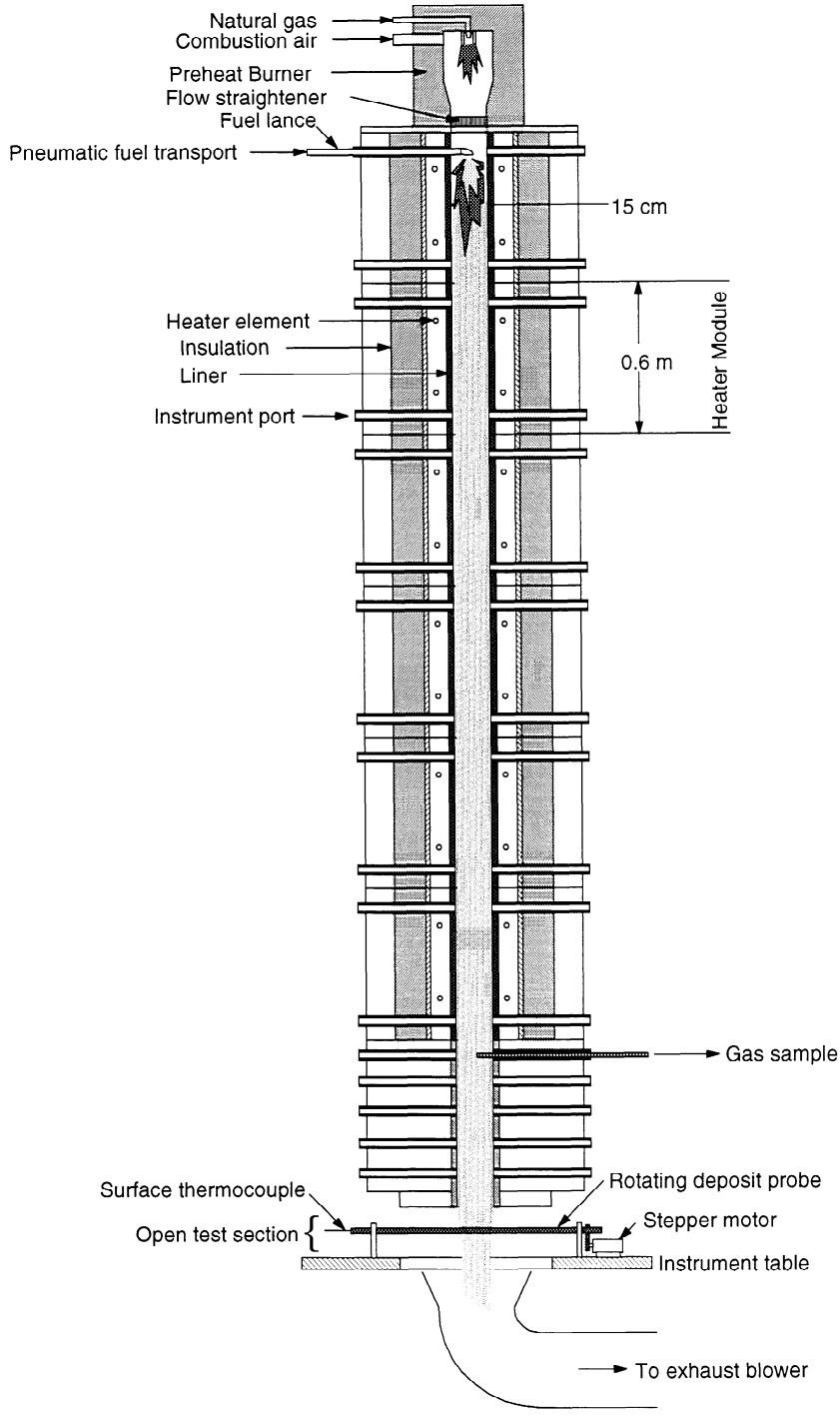

Sandia Multi-fuel Combustor (MFC).

Figure 3. Schematic diagram of the Multifuel Combustor illustrating module designs and open test section.

Diagnostics

A range-finding laser mounted on a precision bearing measures the surface topology and, by difference, deposit thickness along a single line parallel to the probe axis (Figure 4). The measurement range is 0-32 mm, and the resolution is ± 8 μm under ideal conditions, and ± 30 μm under typical black liquor combustion conditions. Successive scans along the same line at regular time intervals resolve the temporal growth rate. A series of scans at different radial positions resolves spatial variations. When the deposit growth rate is small, signal-to-noise ratios are poor. Under these conditions, as were experienced during some of the fume deposition experiments, the deposit thickness could not be reliably resolved *in situ* even after several hours of growth.

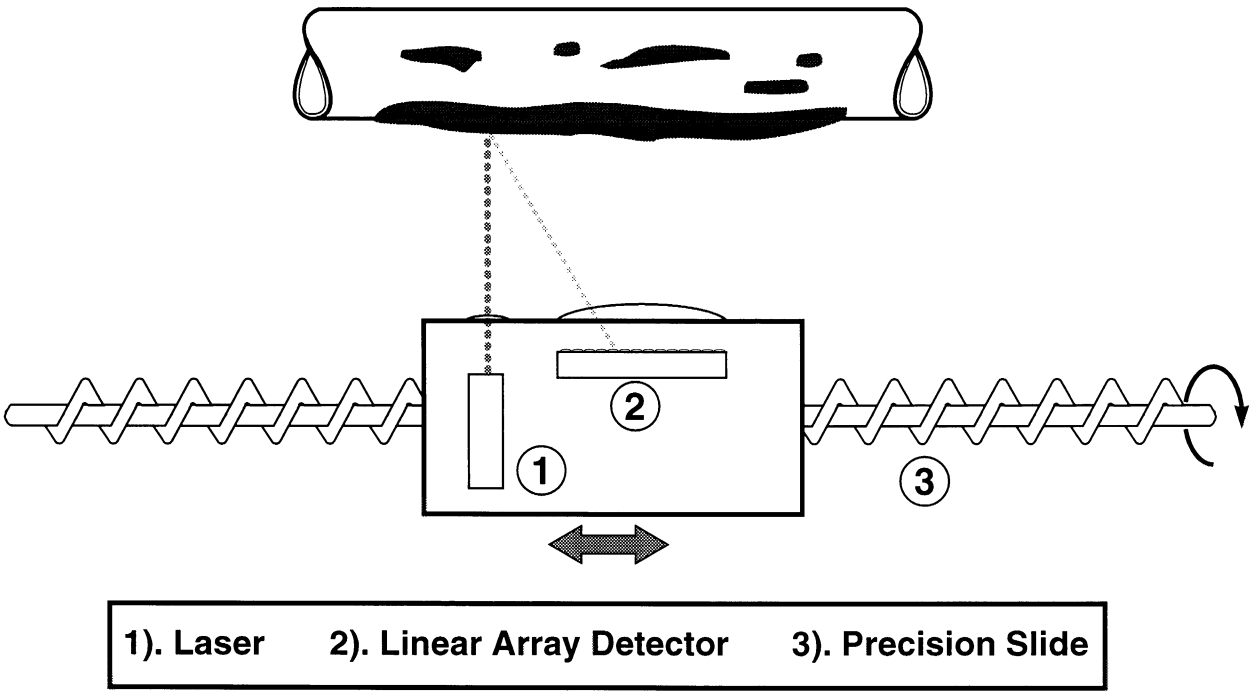

Figure 4. Schematic diagram of the deposit topology diagnostic.

Optical pyrometers are used to measure deposit surface temperature. The measurement technique assumes that all radiation in the instrument line of sight derives from surface emission. Therefore, measurements are made on the shadowed side of the probe with the deposit rotated out of the direction of flow of the gases to avoid surface reflections of flame radiation or with on the windward side with radiation temporarily blocked by some other means. Combustion flows with high particulate loading, such as those commonly experienced in black liquor systems, require that the particles in the line of sight be blocked to prevent scattering of radiation into the diagnostic. Several different pyrometers are used ranges of varying from 250 -850 °C and (400) - 1200 °C, respectively, and with an ideal accuracy of ±0.25 °C and a practical accuracy of ±1 °C if reflected and scattered radiation effects are removed and the probe surface emissivity is known. Over the range of reasonable emissivities for such deposits, the temperature can be characterized within ±15 °C. Deposits grow either axisymmertically, by rotating the probe, or traditionally, with stationary probes. Axisymmetric deposits are used to

characterize thermal conductivities whereas traditional deposits are used to monitor accumulation rates, structures, and mechanisms, the latter being the focus of this investigation. Temperature measurements from three locations on the probe allow temperatures on the remainder of the probe to be interpolated when the deposits are axisymmetric.

Fourier transform infrared (FTIR) emission spectroscopy characterizes spectral radiative properites and composition of the deposit. Spectral emissivities are characterized between 2.5 and 25 μm (4000 to 400 cm^{-1}) except in isolated bands where gas-phase, infrared-active species (principally H_2O and CO_2) interfere. Spectral emissivities can be determined within ±5 percent. Condensed-phase chemical species with identifiable signatures in this wavelength region are qualitatively identified. With respect to species of interest to black liquor combustion, this includes essentially all carbonates, suflates, silicates, some oxides, but few chlorides.

An *in situ,* laser-based diagnostic (PCSV system by Insitec) measures the particle concentration, size distribution, and velocity in the size range of 2-130 μm ideally, and 5-100 μm under most conditions relevant to black liquor combustion. The device is a multibeam system that approximates a point measurement with diagnostic volumes approximately ellipsoidal in shape. The ellipsoidal diagnostic volumes have major and minor axes of about 1 mm and 450 μm for one beam and 0.3 mm and 50 μm for the second beam. The accuracy of the diagnostic, when properly calibrated and aligned, is ±10% or ±1 μm, whichever is larger. Concentrations and velocities are measured with about ±5% accuracy. These accuracies are determined by spinning reticles with known particle sizes through the beam. Real systems typical of black liquor combustion contain high particle loadings. This compromises the measurement by both beam obscuration and multiple scattering in the diagnostic volume such that data reliability for small particles (<5 μm) degrades quickly. This investigation includes particles ranging in size from <0.1 to 50 μm. The smaller particle concentrations are measured using an aerosol spectrometer (discussed later).

Particle mass is determined using a magnetic force restoration technique on a cantelivered probe. This dynamic balance monitors the mass of the growing deposit. The ideal resolution of the deposit mass diagnostic is ±10mg. The mass of the probe, deposit, and some of the electronic control components are determined simultaneously. When the deposit mass accumulation rate is small, instrumental drift becomes a major source of error in the measurements. Under these conditions, as were experienced during some of the fume deposition experiments, the mass of the deposit could not be reliably resolved *in situ* even after several hours of growth. For the low-mass cases, the deposit is rinsed from the probe with water, dried, and weighed with an analytical balance.

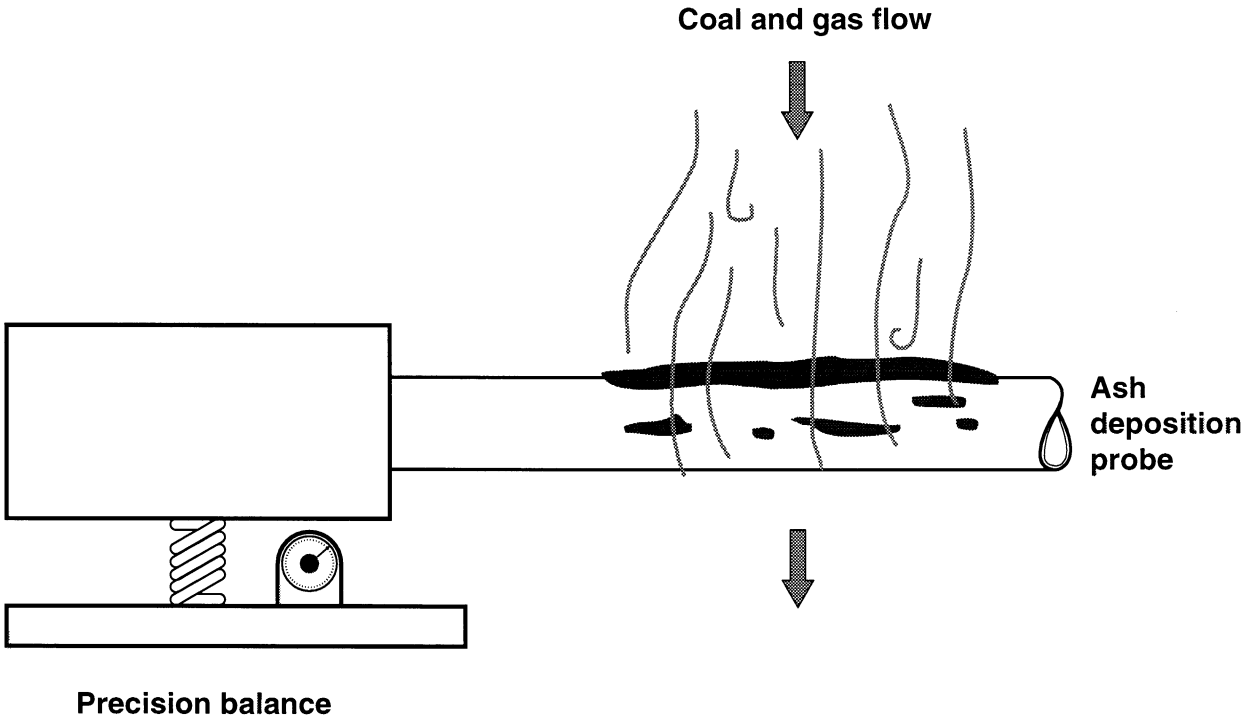

Figure 5. Schematic diagram of the dynamic balance used to determine deposit mass accumulation.

Sampled, Real-time Diagnostics

Sampled, real-time diagnostics include aerosol particle and gas concentration detectors.

An aerosol spectrometer samples and sizes particles in the range of 0.1-7.5 µm. This diagnostic provides complementary analyses to the *in situ* PCSV equipment. The estimated accuracy of the instrument is ±15% and the demonstrated reproducibility in combustion environments is ±7%. This is the primary means of characterizing particle size distributions in these experiments.

A continuous gas analysis system provides continuous monitoring of CO, CO_2, NO_x, O_2, SO_2, and total hydrocarbons (THC). Non-dispersive infrared detectors (NDIR) measure CO, CO_2, NO_x, and SO_2 concentrations. A magneto-pneumatic oxygen analyzer provides oxygen concentrations. A flame ionization detector is used for THC. The analyzers (Horiba models CFA-321, CFA-311, CMA-321, and FIA-HC) are incorporated in a gas sampling system that controls moisture, temperature, pressure and flow rate of sampled gases. The analyzer repeatability is ± 0.5% of full scale when concentrations are greater than 200 ppm and ±1% of full scale for lower concentrations. Zero drift is no more than ±1% of full scale per week for concentrations greater than 200 ppm and ± 2% of full scale per week at lower concentrations. Span drift is no greater than ± 2% of full scale per week. The exception is the THC measurement, which has a ± 1% of full-scale drift per day and a repeatability of ± 1%. Minimum detectable limits are no more than 0.2% of full scale. Analyzers are typically

calibrated before each experiment. In these experiments, these analyzers provided combustion characterization information (exit oxygen content, etc.).

Table 1. Summary of on-line gas analysis systems, techniques, and ranges routinely used in the MFC.

Gas	*Technique*	*Range(s)*
CO	NDIR	0-200/1000
CO_2	NDIR	0-5/25 vol %
NO	NDIR	0-300/1500 ppm
SO_2	NDIR	0-1000/3000 ppm
O_2	magneto-pneumatic	0-5/25 vol %
THC	flame ionization	0-10/30/100/300/1k/3k/10k/30k ppm

Table 2. Summary of interferences between various gas measurements in the MFC gas analysis systems.

Gas	*Analyzed Concentration*	*Interfering Gases* CO	CO_2	NO_x	O_2	SO_2
CO	192.6			0.00E+00		0.00E+00
CO_2 dry	143800.0	0.00E+00		-4.17E-06	-3.48E-03	6.95E-06
CO_2 wet	143800.0			-6.26E-06	-3.48E-03	
NO	961.7	2.08E-04			5.20E-01	0.00E+00
SO_2	944.0	0.00E+00		0.00E+00		
NH_3	193.4			0.00E+00		5.17E-03
H_2O	9000.0 (5°C)	-4.44E-05	0	0.00E+00	0.00E+00	2.22E-04

Interferences from other gases are summarized in Table 2, all of which were measured with nitrogen as the makeup gas. The interference data indicate the fractional response of an analyzer to a gas other than the one being analyzed. The strongest interference is NO with O_2, where a 962 ppm concentration of NO is interpreted by the O_2 sensor as 500 ppm O_2. This interference arises because O_2 and NO_x are paramagnetic, with the strength of the NO and NO_2 paramagnetic susceptibility being roughly 43 and 28 % that of oxygen. Oxygen concentrations are accurately determined so long as they exceed those of NO by approximately an order of magnitude. This behavior is typical of all paramagnetic-style oxygen analyzers and is a primary reason such analyzers cannot be used to measure low oxygen concentrations precisely in combustion flows. The remaining interference ratios are two to five orders of magnitude lower and present little concern under typical combustion conditions. Entries that indicate 0.0 indicate no interference was noted. Blank entries indicate no measurements were made.

Fuel Composition

In these experiments a softwood kraft liquor was fired through an atomizing nozzle. The elemental composition of the liquor is shown in Table 3. For generating predominantly intermediate sized particles (with some fume), the liquor was fired at 33.6% solids in water. For generating only fume particles, the liquor was fired at 2% solids, 28% water, and 70% methanol. Generation of fume particles is through condensation of inorganic vapors. Methanol

increases the temperature in the combustion region (compared to water), which leads to increased vaporization of the inorganics. In addition, elemental sulphur was added to the liquor for some of the fume experiments. In full-scale boilers, fume particles (condensation aerosols) have been analyzed (Tran, 1986) and found to contain on the order of 90% sulphate and 10% carbonate salts. Carryover particles are commonly dominated by carbonate and tend to impact in the superheater rather than penetrate as far back as the generator bank. In the MFC, all of the inorganic matter passes through the reactor so there is no net removal of carbonate. Elemental sulphur is added to the liquor in sufficient quantity (86.3 mg S per gram dry black liquor) to produce alkali salts that have a sulphate to carbonate mass ratio of 9 to 1, similar to that found in recovery boiler convection passes.

Table 3. Composition of black liquor (mass %, dry basis) used in this investigation.

Element	**Mass %**	**Element**	**Mass %**
Carbon	39.4%	Chlorine	0.15%
Hydrogen	2.65%	Sodium	19.3%
Sulphur	4.2%	Potassium	2.27%
Nitrogen	0.12%	Oxygen (by difference)	31.9%

The range of experimental conditions is shown in Table 4. The dependent variables of primary interest were deposit mass and volume accumulation rate and deposit morphology. These were examined as functions of the following independent variables: (1) probe Reynolds number; (2) probe Stokes number; (3) gas temperature; (4) probe surface temperature; (5) gas-probe temperature difference; and (6) particle size distribution. Variation of deposit formation conditions over the ranges indicated in Table 4 shifted the dominant deposition mechanism widely, allowing some assessment of deposit formation rate and property development as a function of deposition mechanism. Separate discussions appear below for deposits generated from fume particles and those generated from intermediate particles.

Table 4. Ranges of experimental conditions used in this investigation.

Condition	Range
Exit gas velocity	3-5 m/s
Exit oxygen	≈4%
MFC exit dia.	15 cm
Target probe diameter	17 & 50mm
Probe Reynolds Number	425, 1200, 2770,
Exit gas temp.	575-800°C
Probe surface temp.	300-600°C
Aerosol mass concentrations:	
Fume particles	0.3 - 0.7 g/m3
Intermediate size particles	16 g/m3

Results and Discussion

Particle Size Distributions

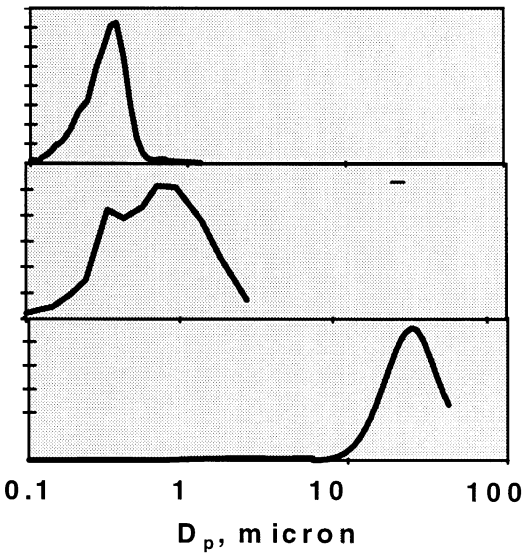

Figure 6 Typical fume, mixed, and intermediate particle size distributions generated during this investigation..

Particle size distributions were produced with mass mean diameters from 0.5 to 20 microns by varying combustion conditions, fuel blend composition and weight percent solids in the fuel. Figure 6 illustrates typical results. Size distributions were measured primarily using the aerosol spectrometer. At the large sizes (5 µm+), additional data were obtained from the PCSV instrument. The agreement between these techniques in the region of overlap was within about 15%. All data were collected immediately before the flow reached the probe.

Qualitative Deposition Observations

The macroscopic and microscopic structure of deposits offer evidence for mechanisms of formation. In the case of fume and intermediate particle deposition, these features share some common properties but differ significantly in important ways. The structures are illustrated with both photographs and scanning electron micrographs (SEMs). In all cases, the images are derived from horizontal cylindrical probes placed in the test section of the MFC. Gas flow is from top to bottom in all figures. The images in a given figure are not necessarily all taken from the same deposit, but all are representative of deposits of the given type.

Fume deposits grow slowly and accumulate somewhat preferentially on the windward side of the probe, which is toward the top in all of these images. Experiments lasting as long as 10 hours produced little more than a 400 µm deposit. Deposits appear reflective and smooth to the eye, but there is not a strong specular reflective component (Figure 7). Primary particle sizes are 100-200 nm (see length bars in images). Top two photographs illustrate portions of a cylindrical probe with (right) and without (left) fume deposit, with fume deposit scraped from the

second frame for contrast. The deposit has an apparently smooth surface that is in fact extremely irregular, comprising long, three-dimensional chains that are slightly more than a single-particle thick.

A microscopic inspection reveals a highly irregular, porous surface comprising strings of particles. The diameter of these strings only slightly exceeds that of the particles from which they are composed. The strings generally grow in a radial direction, but follow generally tortuous paths. Particles in the strings are highly sintered, with individual particle identities barely evident. Crosslinks or bridges between strings are rare. Overall porosity is approximately 80-90 percent.

Deposits from intermediate particles grow rapidly and accumulate predominately on the windward side of the probe (Figure 8). In extreme cases, deposits grow only on the leading side of the probe. Particles accumulate in the direction of the flow, as opposed to radially, in columns that are rooted on single, individual particles that impact on the surface. The columns initially branch frequently, forming dendritic structures with overall diameters many times that of the particles from which the columns are formed. The increases in diameter decrease as the columns grow and their boundaries approach each other.

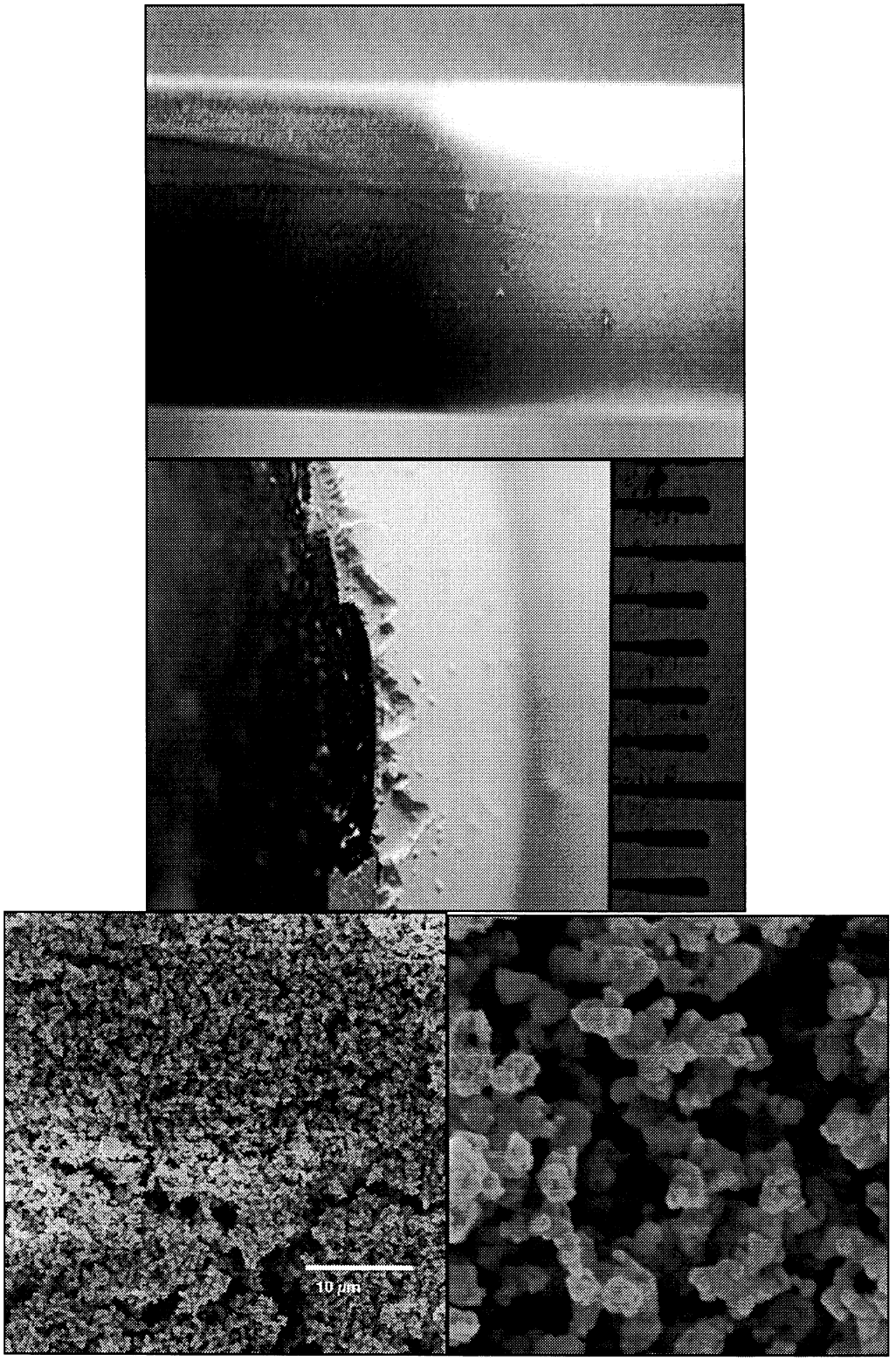

Figure 7. Photographs (top) and SEM photographs of typical fume deposits. Contrast with data from intermediate-sized particles in Figure 8.

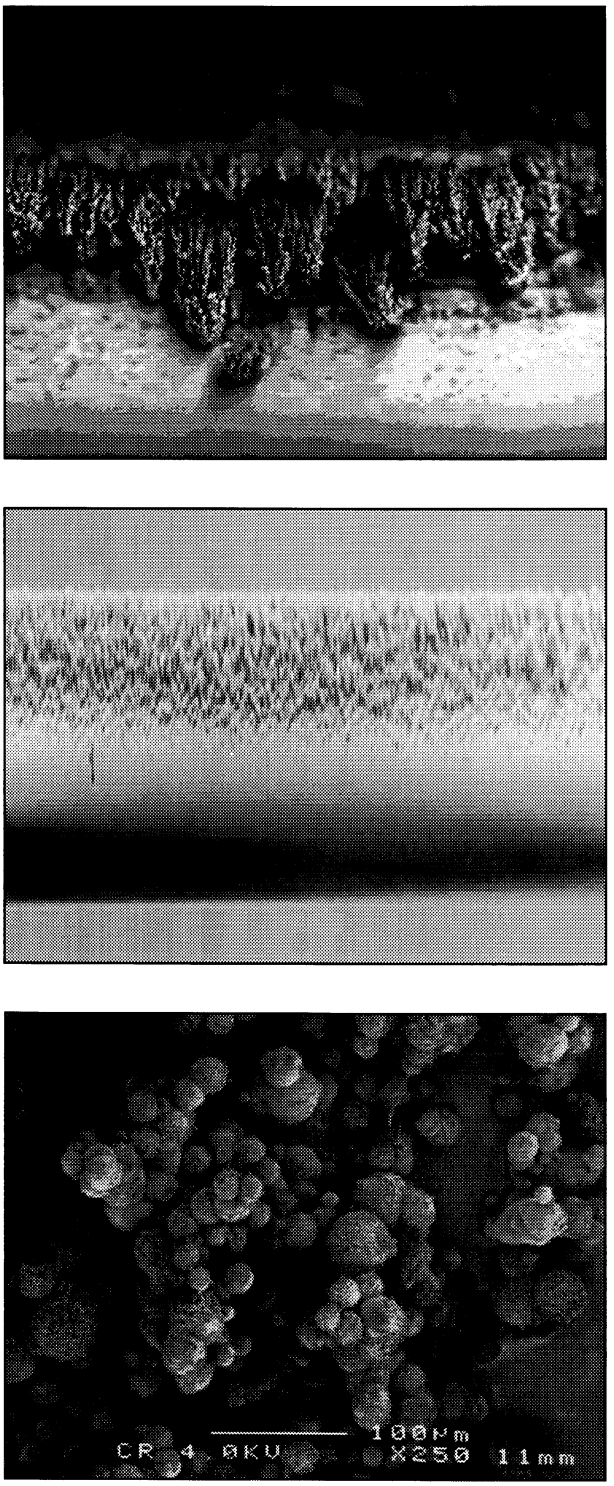

Figure 8. Photographs (top two frames) and SEM image of deposits formed from intermediate sized particles. Primary particles sizes are 10-30 µm. Deposit surface roughness is apparent in both visual and SEM images. Contrast with Figure 7.

The microscopic view of the deposit structure is consistent with this macroscopic image, with relative large particles clearly discernable in the deposit initially. Porosity is fairly high (70-85 %) and the columns have limited connectedness to one another.

The string and column structures of deposits generated from fume and intermediate particles, respectively, have similar mechanistic origin. Particles that adhere upon first impact with the deposit give rise to such structures. Any protrusion from a surface collects particles with much greater efficiency than the immediately surrounding regions. This phenomenon gives rise to the structures. If particles did not adhere upon first impact, far less structured and far more random-packed deposits would result. The intermediate particles arrive at the surface through inertial impaction, giving rise to the strong orientation into the direction of flow of the column growth. Fume particle velocities are influenced by the more random motions of individual gas molecules, giving rise to more random directions of approach to the surface and subsequent growth of tortuous, radially oriented strings. These mechanistic interpretations of the structural data find support in the quantitative data to be discussed next.

Comments from some industrial colleagues indicate that the second image in Figure 8 is the most representative of typical commercial deposits. If this is generally true, these experiments suggest that size distributions in recovery boiler convection passes include more supermicron sized particles than is sometimes believed. We cannot generated deposits with morphologies similar to those in Figure 8 without supermicron particles whose mechanisms of deposition differ fundamentally from submicron particles. Conversely, if supermicron particles can be eliminated or reduced in convection passes, deposition rates will decline sharply.

Quantitative Deposition Observations

The central focus of this work is a determination of the mechanisms determining the rate of deposit growth. Typical data for a fume deposit are illustrated in Figure 9. During this 6-hour experiment, deposit thickness increased to 350 μm, with an attendant rise in deposit surface temperature. The traditional mechanism describing deposition of submicron particles thermophoresis, a process arising from the action of gas molecules on small particles in a temperature gradient. The driving force for thermophoretic deposition scales is the gradient in particle temperature normalized by temperature ($\Delta T/T$). In these data, the deposit surface temperature is seen to be assymtotically approaching a limit slightly below the local gas temperature. It is not apparent, however, that the volumetric rate of growth of the deposit decreases at a rate corresponding to the change in driving force.

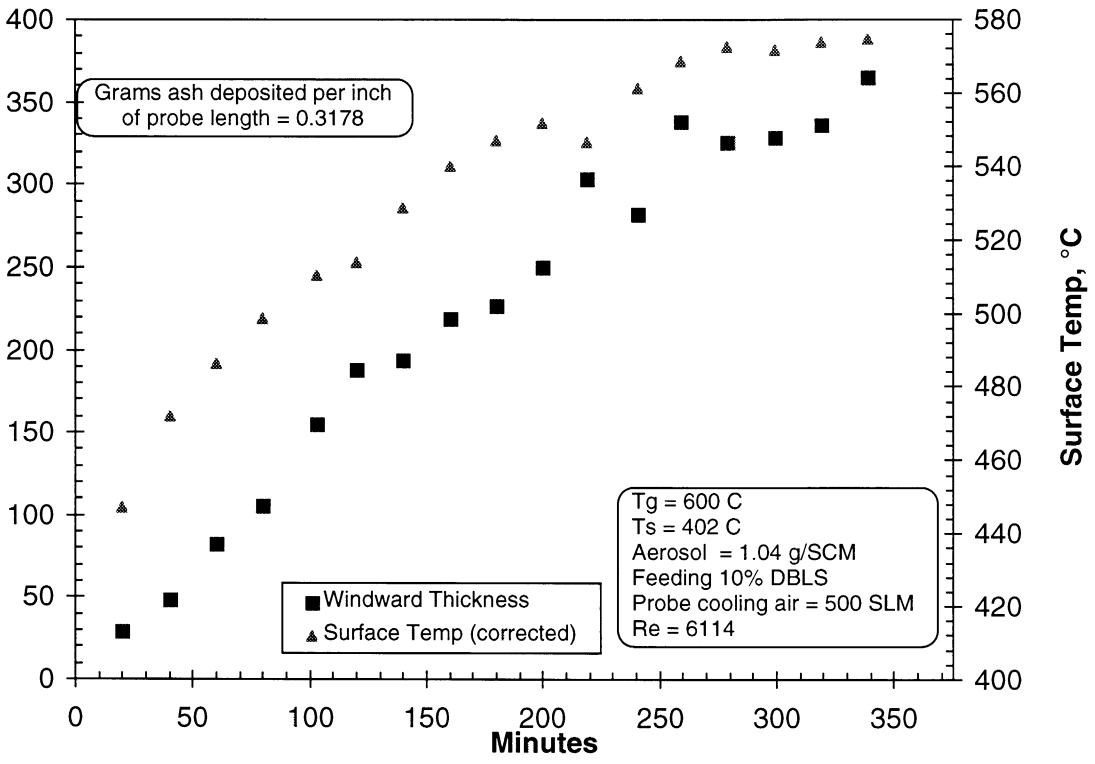

Figure 9 Volumetric rate of growth and change in surface temperature as a function of time for a typical fume deposit.

In a more definitive experiment in which the changes in deposition rate and temperature were monitored well into the region where the surface temperature has become constant, the lack of change in volumetric growth rate is confirmed. The particle size distribution (Figure 10) indicated that essentially all particle mass is less than 1 μm. The volumetric accumulation rate data are illustrated in Figure 11 with temperature data plotted in this case in the form of the thermophoretic driving force. The figure illustrates quite convincingly that the rate of accumulation is essentially unchanged even though the thermophoretic driving force changes by over a factor of five.

These and many other similar, albeit shorter term, experiments with fume data are consistent in this observation. The data are summarized in Figure 12, in which both mass and volumetric rates of deposition are plotted as a function of the initial thermophoretic driving force. The initial thermophoretic driving force is a convenient characteristic parameter as many of these experiments are relatively short term (4 hours or less). The summary plot suggests a weak correlation of rates with driving force, but the correlation is very weak and cannot be distinguished statistically from 0.

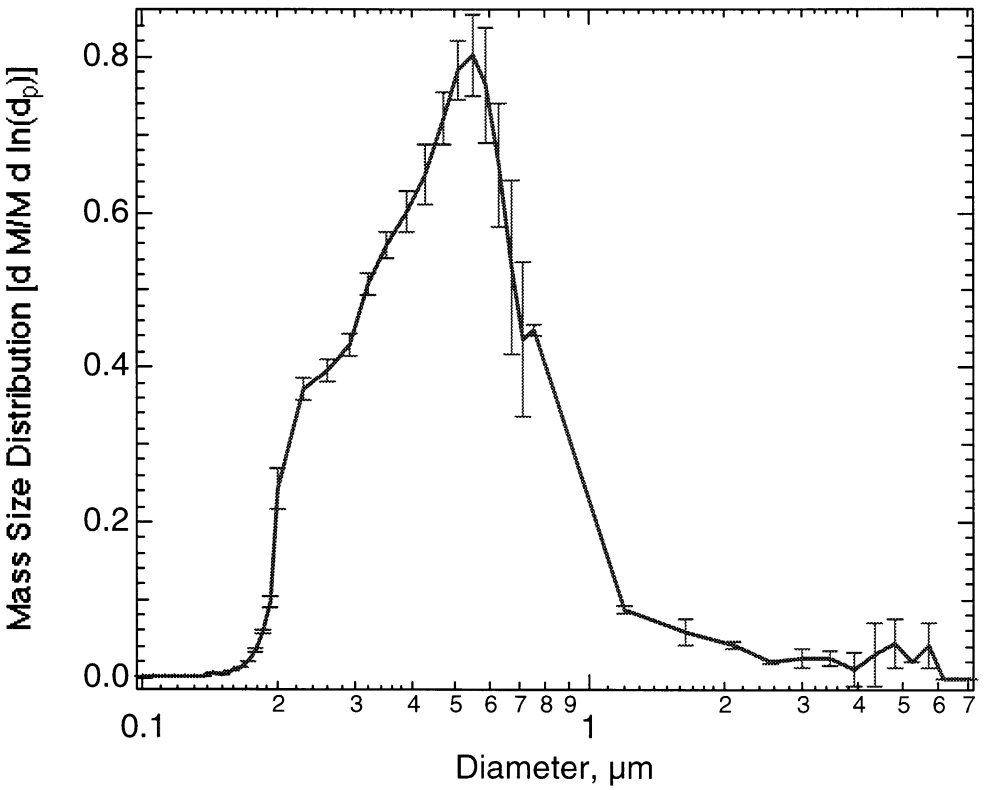

Figure 10 Particle size distribution, with ± 1.96 standard deviations (nominal 95% confidence intervals), during the accumulation of fume deposits.

It would appear that thermophoresis, at least under these conditions, has little influence on the rate of ash deposition. This unexpected result leaves an open question regarding what does control the rate, which question we are currently investigating. It is significant that, while the deposition rates do not appear to correlate with thermophoretic driving force, they are essentially linear in time over a wide range of temperatures, Reynolds numbers, and Stokes numbers.

As particle size increases, thermophoretic deposition becomes increasingly less important and inertial impaction increasingly more important. Inertial impaction rates correlate with particle Stokes number, whereas tube Reynolds number is a more appropriate scaling parameter for heat-transfer-driven processes such as thermophoresis. In our experiments, we match Stokes number under conditions where impaction should dominate and both Stokes and Reynolds numbers for fume deposition. The variation of particle impaction rate with Stokes number is illustrated in Figure 13.

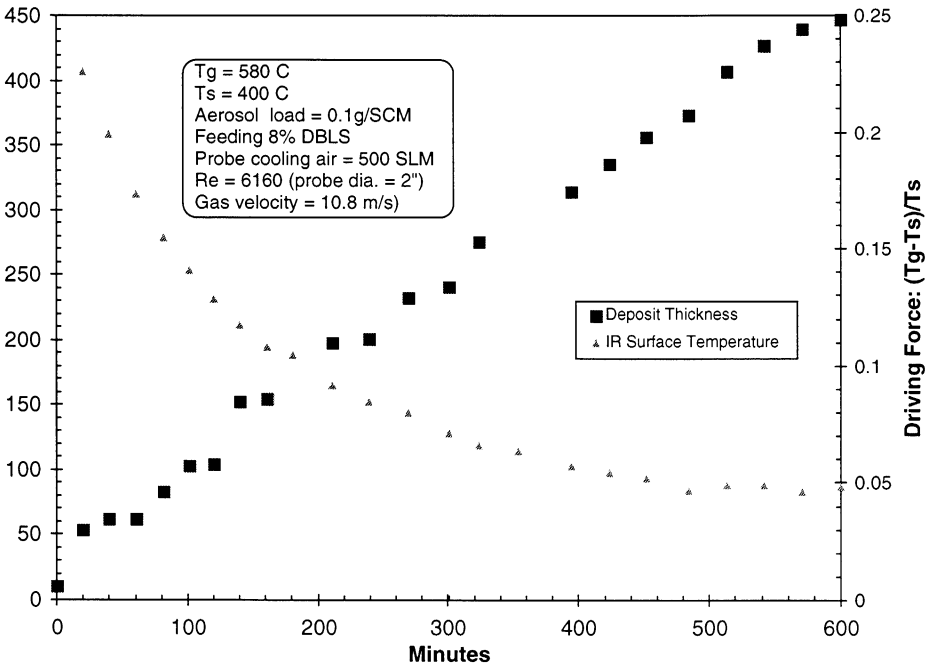

Figure 11 Volumetric rate of growth and change in surface temperature as a function of time for a typical fume deposit.

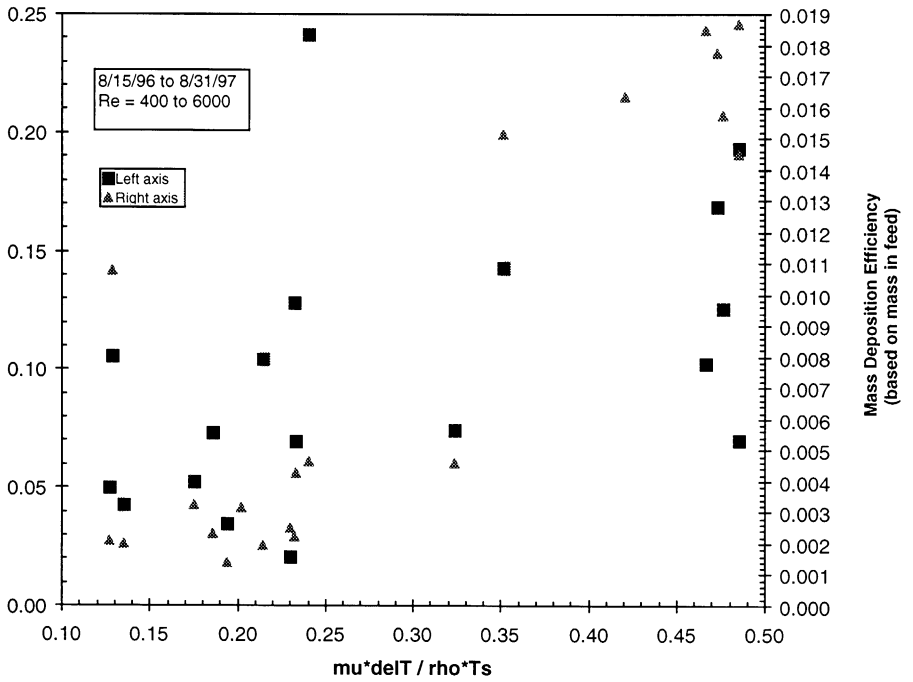

Figure 12 Summary diagram of fume deposition data as a function of initial thermophoretic driving force.

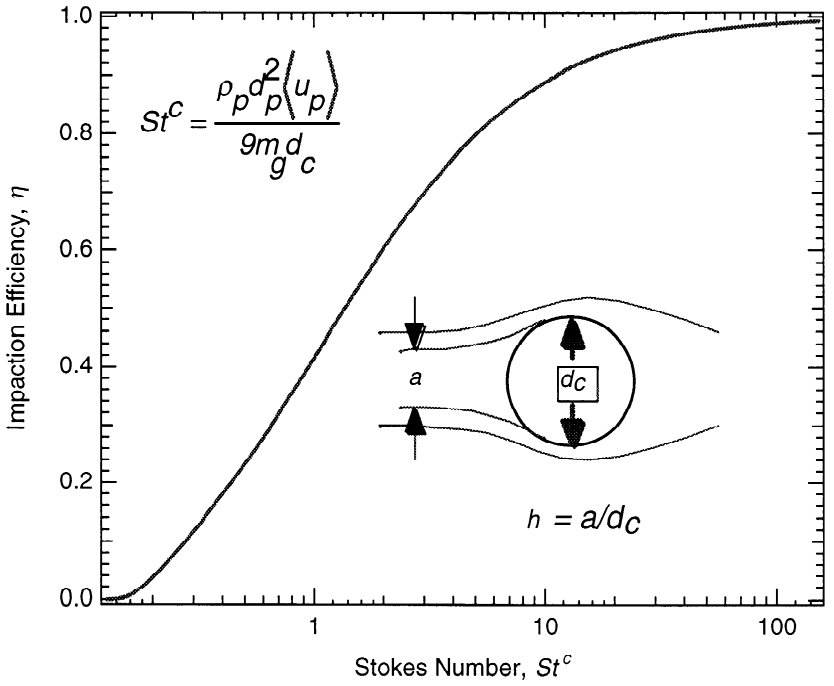

Figure 13 Particle impaction efficiency as a function of Stokes number.

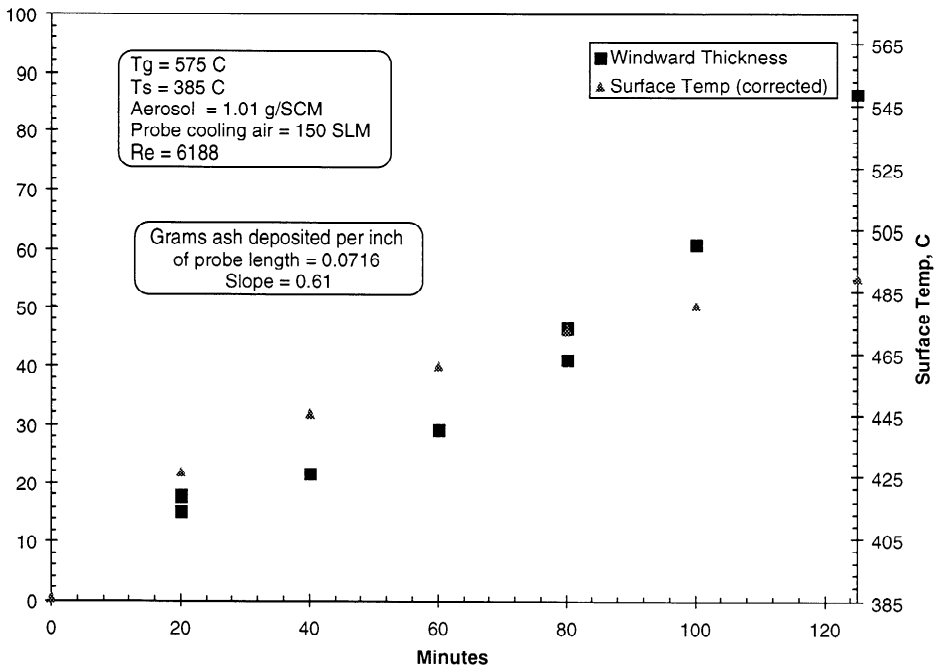

Figure 14 Volumetric deposition rate and temperature as a function of time for intermediate particles.

Experimental deposition rates with slightly larger particle size distributions, including both fume and intermediate particles, are illustrated in Figure 14 and is again seen to be constant with respect to time. As size increases, the same trends are observed. That is, particle deposition rates are constant with respect to time but increase rapidly with increasing particle size. This is consistent with theoretical expectations.

Implications to Commercial Operation

Very recent work on char bed burning[3] has shown that a significant fraction (1-9%) of the inorganic matter in burning char is released as intermediate size particles. The concentrations of these particles have also very recently been reported to be significant in kraft recovery boilers[4]. Combining these findings with the results reported here, we would expect that the concentration of intermediate particles at the generator bank entrance would be of the order of 1-10 g/Nm^3. The overall collection efficiency of these particles, based on the results in the present study, is 20-40%[5]. This suggests deposition rates of 0.3-0.4 mm/hr for a concentration of 1 g/Nm^3, with slightly higher rates expected in the superheater region than in the boiler bank.

These rates can be converted to elapsed times between water washing and plugging for a given soot-blower efficiency[6]. The results, plotted as a function of soot blower efficiency, are shown in Figure 15. They indicate that boiler operation between water washes could be as short as 10 days or as long as 6 months, depending on soot blowing efficiency, where intermediate size particles are dominant in growing recovery deposits. The times indicated in Figure 15 would be shorter for higher intermediate particle loading.

---

[3] S. H. Kochesfahani, PhD thesis, University of Toronto, in progress.
[4] P. Mikkanen, personal communication.
[5] Collection efficiency is defined here as the fraction of particles in the region swept by a heat transfer surface that actually collect on the surface.
[6] Soot-blower efficiency is defined here as the fraction of deposited material removed during each soot blowing cycle.

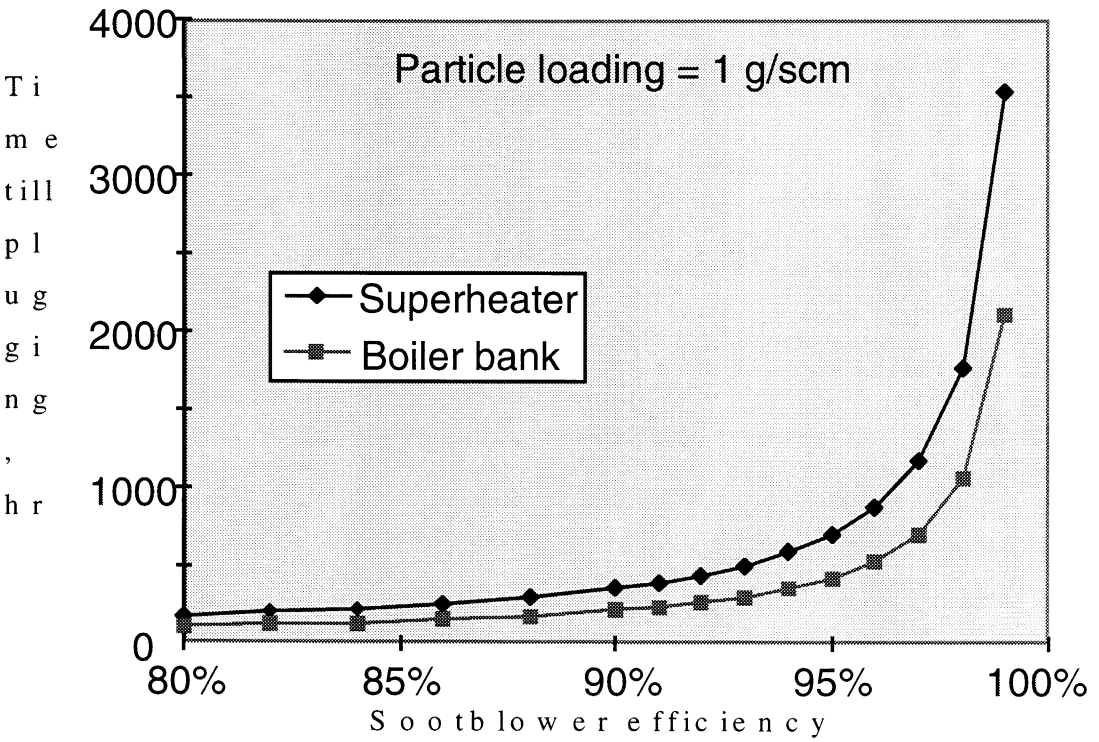

Figure 15 Estimated time for a clean recovery boiler to plug versus soot blowing efficiency for an intermediate particle loading of 1 g/Nm3.

The results obtained in this investigation on fume deposition rates indicate that thermophoresis is not likely the controlling factor in the growth of fume deposits in kraft recovery boilers. Based on the deposition rate data obtained, one can also estimate an operating time between water washing and plugging for fume deposition. For a fume loading of 20 g/Nm^3, typical deposition rates would be 3-6 mm/hr, with rates 50% higher expected in the superheater region than in the boiler bank. Operating times between water washing, calculated as for intermediate particle deposition, are plotted as a function of soot blower efficiency in Figure 16. They indicate that boiler operation between water washes could be as short as 10 days or as long as 4 months, depending on soot blowing efficiency, where fume particles are dominant in growing recovery deposits. The times indicated in Figure 16 would be shorter for higher fume loading.

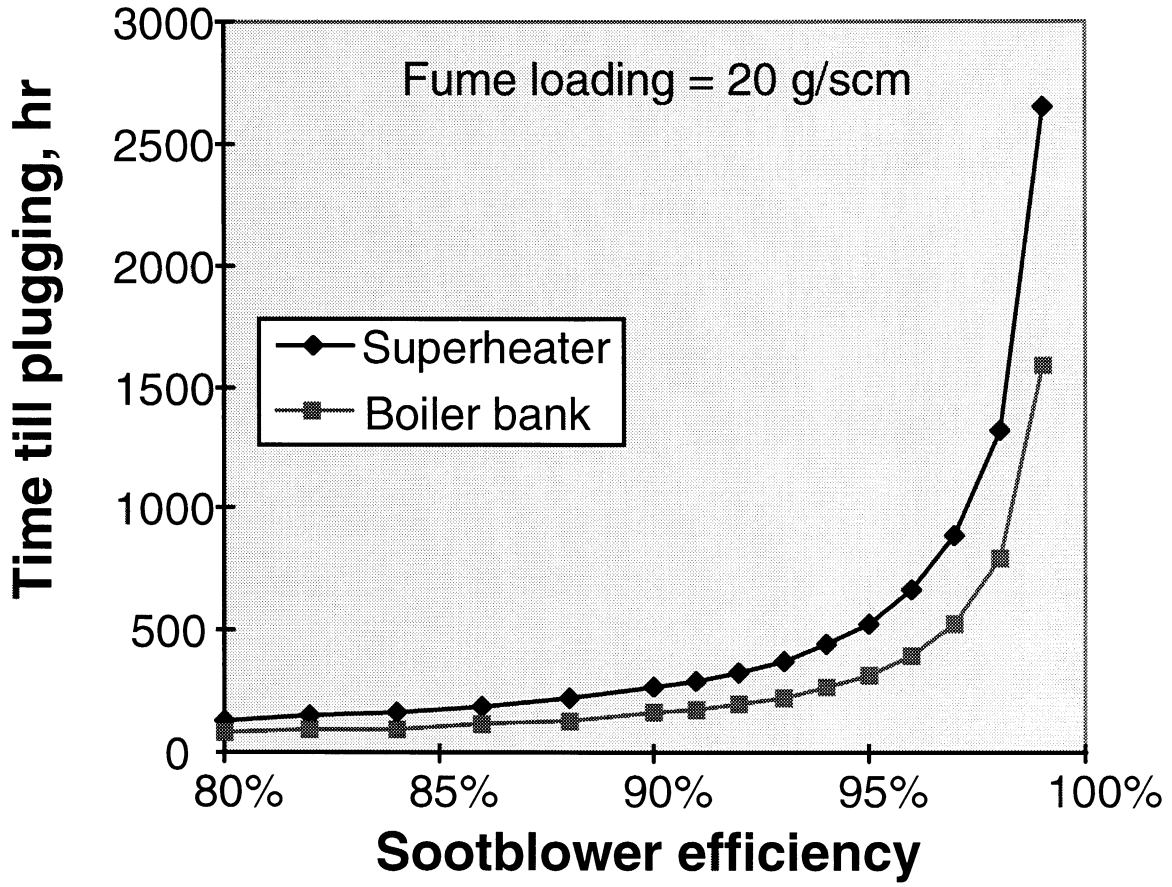

Figure 16. Estimated time for a clean recovery boiler to plug versus soot blowing efficiency for a fume loading of 20 g/Nm^3.

Conclusions

Experimental data regarding deposition of fume particles (0.01-1 μm) and intermediate particles (1-100 micron) black-liquor particles on tube surfaces are available under laboratory conditions that closely simulate the range of conditions in commercial recovery boilers. The objective in collecting these data was to determine the mechanisms and rates of particle depostion under conditions typical of a recovery boiler. Experimental conditions that were varied independently during these experiments include particle size distribution, particle loading, tube Reynolds number, tube Stokes number, gas temperature, tube temperature, and the difference between tube and gas temperature. Not a full factorial design. The dependent variables include deposit volumetric growth rate, mass growth rate, deposit morphology, deposit emissivity, and deposit surface temperature.

The six primary conclusions from this work include: (1) the fume deposition mechanism does not appear to be controlled by thermophoresis, as we had hypothesized at the beginning of the experiments; (2) fume and intermediate particles deposit at rates linear in time under a wide variety of conditions; (3) essentially all particles that strike the surface adhere to it under a wide range of conditions; (4) initial microstructures of both fume and intermediate deposits include

connected beads with few bridges between them; (5) under practical conditions, deposit strength is determined to a large extent by the connectedness of the beads and to a lesser extent on sintering of particles within the beads; and (6) the time between sootblowing can be estimated from the data and agrees reasonably well with commercial experience.

These conclusions logically fall into the three categories of mechanistic information (conclusions (1) through (3)), deposit microstructure (conclusions (4) and (5)) and practical application (conclusion (6)). The implications of the conclusions in these three categories are significant.

These data are quite definitive in illustrating that thermophoresis does not control the rate of deposition of fume particles, contrary to our initial hypothesis. We currently are pursuing hypotheses regarding the correct mechanism. While fume deposition rates do not decrease as deposit surface temperature increases, deposition rates do indicate a modest correlation with initial temperature. Given that the rates of particle arrival are not influenced by the difference in gas (particle) and deposit surface temperature, the remainder of the observations are consistent with theory. That is, the deposits grow linearly in time because essentially all particles that contact the deposit surface adhere to it immediately.

Both fume and intermediate particles generate deposit microstructures that include long, connected, strings of particles in the direction of deposit growth. Bridges between these structures perpendicular to the direction of deposit growth are rare. Intermediate sized particles grow structures that initially branch out rapidly from a single point of origin (i.e., are dendritic) and then grow with a more uniform diameter which is several times larger than the average particle diameter. Fume deposits also have chain structures, but they have diameters that are typically closer to the average particle size and little branching, or dendritic, structure. The observed linear volumetric growth rate with time suggest that deposits have not sintered appreciably on a macroscopic scale during the course of our experiment (up to 10 hours with surface temperatures approaching 600 °C). We suspect higher temperatures will lead to significant macroscopic sintering, in which separate particle chains bridge and sinter to one another. We also believe that the observed slow rates of bridging between such chain-linked structures resolves the disagreement between the slower rates of sintering observed in commercial practice compared to laboratory experiments with pressed pellets of crushed deposit materials. Individual particles in the gases exhibit high sintering rates upon colliding with the deposit, in contrast to the slow sintering rates of particle dendrites.

The observed laboratory rates of deposition can be used to estimate the time between soot blowing in practical systems. These estimates are consistent with general commercial experience.

Acknowledgements

This work was sponsored by the US DOE Office of Industrial Technology and a consortium of industries, including Mitsubishi Heavy Industries, Kvaerner Pulping, Weyerhaeuser, Ahlstrom Machinery, Babcock and Wilcox, ABB-Combustion Engineering, and International Paper. The authors are grateful for both their financial support and technical reviews of the work.

DUES-FUNDED PROJECT SUMMARY

Project Title:	Control of Non-Process Elements in Kraft Pulp Mills and Bleach Plants
Project Code:	
Project Number:	F017-04
PAC:	Chemical Recovery
Division:	Chemical Recovery and Corrosion
Project Staff	
Faculty/Senior Staff:	J. Frederick, W. Schmidl, A. Rudie
Staff:	
FY 98-99 Budget:	TBA
Allocated as Matching Funds:	$12,847
Time Allocation	
Faculty/Senior Staff:	J. Frederick (10%), W. Schmidl (35%), A. Rudie (-)
Support:	
Supporting Research	
M.S. Students:	None
Ph.D. Students:	None
External:	G. Rorrer, M. Laver, Oregon State University

RESEARCH LINE/ROADMAP: Environmental Performance. 4. Reduce water usage in Bleached Kraft Pulp production to 2500 gallons per ton.

PROJECT OBJECTIVES:

The objective is to provide the pulp and paper industry with an equilibrium calculator capable of handling accurately dissolved inorganic ions, their complexation behavior with organic matter, their adsorption on wood pulp fibers, and inorganic precipitates. The simulator should be compatible and interfaceable with the major process simulators used by the pulp and paper industry.

PROJECT BACKGROUND:

Non-process elements are becoming a major problem in both kraft pulp mills and bleach plants as water use is reduced. A limiting factor for these mills is that there is currently no way to predict accurately the level to which critical elements such as Al, Cl. Fe, K, Mg, Mn, Si, and other metals will accumulate as chemical cycles are closed more tightly. The process simulation tools available lack the capability for predicting the equilibrium distribution of these elements between inorganic ions, dissolved organometal complexes, ions adsorbed on wood pulp fibers, and inorganic precipitates.

Work in this area was begun in 1994 by IPST, and in 1996 by Oregon State University under the DOE/Agenda 2020 program. These programs were brought together when Jim Frederick moved from OSU to IPST. FY99 will be the final year of the OSU work under DOE/Agenda 2020.

SUMMARY OF RESULTS:

Data bases for the thermodynamic properties and activity coefficient parameters for the Pitzer method have been assembled. Calculations to evaluate the accuracy of predicted solubilies for sodium salts in inorganic soilutions have been completed with successful results. Calculations to evaluate the accuracy of predicted solubilies for some NPE's (Ba, Ca, Mg, Mn) in mill green and white liquors were less successful. Barium's solubility was predicted accurately, but the solubility of the other elements were off by a factor of up to several orders of magnitude. Both the sampling method and the thermodynamic and activity coefficient data are being re-evaluated.

Extensive data on the solubility of aluminum and silicon in green and white liquors have been obtained. Additional data on the impact of magnesium ion, $Ca(OH)_2$, and TiO_2 were also obtained. The crystalline aluminum- and silicon-containing species in the precipitate have been identified by x-ray diffraction analysis. Amorphous aluminum- and silicon-containing precipitate species will be identified by mass balance once chemical analysis of the precipitates have been completed.

A large amount of data has been obtained for adsorption of metal ions on wood pulp fibers. Part of this data has been obtained by Alan Rudie and Pat Bryant at IPST, and part by Greg Rorrer at Oregon State University. The effects of temperature, ion concentration, and the carboxylic and phenolic hydroxyl content on the amount of cations adsorbed on wood pulp fibers have been investigated. The experimental measurements will continue, and modeling of the adsorption behavior will begin early in FY98. Greg Rorrer will spend four months (4/99-7-/99) at IPST on this project as part of his sabbatical leave.

Work on characterizing the dissolved organic matter in black liquor and bleach plant effluent streams has been ongoing at OSU (by Murray Laver) for the past 18 months, and has also begun here at IPST (by Alan Rudie). Organic matter from black liquor and bleach plant effluents have been fractionated, and the functional groups identified. Preliminary experiments to measure the complexing capacity of dissolved organic matter have been completed. This will constitute a major part of the FY99 work.

GOALS FOR FY 98-99:

1. Measurement of stability constants for wood organics with metal ions.
2. Correlate stability constants with chemical properties of organic matter.
3. Correlate adsorption parameters with functional group content of fibers.
4. Complete the evaluation of the inorganic data base.
5. Develop an organo-metal equilibrium calculator.
6. Obtain additional data for mill liquor, bleach filtrates, and pulp streams.
7. Predict the solubility limits of metals in mill liquor and bleach filtrate streams.
8. Evaluate the estimation procedure.
9. Write final DOE report.

DELIVERABLES:

1. An equilibrium calculation software package for metal ions in bleached kraft pulp mills which includes an equilibrium solver, a thermodynamic data base for inorganic ions, and a data base for the stability constants of dissolved organic matter from bleach filtrates and spent pulping liquors with metal ions.
2. A "user's manual" that includes a set of example applications to pulp mill and bleach plant problems.

SCHEDULE:

(See following page)

ID	Task Name
1	1. Measure stability constants for wood organics with metal ions
2	2. Correlate stability const's with chem. prop's of organic matter
3	3. Correlate adsorption parameters with fiber functional groups
4	4. Complete the evaluation of the inorganic data base
5	5. Develop an organo-metal equilibrium calculator
6	6. Obtain additional data for NPE solubility in mill streams
7	7. Predict solubility limits of metals in mill streams.
8	8. Evaluate the estimation procedure.
9	9. Write final DOE Report

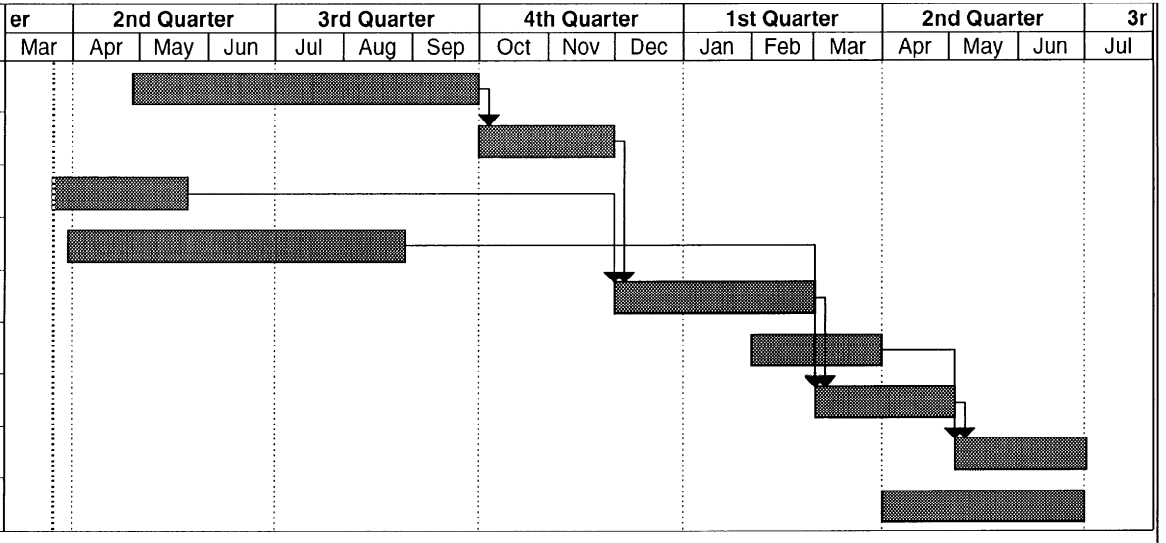

51

Project: Project1
Date: Mon 3/23/98

Task
Progress
Milestone
Summary
Rolled Up Task
Rolled Up Milestone
Rolled Up Progress

The Distribution of Non-Process Elements in Pulp Mill and Bleach Plant Process Streams. 1. Calculating Precipitation of Inorganic Species

W. J. Frederick, G. W. Schmidl, and C. P. Woitkovich
The Institute of Paper Science and Technology
500 - 10th Street NW
Atlanta, GA 30318

S. A. Sinquefield
Department of Chemical Engineering
Oregon State University
Corvallis, OR 97331

ABSTRACT

Non-process elements such as Ca, Fe, Mn, etc. can adsorb on pulp fibers, form complexes with dissolved organic matter, precipitate from solution, or remain in solution as inorganic ions. In designing purge strategies for these elements from pulp mills and bleach plants, it is important to be able to predict what their distribution will be between those adsorbed on fibers, remaining in solution as inorganic ions and ion-organic complexes, and precipitated from solution. The logical first step in developing or evaluating a calculation procedure for the distribution of non-process elements is to address the issue of prediction of precipitation of inorganic salts from solutions of ionic strengths from nearly zero to 4 or more.

In the study reported here, a chemical equilibrium estimator was used to predict the solubility of several non-process elements in green, and white liquors. Free energy data for the ionic species and precipitate phases and ion activity coefficients were calculated from data bases and an activity coefficient model included with the chemical equilibrium solver. The predicted solubilities were compared with both published solubility data for multicomponent salt systems and data from three kraft pulp mills. The agreement between the measured and predicted was generally good for both green and white liquor streams.

INTRODUCTION

With reduction in water use in kraft pulp mills, bleach plants, and paper mills, the concentrations of both inorganic and organic materials accumulate to higher concentrations than earlier encountered. This paper deals with the behavior of inorganic species that are not part of the pulping or bleaching chemicals - often referred to as non-process elements (NPE's) - in pulp mill chemical cycles. Non-process elements include elements such as aluminum, barium, calcium, chloride iron, potassium, magnesium, manganese, silicon, and other elements. Of these, potassium and chloride are very soluble and difficult to purge from aqueous pulp mill streams without special processes and equipment. The others are much less soluble in alkaline liquors or as sulfates. When they accumulate in the recovery cycle or bleach plant, they may deposit as scales on process equipment. Some interfere with process operation - for example iron and manganese decrease the efficiency of bleaching with oxygen-based agents, and magnesium and silicon can interfere with settling or filtration in green and white liquor clarification.

Management of these NPE's in kraft pulp mills and bleach plants requires the capability to predict how they split with process streams. Figure 1 shows how these elements can distribute themselves between pulp fibers, dissolved organic matter, and the solution phase. Cations can adsorb onto pulp fibers or form complexes with dissolved organic matter. Inorganic ions can precipitate as solid phases, either as scale on in suspension, or remain in solution. The amount of any given element in each of these states depends on equilibrium and perhaps rate constraints. We need to be able to predict the equilibrium distribution of non-process elements between these pulp fibers, complexes with dissolved organic matter, inorganic precipitates, and ions in solution.

Currently the capability to predict the solubility of inorganic matter in aqueous solutions far exceeds the capability to predict adsorption on pulp fibers and complexation with dissolved

organic matter. Methods for estimating the activity coefficients of inorganic ions in solution, the weak link in calculation solubilities in multicomponent inorganic solutions, were established in 1970's and 80's (e.g. 1-4). Equilibrium calculators that include data bases of thermodynamic properties of inorganic salts and ions in aqueous solution, and which include or can incorporate these activity coefficient estimators, are now readily available (e.g. 5-8). They are being used industrially in many areas.

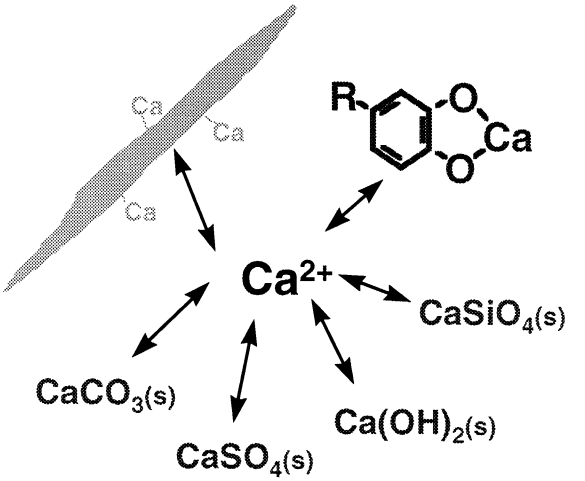

Figure 1. Possible distribution of cations in e.g. brown stock during washing as illustrated for calcium ion.

The objective of this paper is to assess the ability of equilibrium simulation for predicting the solubility of non-process elements in aqueous solutions comparable in composition and ionic strength to green and white liquors.

METHODS

Comparisons were made between experimental data and calculated solubilities of various inorganic salts. Most of the calculations were made using the Non-ideal Aqueous ELectrolyte Simulator (NAELS) developed by Sinquefield (5). NAELS was chosen because it was developed specifically for applications in the pulp and paper industry. It uses minimization of the total Gibbs free energy of the system to predict the solubility of inorganic salts in aqueous solutions. It contains a limited thermodynamic data base of inorganic salts and inorganic ions in aqueous solution, but nearly all of the ions it contains are of interest in kraft pulp mills and bleach plants. NAELS uses the Pitzer method for predicting ion activity coefficients. The Pitzer method considers the interactions of ion pairs and triplets in solution. The Pitzer method normally provides accurate estimates of ion activity coefficients to ionic strengths well above the range (5-10 molal) encountered in green and white liquors. By comparison, activity coefficient estimators based on only binary ion interactions are usually accurate only to 4-5 molal. A predecessor of NAELS, called ISIS (12), was used in one set of calculations reported here. In another, a data fitting method was employed to obtain the chemical potentials and ion interaction parameters for activity coefficient estimation (13).

Experimental data in three categories were used to evaluate the accuracy of the equilibrium simulations:

- major chemical species (sodium and potassium salts) were used to assess the accuracy of the equilibrium simulator for the major species in green and white liquors[1],
- minor chemical species (NPE's) in solutions of ionic strength and hydroxide concentrations comparable to green and white liquors were used to assess the ability of the simulator to predict the behavior of specific NPE's, and
- concentrations of NPE's in actual green and white liquors as measured in mill studies were used to assess the ability of the simulator to predict NPE solubility behavior in mill process streams.

Thermodynamic property and activity coefficient parameters available in the literature were-

[1] Since the activity coefficients of the minor species are almost entirely controlled by the concentrations of the major species and their interactions with them, it is essential that an equilibrium simulation program be able to predict accurately the solubility of the major species.

compiled by Sinquefield (5) in the NAELS data bases. They were used in the equilibrium simulations (5).

RESULTS

Major Species In Green And White Liquor

Figure 2 shows the solubility of NaCl and KCl in aqueous solutions at 25°C. The data points and curves are the solubility limit of solutions which contain various amounts of the two salts at saturation. Note that both the data and calculated curves have a break point at approximately 5.0 mol NaCl/kg water[2], 2.2 mol KCl/kg water. This point is the invariant point. To the left of it, the precipitate phase at equilibrium is KCl. To the right, it is NaCl. NAELS predicts the solubility of NaCl and KCl in water at 25°C with an accuracy acceptable for many process applications.

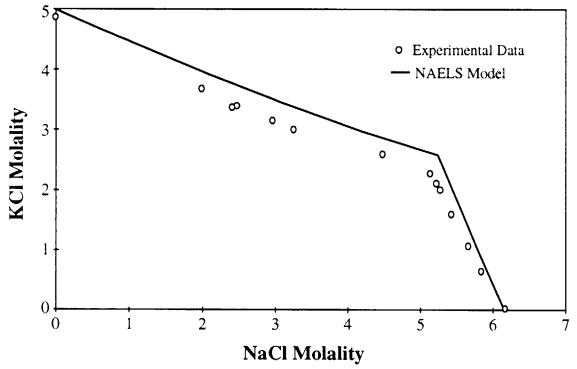

Figure 2. Solubility behavior for the system NaCl - KCl - water at 25°C. Data are from Linke and Seidell (11).

Figure 3 shows the solubility behavior of sodium sulfate and sodium carbonate in equilibrium with their decahydrates at 25°C. The solubility behavior of this system is unusual in that the equilibrium sulfate concentration first decreases slightly, then rises slightly, and finally drops steeply as the sodium carbonate concentration is increased. The abrupt drop in Na_2SO_4 solubility is challenging to predict. The NAELS equilibrium simulator predicts well the shape of the solubility curve. The actual solubility data deviate from the predicted curve by at most 0.25 mol/kg water along both branches of the data. The greatest deviation occurs at the invariant point where NAELS predicts too high a sulfate concentration by 0.2 mole/kg water and too high a carbonate concentration by 0.25 mol/kg water. As with the NaCl - KCl system. The equilibrium predictions are sufficiently accurate for many industrial applications

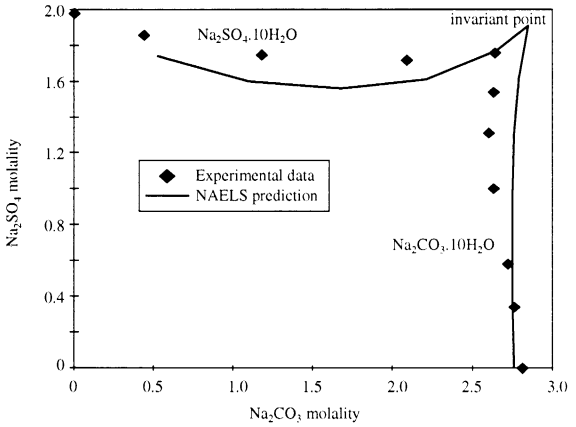

Figure 3. Solubility behavior for the system Na_2SO_4 - Na_2CO_3 - water at 25°C. Data are from Linke and Seidell (11).

When more accurate predictions of solubility are needed and accurate solubility data are available, a data fitting method can be employed to obtain the chemical potentials and ion interaction parameters for activity coefficient estimation (13). Figure 4 compares solubility data for the system Na_2SO_4-Na_2CO_3-NaOH-water at 100°C with calculated values based on the chemical potential and ion activity coefficient parameters extracted (13) from experimental data (10) for this system at 100°C. This system is of interest because it describes the precipitation of burkeite[3] from aqueous sodium salt solutions. It can been used in most cases to represent green and white liquor where the solubilities of minor species (NPE's) are determined by the

[2] Unless otherwise noted, all concentrations are expressed as mass or moles per kg water.

[3] Burkeite is a double salt, $2Na_2SO_4 \bullet Na_2CO_3$ which has a unique crystalline structure and is not simply a physical mixture of Na_2SO_4 and Na_2CO_3.

solubility of their carbonates, sulfates, or hydroxides. The region of interest for kraft pulp mills is the shaded region in the left side of the graph.

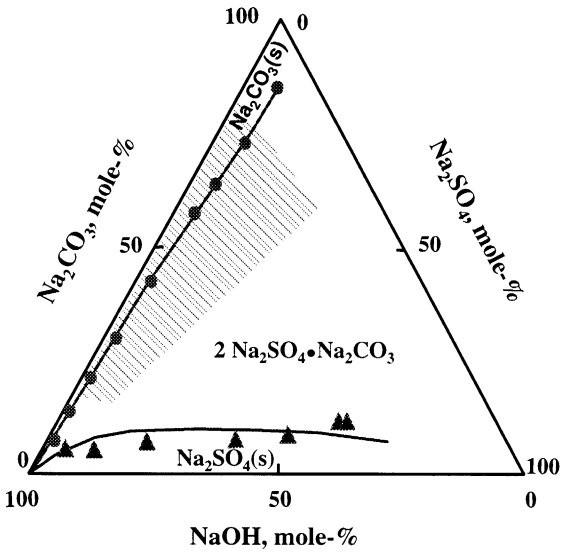

Figure 4. Ternary diagram for the distribution of the solid (precipitate) phases in equilibrium with aqueous solutions of Na_2SO_4-Na_2CO_3-NaOH. Data are from Green and Frattali (10). The solid lines were calculated by Kim (13).

The data plotted in Figure 4 are as the invariant lines which divide the regions where Na_2CO_3 or burkeite, and Na_2SO_4 or burkeite are the solid (precipitated) phases in equilibrium with the aqueous solution. The predictions agree well with the experimentally determined invariant lines for both Na_2CO_3-burkeite and Na_2SO_4-burkeite.

The solubility behavior of this three salt system is more difficult to predict than that of Na_2SO_4 - Na_2CO_3 - water at 25°C for two reasons. First, there are more ions involved, and second, both sulfate and carbonate can combine with sodium or hydrogen ions to form monovalent anions (e.g. $NaSO_4^-$, HSO_4^-). As illustrated here, the data fitting approach often results in more accurate predictions of solubility behavior in more complex systems.

Non-Process Elements In Moderate To High Ionic Strength Media

Comparisons of data and predictions for aqueous solutions that contain non-process elements of interest and more than one salt are limited by the availability of reliable experimental data.

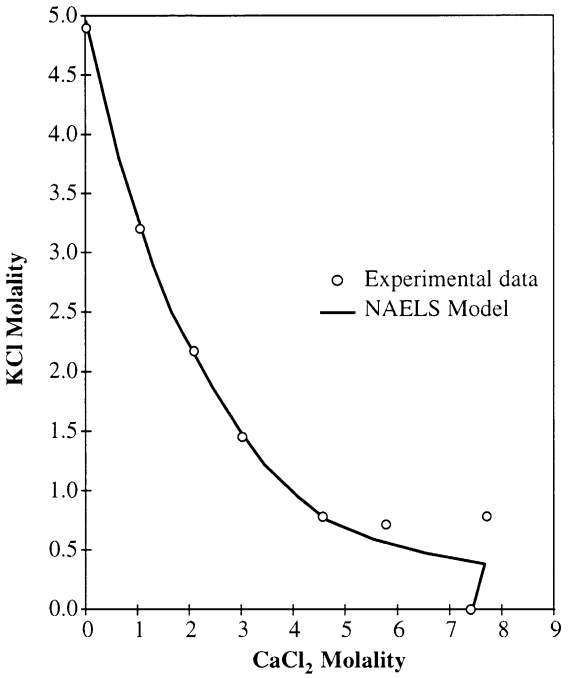

Figure 5. Solubility characteristics of the system $CaCl_2$-KCl - water at 25°C. The data points are from Linke and Seidell (11).

Figure 5 compares the predicted and measured solubility for the system $CaCl_2$-KCl-water at 25°C. The NAELS equilibrium simulator predicts the data very accurately up to a $CaCl_2$ molality of 4.6. At higher $CaCl_2$ molalities, it underestimates the KCl solubility by up to a factor of 2, but it does predict the $CaCl_2$ concentration at the invariant point within 0.3 molal units.

Figure 6 shows the predicted solubility limit for the system $MgCl_2$-$CaCl_2$ - water at 25°C. This system is complicated because there are three invariant points along the solubility curve and therefore three different solid phases can precipitate. The invariant points as predicted by the NAELS equilibrium simulator are shown as stars in Figure 6. NAELS predicts both the solu-

bility limit and the invariant points quite well for this system.

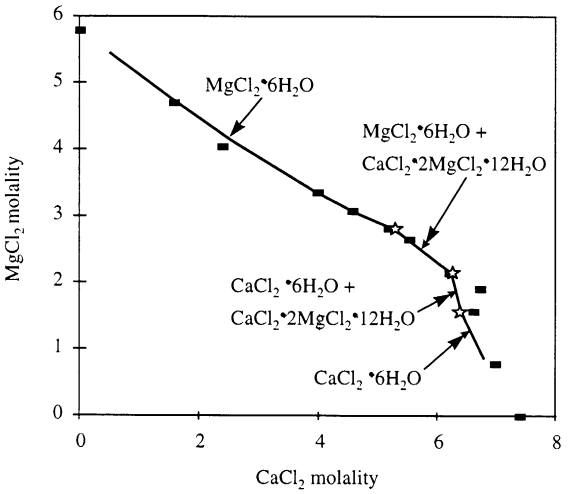

Figure 6. Solubility curve and data for the system $MgCl_2$ - $CaCl_2$ - water at 25°C. The data points are from Linke and Seidell (11) while the solid curve was calculated using NAELS. The stars represent invariant points calculated with NAELS.

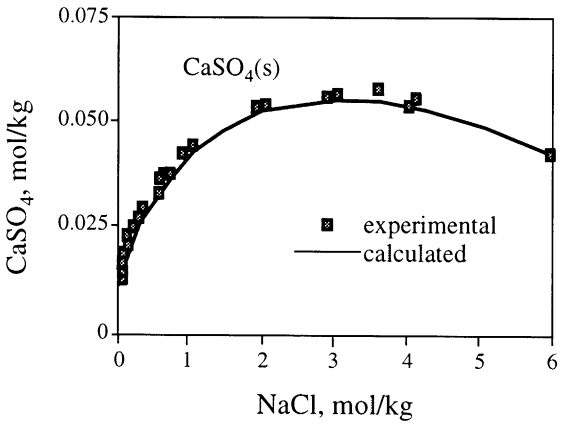

Figure 7. Solubility of $CaSO_4$ in NaCl solutions at 25°C. From (12).

Figure 7 compares experimental solubility data for $CaSO_4$ in aqueous NaCl solutions with predicted solubilities. The predicted values were calculated using a precursor to NAELS which used the same activity coefficient estimation method (Pitzer's) and a similar free energy data base. The solubility of $CaSO_4$ in NaCl solutions, which is two orders of magnitude lower than that of other systems modeled in this study, is predicted very accurately by this method. This result supports the concept that non-process element concentrations at saturation can be predicted accurately even though they may be several orders of magnitude lower in concentration than the sodium salts present in green or white liquor.

Mill Data

Calculated solubilities of barium, calcium, magnesium, and manganese were compared with measured concentrations of these elements in clarified green and white liquors from three kraft pulp mills. The clarified green and white liquors data are averages of six samples collected at regular time intervals under steady operation They were analyzed by ICP for total concentrations of metals without further removal of suspended solids, and the suspended solids were also measured. The experimental results, shown in Table 2, were the total element contents of the clarified green and white liquors before suspended solids removal, minus the contribution of metals in the suspended solids. The corrections were made by assuming that the dregs or lime mud solids and the suspended solids had the same composition. Except for the calcium results, these corrections were minor.

Table 1. Concentrations of sodium and potassium salts in the simulated clarified green and white liquors.

Species[a]	g/L as Na_2O	g/L as species
Green Liquor		
NaOH	15	19
Na_2S	40	50
Na_2CO_3	120	205
Na_2SO_4	15	34
White liquor		
NaOH	108	140
Na_2S	40	50
Na_2CO_3	27	46
Na_2SO_4	15	34

[a]2.5 atom-% of the cations associated with these species were potassium.

The calculated solubilities in Table 2 are for 95°C solutions. The concentrations of sodium and potassium salts in the clarified green liquor used in the calculations were as shown in Table 1.

The amounts of Ba, Ca, Mg, and Mn included in the equilibrium simulation were 0.1 g $BaCO_3$/kg water, 0.5 g $CaCO_3$/kg water, 0.2 g $MgCO_3$/kg water, and 0.2 g $MnCO_3$/kg water.

For green liquor, NAELS predicted the following precipitate phases for the four NPE's. In green liquor they were $BaCO_3$, $CaCO_3$, $Mg(OH)_2$, and $Mn(OH)_2$. In white liquor, they were $BaSO_4$, $CaCO_3/Ca(OH)_2$, $Mg(OH)_2$, and $Mn(OH)_2$.

The measured and predicted equilibrium concentrations for these NPE's are compared in Table 2. The predicted barium concentrations agree reasonably with the experimental data. The predicted calcium concentrations are low by a factor of 2-20. The measured magnesium and manganese concentrations are much higher than the predicted ion concentrations. There are two factors that may account for this. One is that the suspended solids in the clarified green and white liquors may have had a different composition than the dregs or lime mud solids. This is known to be the case for free lime suspended in white liquor, and was likely the case for magnesium. The other factor is the formation of metal hydroxide cations (e.g. $MgOH^+$). These cations, which form at high alkalinity, can increase the total dissolved Ca, Mg, or Mn in solution.

CONCLUSIONS

The NAELS equilibrium simulator generally predicted well the solubilities of sodium and potassium salts in aqueous solutions.

Comparison of predicted versus measured solubilities of various non-process elements in solutions that contained more than one salt were difficult to perform because of the lack of reliable, readily available solubility data for such systems. For those compared, the NAELS equilibrium simulator predicted reasonable results.

The NAELS equilibrium simulator predicted the solubility of barium in clarified green and white liquors with good accuracy and the solubility of calcium within a factor of 20, but way underpredicted the solubilities of magnesium and manganese. The differences may have occurred because the liquors contained suspended solids which contained significant amounts of calcium and magnesium, or possibly because of the formation of metal hydroxide cations.

ACKNOWLEDGMENTS

Much of this work was part of the M.S. thesis of Scott A. Sinquefield. Partial support for him was provided by a consortium of the following companies: Associated Pulp and Paper Manufacturers (Australia), International Paper Company, Mead Corporation, Union Camp Corporation, Westvaco Corporation, and Weyerhaeuser Company.

The data on concentrations of non-process elements in clarified green liquor were obtained by Patrick S. Bryant as part of his research at IPST.

REFERENCES

1. Bromley, L.A., 1973, *AIChE J.*, 19:313.
2. Meissner, H.P., 1980, "Prediction of activity coefficients of strong electrolytes in aqueous systems" in *Thermodynamics of Aqueous Systems With Industrial Applications*, ACS Symp. Ser. 133, p. 496.
3. Pitzer, K.S., *Activity Coefficients in Electrolyte Solutions*, Vol. 1, CRC Press, Boca Raton, Florida, (1979) p. 157.
4. Chen, C-C., Britt, H.I., Boston, J.F., Evans, L.B., *AIChE J.*, 25(5):820-831 (1979) and 26(5)::877 (1980).
5. Sinquefield, S. A., M.S. Thesis, Oregon State University, 1991.
6. Outokumpu Research Oy, *HSC Chemistry for Windows*, User's Guide Version 2.0, May 31, 1994.

7. OLI Systems, Inc. *OLI Software Manual.* Morris Plains, NJ: OLI Systems, Inc., January, 1996.

8. Eriksson, G., Hack, K., 1990, "ChemSage - a computer program for the calculation of complex chemical equilibria," *Met. Trans. B.* 21B, 1013-1023.

9. Grace, T.M., 1976, "Solubility limits in black liquors," *AIChE Symp. Ser.* 72(157):73-82.

10. Green, S., Frattali, J., 1946, *J. Am. Chem. Soc.*, 68:1789-84.

11. Linke, W.F., Seidell, A., *Solubilities of Inorganic and Metal-Organic Compounds*, Am. Chem. Soc., Washington, D.C., Vol. I (1958), Vol. II (1965).

12. Kelly, B., Frederick, W.J., "An equilibrium model for trace element solubility in aqueous inorganic solutions," in *Applications of Chemical Engineering Principles in the Forest Products and Industries*, F. Kayahan and B. Krieger-Brockett, editors. AIChE Forest Products Division Symposium Series, vol. 1, 1986.

13. Kim, H.C. "A study of chemical equilibria for strong electrolytes in aqueous inorganic solutions," M.S. project report, Oregon State University, Department of Chemical Engineering, June 5, 1987.

Table 2. Predicted and measured concentrations of various non-process elements in clarified green and white liquor.

Analyte	Suspended solids-free liquor[a]			Simulated green or white liquor
	Liquor A	Liquor B	Liquor C	
Green Liquor				
Total solids, %	19.7	20.3	21.0	20.0
Ba, mg/kg	1.5	1.6	2.9	1.3
Ca, mg/kg	15	21	17	1.1
Mg, mg/kg	1.9	5.5	5.8	$3x10^{-4}$
Mn, mg/kg	2.5	1.6	3.1	$7x10^{-4}$
White Liquor				
Total solids, %	17.3	18.0	19.5	19.0
Ba, mg/kg	0.8	0.3	0.5	1.4
Ca, mg/kg	85	9.7	21	4.8
Mg, mg/kg	1.7	2.9	2.1	$3x10^{-6}$
Mn, mg/kg	2.0	1.8	3.1	$2x10^{-5}$

[a]Corrected for the amount of each element in the suspended solids by assuming that the suspended solids had the same elemental composition as the dregs solids. The amounts of suspended solids were 69, 127, and 260 mg/kg water respectively for green liquors A, B, and C. For the white liquors, they were 298. 407, and 201 mg/kg water respectively.

THE SOLUBILITY OF ALUMINOSILICATES IN KRAFT GREEN AND WHITE LIQUORS

P. N. Wannenmacher
Department of Chemical Engineering
Oregon State University
Corvallis, OR 97331, USA

Wm. James Frederick
The Institute of Paper Science and Technology
Atlanta, GA 30318, USA

K.A. Hendrickson
Weyerhaeuser Company
Springfield, OR, USA

K.L. Holman
Weyerhaeuser Company
Tacoma, WA, USA

ABSTRACT

A consequence of "closed" kraft mill operation is the risk of aluminum and silicon build-up in the process recovery cycles. As the Al and Si concentrations increase, the management of the black liquor evaporators and the lime cycle become more difficult. This paper presents the results of 2-day "equilibrium" solubility tests for Al and Si in unclarified kraft mill green and white liquors. The results show that efficient green liquor dregs removal can reduce the Al and Si concentrations to relatively low values. These concentrations can be reduced further by the addition of magnesium compound such as $MgSO_4$.

INTRODUCTION

The deposition of aluminosilicates in black liquor evaporators has become an increasingly important problem as water use is reduced in kraft pulp mills [1&2]. Aluminum and silicon species are more soluble in alkaline pulping liquors than are most other non-process elements. The dominant natural purge point for aluminum and silicon from the recovery cycle is the green liquor dregs. However, because they are often more soluble in white liquor, they are likely to accumulate in white liquor due to ineffective green liquor dregs removal and dissolution of aluminum and silicon from make-up lime. Removal of aluminum and/or silicon by addition of magnesium to green liquor has been evaluated but never commercialized.

The objective of this work is to (1) show what the solubility levels of aluminum and silicon in green and white liquors are, and (2) define strategies for effective removal of aluminum and silicon from the liquor cycles of kraft pulp mills.

EXPERIMENTAL

Aluminum and silicon equilibrium experiments were conducted using unclarified kraft mill green and white liquors as the starting solutions. The liquors were then augmented with various amounts of aluminum and silicon ($AlCl_3 \bullet 6H_2O$ and $Na_2SiO_3 \bullet 9H_2O$) to achieve the desired starting concentrations. An additional 0-2000ppm of aluminum and silicon were added to the original mill liquors. In addition to varying the aluminum and silicon concentrations, various amounts of CaO, TiO_2 and $MgSO_4$ were also added to test their effectiveness for removing aluminum and silicon from the liquors. A series of experiments were also conducted to check what effect high potassium concentrations would have on the equilibrium values. The majority of the experiments were conducted for a 48-hour equilibration time[1]. The equilibrium runs were conducted using 500ml sealed polypropylene sample bottles, placed in an air heated orbital shaker controlled at 95°C and 180–200RPM. Extreme care was taken to keep the liquors at the initial mill withdrawal temperature (~95°C) throughout all stages of each experiment - from mill withdrawal time through final sample preparation. Final equilibrated samples were hot vacuum filtered through a 10μm/2μm filter paper "sandwich" using all plastic labware. Prior to filtrate ICP and AA analysis, the sample

[1] We denote the total dissolved aluminum and silicon content as [Al] and [Si] respectively. The total dissolved aluminum and silicon content after equilibration is indicated by $[Al]_{eq}$ and $[Si]_{eq}$ respectively.

solutions were microwave acid digested with concentrated nitric acid to mitigate precipitate and gel formation.

EXPERIMENTAL RESULTS

Aluminosilicate Solubility in Green Liquor

Figure 1 shows the change in concentrations of [Al] and [Si] with time in green liquor for three different initial aluminum and silicon concentrations. Note that the corresponding [Al] and [Si] pair have the same dashed line type. An inverse concentration effect can be seen in the data - if there is a high [Si] there is a corresponding low [Al] and vice versa. The Al and Si concentrations continue to change with time up to 48 hours (when the experiments were stopped). It can be seen that for very high initial Al and Si concentrations that the 24-hour values are still higher than the 48 hour values. However, for initial Al and Si concentrations, below 400ppm, it appears that the 24 and 48 hour data are approaching and close to a true equilibrium point. Some data "variability" can be seen in this and subsequent graphs of the experimental data. At this point it is difficult to discern whether this variability is due to different "favored" compound formation or whether this is a manifestation of some type of interaction/blocking associated with the analysis instrumentation (reanalyzing individual samples routinely gave acceptable reproducibility). It was hoped that the X-ray analysis of the precipitates would clarify this annoyance, prior to the deadline of this manuscript, but at this point the cause is still illusive.

Figure 2 shows the same data as Figure 1, only re-plotted as [Al] vs. [Si], with the addition of all the 2-day "equilibrium" data. The initial concentrations of this 2-day data are not shown for figure clarity, since many different initial concentrations were tested. When all the 2-day data is plotted a stretched Z shape can be seen. This would suggest the formation (precipitation) of possibly three different species of Al-Si compounds. At the time of the writing of this paper no such trends could be ascertained from the X-ray analysis of the filtered precipitates. The most prevalent minerals found in these runs were $CaCO_3$ (calcite - as would be expected in unclarified green liquor), $Na_6Ca_2Al_6Si_6O_{24}(CO_3)_2 \bullet 2H_2O$ (cancrinite), and $Na_6Al_6Si_6O_{24}$ type zeolite compounds.

The data seem to "find" their equilibrium values in an arch-like projection. A rough estimate of a final 2-day "equilibrium" can be found by starting at the 5,000, 5,000ppm point on Figure 2 and drawing a line from that starting point through the anticipated initial concentration, until the line crosses the 2-day equilibrium data points.

The addition of various concentrations of CaO, TiO_2 and K_2CO_3 were tested. The results from all of these tests showed no significant deviation from the $[Al]_{eq}$ and $[Si]_{eq}$ values plotted in Figure 2.

Aluminosilicate Solubility in White Liquor

The relationship between $[Al]_{eq}$ and $[Si]_{eq}$ in a mill white liquor is shown in Figure 3. Data for fresh as well as re-burned lime are presented, although the differences in behavior don't seem to be substantial. Again the initial concentrations are excluded from the graph for figure clarity. A bend can be seen in this data at [Al]~300ppm, but again, as with the green liquor no such trends could be ascertained from the X-ray analysis results of the filtered precipitates. The mineral species of interest are $Na_8Al_6Si_6O_{24}\text{-}X \bullet nH_2O$ type compounds, where X is (SO_4) for (vishnevite) and $(NO_2)_2$ for one of the zeolite structures. The major constituent of the solid phase was $CaCO_3$ (calcite), as would be expected since unclarified white liquor was used as the starting solution. The white liquor $[Al]_{eq}$ and $[Si]_{eq}$ concentration can also be roughly estimated much like the green liquor, however the "pivot point" is 5,000(Al) and 20,000(Si) rather than the 5,000, 5,000 point that was used on the green liquor plot.

Effect of Magnesium Ion on Aluminosilicate Solubility in Green and White Liquors

Magnesium ion has been reported to reduce the solubility of aluminum in green liquor [3]. Figure 4 shows that for the same green liquor to which $MgSO_4$ as well as aluminum and silicon salts were added simultaneously, $[Al]_{eq}$ and $[Si]_{eq}$ were both reduced. For $[Al]_{eq}$ above 100ppm, $[Al]_{eq}$ and $[Si]_{eq}$ are decreased by about a factor of two by $MgSO_4$ addition. However, for $[Al]_{eq}$ below 100ppm, $[Al]_{eq}$ was decreased somewhat more, depending on the amount of magnesium added. At the highest magnesium addition level, 5:1 (Mg:Si), $[Si]_{eq}$ was nearly independent of $[Al]_{eq}$. Adding even small amounts of magnesium ion (1:5 Mg:Si) had a smoothing-linearizing effect on the Z shape shown in Figure 2, although there was no notable change in the $[Al]_{eq}$ and $[Si]_{eq}$ concentrations. For magnesium ion concentrations equal to [Si] a slight deviation from the 2 day equilibrium values can be seen at high

[Si] and low [Al]. The same effect was observed when $MgCO_3$-$Mg(OH)_2$ was added instead of $MgSO_4$. Preliminary analysis of the X-ray diffraction data on the magnesium fortified green liquor data shows a few instances of $Mg_6Al_2(OH)_{18}\bullet 4H_2O$ (meixnerite) and zeolite formation, but not in enough quantities to explain the removal of the aluminum and silicon from the solution. A possible explanation is that an amorphous compound was formed which the X-ray diffraction will not identify. Chemical analysis of the precipitate phases is under way to determine if there may have been other compounds that were not identified by the X-ray diffraction analyses.

Figure 5 shows how the amount of magnesium addition effects the final $[Al]_{eq}$ and $[Si]_{eq}$ values for a 2-day run. The two extreme right diamonds are the starting Al-Si concentrations. The first column in the graph legend is for the high [Al] starting point (1000ppm) – likewise the second column is for the low [Al] starting point (120ppm). It can be seen that for low magnesium addition the equilibrium values are approximately the same as for when no magnesium is added, however as the Mg:Si ratio increases above 1:1 the equilibrium values swing down and to the left until, as seen in Figure 4, the $[Si]_{eq}$ is no longer a function of $[Al]_{eq}$.

White liquor experiments with magnesium addition were conducted only with the 1:1 (Mg:Si) ratio. This data gave the same type of characteristics as is shown in the green liquor plots.

STRATEGIES FOR EFFECTIVE ALUMINUM AND SILICON REMOVAL

Addition of magnesium sulfate or carbonate to green liquor can be effective in removing both aluminum and silicon from green liquor. Addition at a 5:1 ratio of Mg to Si (atoms Mg/atoms Si) in raw green liquor can reduce silicon levels by a factor of 10 (from 500 to 50ppm) and aluminum levels by a factor of 20 (from 40 to 2ppm) when compared to clarified green liquor concentrations without magnesium addition. The process works well at 95°C and normal green liquor pH. There is no need to reduce temperature or for carbonation of the green liquor.

Gel formation was only encountered for extreme initial concentrations of Si (>3,000ppm). The 2-day equilibrium values for [Si] corresponded directly with the amounts of Al and Mg added to the solution. For an initial [Al] of ~1,800ppm and Mg ion addition equal to the [Si] (~3,300ppm), the 2-day $[Al]_{eq}$=100ppm and $[Si]_{eq}$=17ppm. The comparable run with only 280ppm Al and no Mg gave $[Al]_{eq}$=19ppm and $[Si]_{eq}$=2,200ppm – severe gel formation occurred on this run.

The solubility of aluminum and silicon is greater in white liquor than in green liquor, especially in the higher [Si], lower [Al] region.

CONCLUSIONS

Aluminum and silicon can be removed effectively from green liquor by precipitation with magnesium salts and efficient dregs removal. For typical kraft mills, [Si] in the clarified green liquor can be reduced to less than 100ppm. [Al] can be reduced to at least 100ppm and perhaps below 10ppm depending on the ratio of Al/Si in the smelt entering the dissolving tank.

Dregs carry-over will result in unnecessarily higher [Al] and [Si] in white liquor.

Aluminum and silicon are readily extracted from lime. Use of a low aluminum and silicon content lime is especially important in minimizing the content of these elements in white and black liquors.

ACKNOWLEDGEMENTS

The Weyerhaeuser Company through an AARC grant provided partial support for this work and one of the authors (Wannenmacher). The efforts of David Rothbard and IPST are gratefully acknowledged for the SEM and X-ray analysis of the precipitate samples.

REFERENCES

1. Ulmgren, P., "The Removal of Aluminium from the Recovery System of a Closed Kraft Pulp Mill" Proc. 1985 Int'l. Chem. Recovery Conf., TAPPI Press, Atlanta, p. 299.

2. Theliander, H., "Si and Al Inputs and behaviour in the Recovery Cycle" Proc. 1996 Minimum Effluent Mills Symposium, TAPPI Press, Atlanta, p. 295.

3. Ulmgren, P., "Non-Process Elements in a Bleached Kraft Pulp Mill with Increased System Closure" Proc. 1996 Minimum Effluent Mills Symposium, TAPPI Press, Atlanta, p. 17.

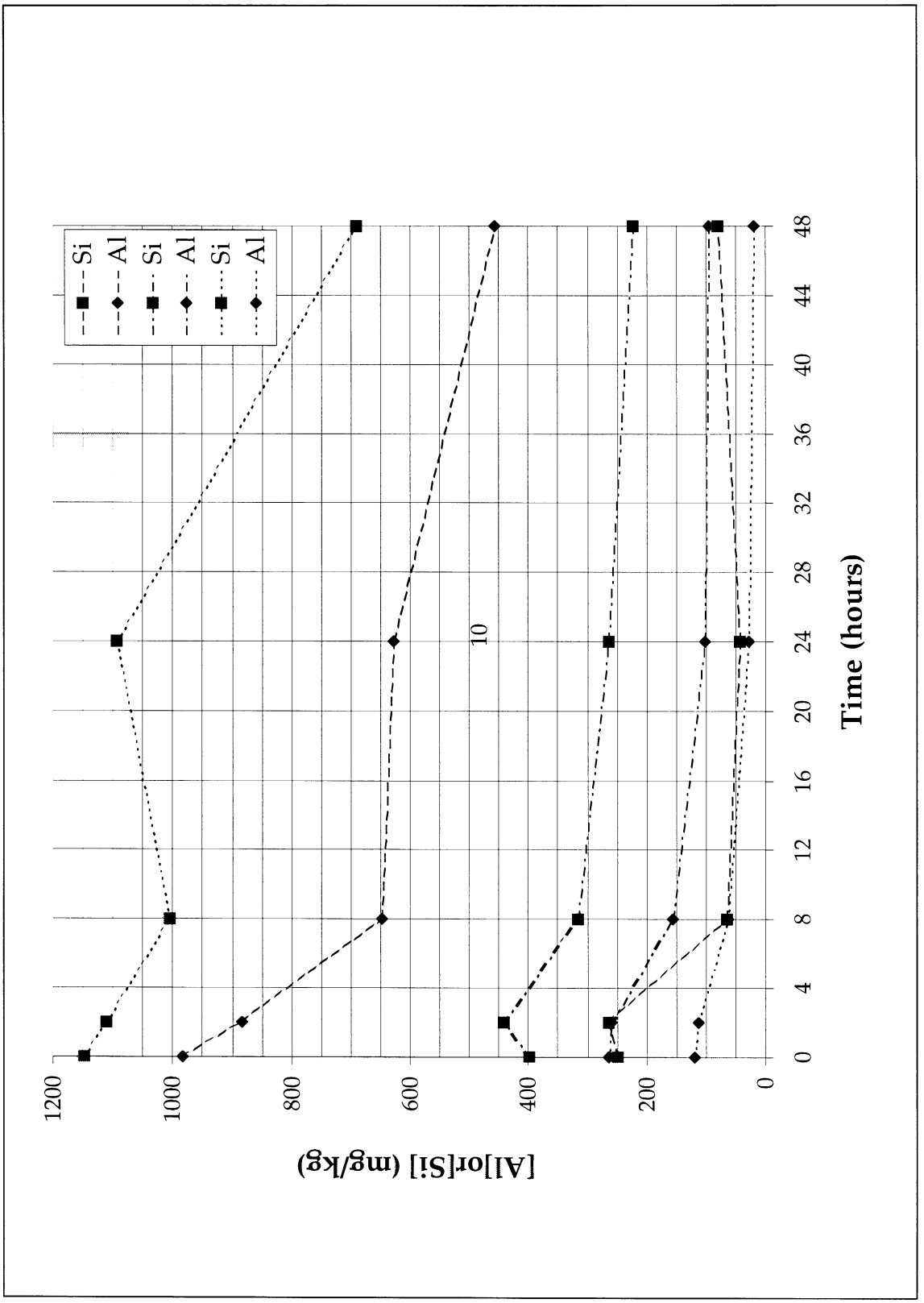

Figure 1. Aluminum and silicon concentrations versus time for three different addition levels of aluminum and silicon. Data are at 95°C.

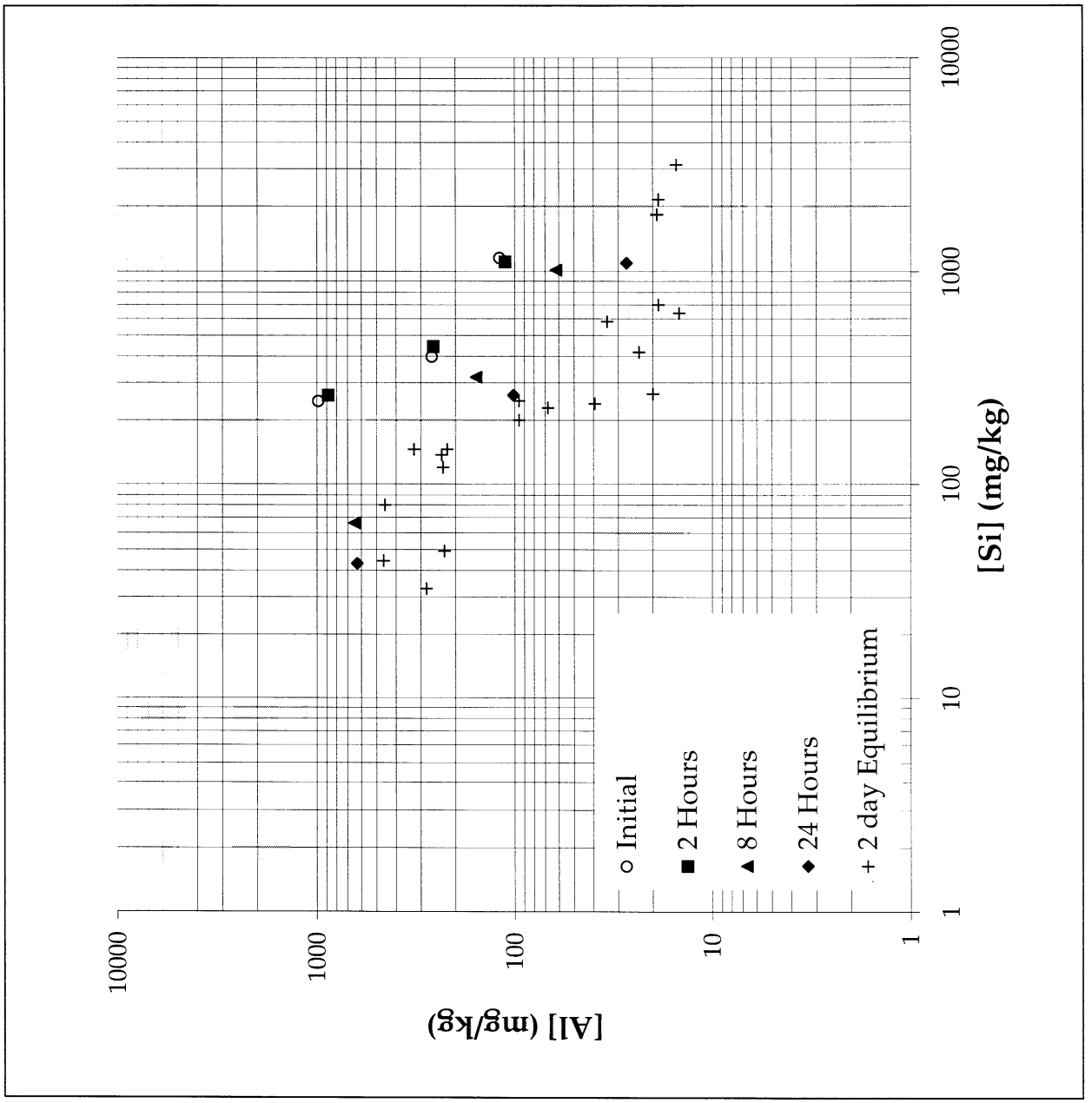

Figure 2. The approach to equilibrium for aluminum and silicon in green liquor at 95°C.

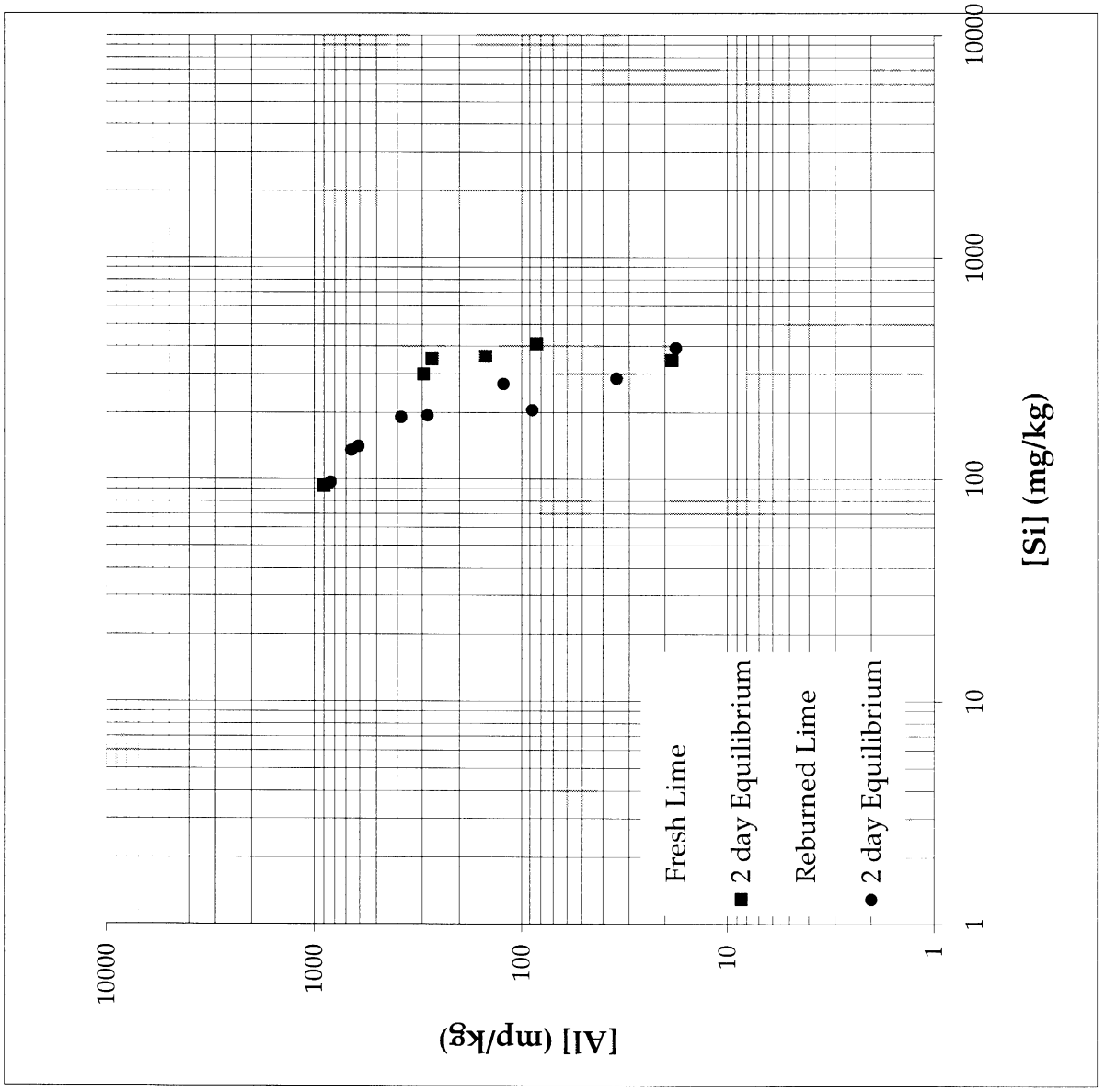

Figure 3. The solubility of aluminum and silicon in white liquor at 95°C.

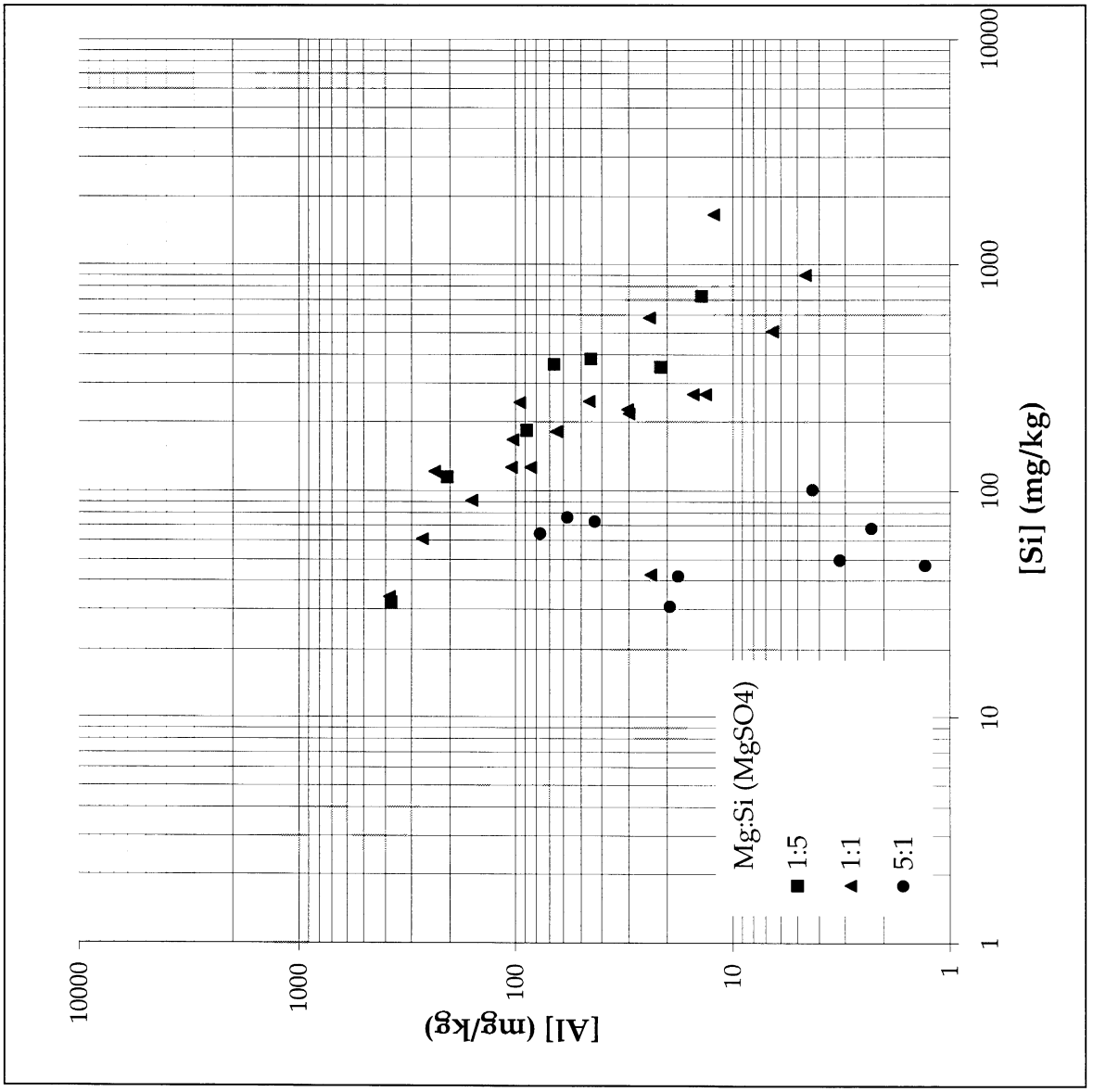

Figure 4. Effect of magnesium addition to green liquor on [Al]eq and [Si]eq over a wide range of starting conditions; 90°C.

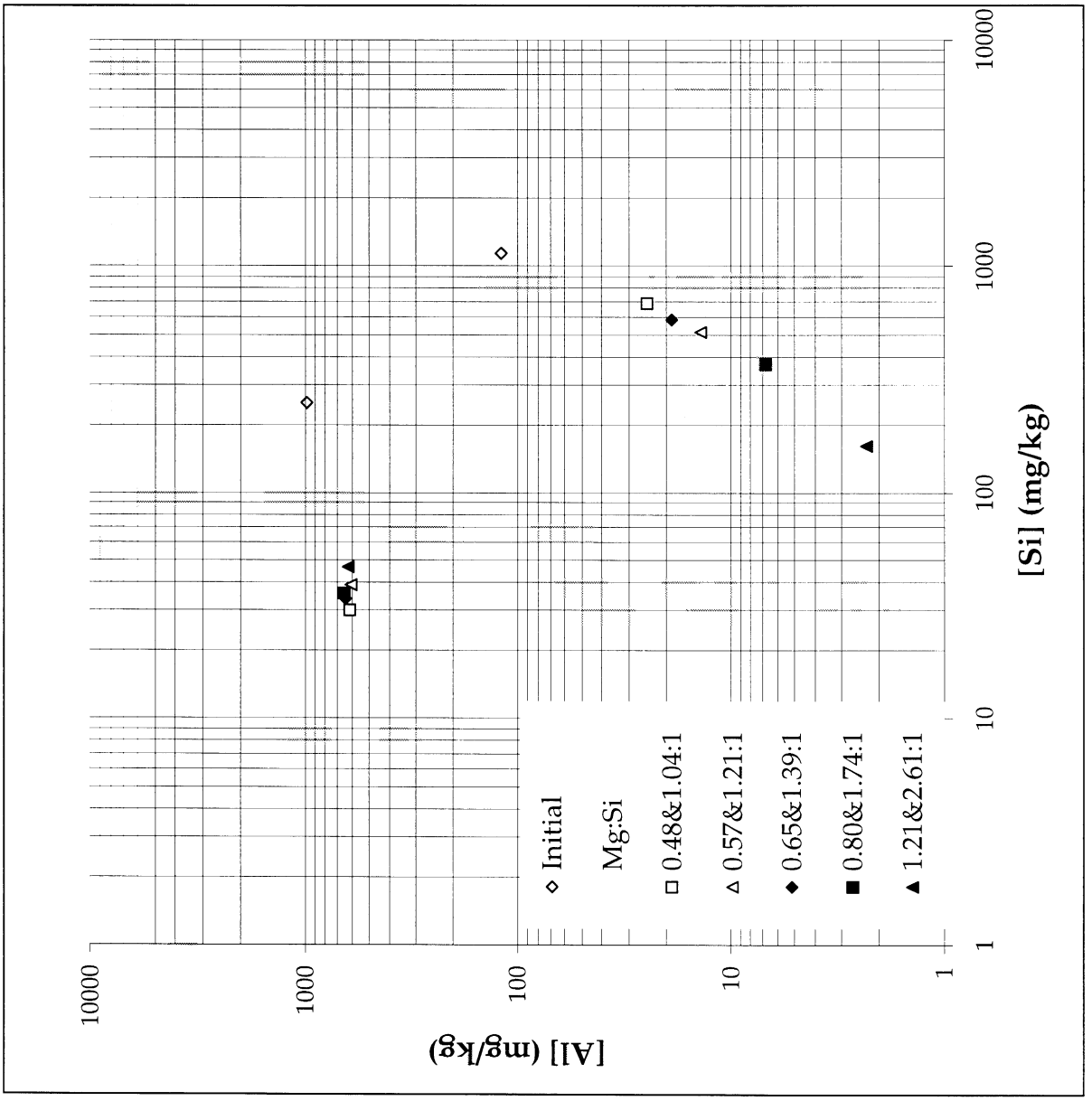

Figure 5. Effect of magnesium to silicon ratios on $[Al]_{eq}$ and $[Si]_{eq}$ in green liquor for two initial Al and Si charges; 90°C.

DUES-FUNDED PROJECT SUMMARY

Project Title:	Closed Mill Salt Recovery
Project Code:	
Project Number:	F01706
PAC:	Recovery
Division:	Chemical Recovery and Corrosion
Project Staff	
Faculty/Senior Staff:	P. Pfromm
Staff:	H.-J. Rapp (post-doc, until 6-98), D. Taylor (Senior Technician)
FY 98-99 Budget:	July 97 to June 98: Cumul. Budget $166,000 Allocated as Matching Funds (Salary+Fringe+ Overhead P. Pfromm): F01702 VOC Control, Agenda 2020: $8423 (7-97 to 6-98); F01703 Elimination of the Calcium Cycle, Agenda 2020: $20,236 (7-97 to 6-98)
Time Allocation	
Faculty/Senior Staff:	P. Pfromm: 35%
Support:	H.-J. Rapp: 100%, D. Taylor: 75%
Supporting Research	
M.S. Students:	D. Englehart
Ph.D. Students:	E. Watkins
External:	None

RESEARCH LINE/ROADMAP: Environmental Performance 4. Reduce Water Usage in Bleached Kraft Pulp production to 2500 gallons per ton.

PROJECT OBJECTIVE:

Evaluation of selective removal of chloride and potassium from low-effluent kraft pulping by electrodialysis of dissolved electrostatic precipitator catch (ESP catch) is the purpose of this project. Concentrations in the liquor streams can then be controlled to avoid corrosion and recovery boiler plugging.

PROJECT BACKGROUND:

RAC recommended area I, as of 11-16-1994, "Minimize the Environmental Impact"

Subgoal: Develop separation technologies for Non Process Elements (NPE's).

Subtask d: Eliminate unwanted chlorine compounds (no end-of-pipe).

The removal of chloride from the kraft pulping operation is necessary due to the negative impact of increased chloride concentrations on recovery boiler operation (sticky deposits), and corrosion. One method of chloride control is to discard large amounts of the ESP catch. On the other hand, if the chloride could be removed selectively, the ESP catch could be recycled, resulting in a direct payback due to savings in chemical makeup. In addition, the inorganics discharged to waste treatment and to the environment would be very significantly reduced.

Currently, crystallization of an ESP catch slurry is being tested by Champion International for chloride and potassium control. The simplicity of the membrane process proposed here, in addition to ease of operation and low energy demand are the motivation to explore this technology.

The chloride purge stream from crystallization will contain organics. That is not the case for electrodialysis, where all organics are recycled with the saltcake to the recovery boiler, and a purely inorganic salt solution is discharged.

The total chloride removal capacity from the ESP catch by any technique may not be sufficient for some bleach plant closure schemes. If proven feasible for actual ESP catch in presence of organics, electrodialysis for chloride control could be used in the bleach plant. This is not directly possible for evaporation/crystallization.

Benefits

The benefits of selective chloride removal from the ESP catch by electrodialysis are:

- Reduced chemical makeup (direct payback)
- Reduced environmental impact
- Reduced washing frequency for the recovery boiler (increased productivity)
- Reduced corrosion

The advantages of electrodialysis vs. alternative processes (evaporation/crystallization, ion exchange) are:

- Continuous process
- No organics entrained in the chloride purge
- No regeneration chemicals needed
- Simple startup/shutdown
- Chloride removal rate is easily adjusted
- Low energy requirements
- Low space requirements

SUMMARY OF RESULTS:

Goals for 1997/98, per PAC Report by P. Pfromm, Spring 1997, versus current status:

1) Complete pilot test and evaluation. DONE
2) Clarify all liability/insurance issues. DONE, February 1997:
3) Install membranes (H.-J. Rapp in Plainfield, IL)., February/March 1997 DONE
4) Ship unit by truck to host mill., March 1997 DONE
5) Install, modify unit as needed. March/April 1997 DONE
6) Start pilot test runs. April 1997 DONE
7) Ship unit back to U.S. Filter HPD. Fall 1997 DONE, Winter 97 (delay due to extended tests).
8) Evaluate runs, update full scale design. DONE, see Member Report 3 on this project, issued October 1997..
9) Issue member report on pilot runs. DONE, see Member Report 3.
10) Publish laboratory data with Asahi membranes. DONE, submitted to Journal of Membrane Science, January 1998.

11) Detailed laboratory runs on Na/K selectivity. Confirm K/Na selectivity for monovalent selective Asahi membranes.
IN PROGRESS, delayed due to emphasis on pilot test.
12) Investigate alternative membranes for Na/K separation (immobilized crown ethers, surface modification of existing membranes).
IN PROGRESS, literature research, cooperation with N. Vadat, Tuskeegee, A. Ragauskas, IPST
13) Add high charge density/high molecular weight cationic polymer to surface of standard membranes, test K/Na selectivity. Involve chemist for membrane polymer modification using K selective organics.
IN PROGRESS, proposal with A. Ragauskas in preparation.

Goals for 1997/98, per PAC Recommendations/Feedback after Spring meeting 1997:

1) Continue field trials. DONE
2) Develop head-to-head cost comparison...SEE BELOW

Recommendations/Feedback after Fall meeting 1997:

1) Complete field trials and cost comparison with the crystallizer process.
IN PROGRESS, Field trials complete, cost comparison under way with the help of US Filter/HPD, G. Delaney
2) Pending final outcome...finding a supplier....commercialize.
IN PROGRESS, US Filter/HPD would be the natural source.
Alternatively, capital cost for full scale ED equipment from the manufacturer Asahi is being evaluated. Concept: IPST sizes stack based on mill material analysis. Mill purchases ED stack&power supply, and builds the peripheral equipment (3 pumps+tanks, flowmeters, slurry tank, transfer lines+pumps). IPST facilitates (startup, training etc.).

Please see IPST Member Report, Project F017, Report 3, issued October 8, 1997. Copies have been mailed to PAC members before the Spring 1998 meeting. Copies are also available at the PAC meeting, or contact P. Pfromm, 404-894-5305 to receive a copy.

Summary of recent results, beyond Member Report 3:

Post mortem of pilot scale system after field trial

The system was shut down and shipped back to US Filter/HPD's laboratories in Plainfield, IL. H.-J. Rapp disassembled the electrodialysis stack (remove membranes). No damage was visible, except for a small cut in one of the membranes facing an electrode chamber. Since the hydrostatic pressure in all hydraulic circuits was kept constant, no large leaks are caused by such a small failure of one of the membranes. In the future special NAFION membranes should be used at the electrodes, for their mechanical and chemical stability when compared to standard membranes.

Issues of pre-filtration, additional non-process element removal

The feed (ESP dust solution) coming from the ESP dust slurry tank was pre-filtered for the initial portion of the pilot test (10 micron cartridge filter). For the final part, all pre-filtration was

removed and raw ESP dust solution was treated successfully without deterioration of the stack performance for about 150 hours of run time (Figure 1).

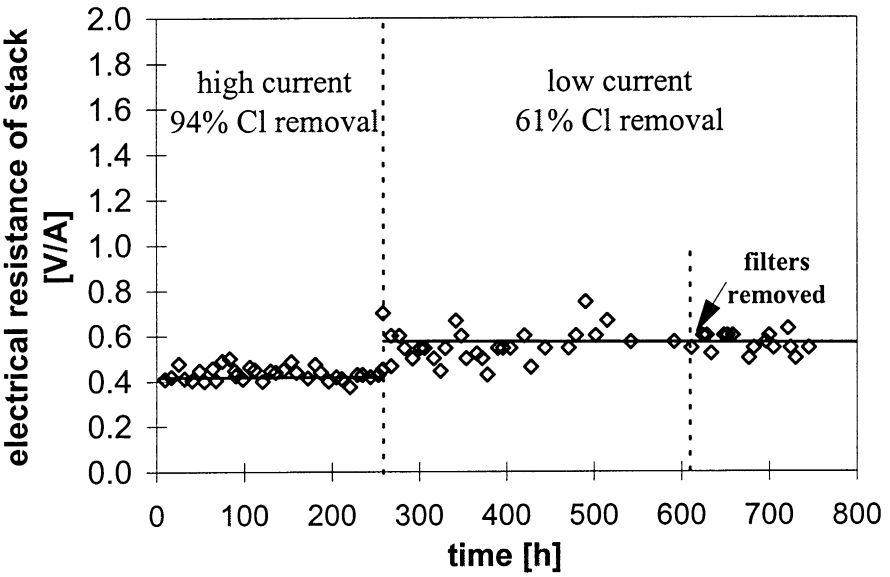

Figure 1: Electrodialysis Stack performance, entire pilot test. No deterioration is detected when the pre-filter is removed.

The sludge removed by the pre-filters contains significant amounts of non-process elements (see Table 1). The calcium content is high, as could be expected due to low solubility of calcium compounds. On the order of 50 kilograms per day of this sludge would be removed from the recovery cycle for a 1000 ton per day mill with chloride removal (assumed 500 kilograms chloride removed per day) by electrodialysis. This could be seen as a small additional benefit of NPE removal.

Aqueous soluble metals in ashed solid residue	**Insoluble** metals in ashed solid residue
sodium: 31.7%	sodium: 2.2%
calcium: 0.2%	calcium: 23.6%
potassium: 6.7%	potassium: 0.2%
manganese: 293 ppm	manganese: 8.1%
zinc: 81 ppm	zinc: 5.0%
magnesium: 50 ppm	magnesium: 3.1%
iron: 34 ppm	iron: 2.3%
aluminum: 606 ppm	aluminum: 1.5%

Table 5. Soluble and insoluble metals in ashed filter residue (filter residue of raw ESP dust slurry filtered through 10 micron cartridge filters).

GOALS FOR FY 98-99 (June 1998 to May 1999):

Personnel:
Post-doc H.-J. Rapp will leave the project in June 1998. Personnel requested here is 35% P. H. Pfromm, 75% A. Taylor. The following is a plan for laboratory and tech transfer work:

Objective A: Technology transfer, electrodialysis of ESP dust
A1. Continue work with US Filter/HPD for full scale application
A2. Address recycling of sulfate rich solution.
A3. Further pilot scale tests if financial support from a host mill is supplied (lease/transport unit, on site support, support for analytical services). IPST's membranes would be used.

Objective B: K/Na selective membrane separation:
B1. Run K/Na sulfate mixture with conventional membranes to obtain baseline for K/Na selectivity.
B2. Run composite anion/cation exchange membrane to quantify improvement of K/Na selectivity (anion exchange membrane as a size/charge selective "filter" for cations)
B3. Consider new chemistries for K selective membranes (with A. Ragauskas)
B4. Test new chemistry initially as resin.

Objective C: Ion exchange for combined chloride/potassium removal from green liquor.
Previous work: MS student D. Englehart is completing study on selective potassium removal from green liquor with commercial ion exchange resins.
C1. Literature update
C2. Select commercial anion exchange resin.
C3. Bench-scale tests

DELIVERABLES:

1) Baseline K/Na selectivity of Asahi ion exchange membranes, quantitative measure of K/Na selectivity improvement by cation exchange membrane as "filter".
2) Bench scale results of selective Cl removal from simulated green liquor by conventional ion exchange (equilibrium isotherms).
3) Proposal on new chemistry for K/Na separation by electrodialysis.

PROPOSED SCHEDULE, F01706

March 98' June 98' September 98' December 98' March 99'

Objective A:
Tech. Transfer, ED of ESP dust
A1. Continue work with
US Filter/HPD

A2. Address recycling of
sulfate rich solution

A3. Further pilot scale test

Objective B: K/Na selective membrane separation
B1. Run K/Na with conventional membranes...

B2. Run composite anion/cation membrane...

B3. Consider new chemistries...

B4. Test new chemistries

Objective C: Ion exchange for combined chloride/potassium removal from green liquor
C1. Literature update

C2. Select commercial anion exchange resin

C3. Bench-scale tests

Highlights of Externally Funded and PhD Projects

DOE FUNDED PROJECT

Sponsor: DOE Agenda 2020, Energy Performance Task Group

Project Title:	Elimination of the calcium cycle: direct electrolytic causticizing of Kraft smelt
Project Code:	
Project Number:	4182
PAC:	Recovery
Division:	Chemical Recovery and Corrosion
Project Staff	
Faculty/Senior Staff:	P. Pfromm, J. Winnick (Georgia Tech)
IPST Staff:	D. Taylor (Senior Technician); Research Services Division
FY 98-99 Budget:	August 97 to August 98 (1 year project): $180,000 total
Time Allocation	
Faculty/Senior Staff:	P. Pfromm, J. Winnick, ~1 month each (Pfromm from IPST matching funds)
Support:	D. Taylor: 12.5%
Supporting Research	
M.S. Students:	
Ph.D. Students:	R. Wartena (Georgia Tech)
External:	This project is external

RESEARCH LINE/ROADMAP:

PROJECT OBJECTIVE

Show on the laboratory scale that electrolysis of a sodium sulfide/sodium carbonate salt smelt in presence of steam at the cathode and a sacrificial carbon anode will result in causticizing of the smelt without any significant sulfur loss:

1. production of hydroxide and hydrogen from steam at the cathode
2. release of carbonate as carbon dioxide at the cathode

PROJECT BACKGROUND

The Gibbs free energy change was calculated at 1100 K. It is clear that formation of CO_2 from $CO_3^=$ at the carbon anode is the expected reaction. This is **only** the case with the sacrificial carbon anode.

$$\mathbf{2Na_2CO_3 + C + 4H_2O \xleftrightarrow{4e^-} 4NaOH + 3CO_2 + 2H_2 \quad \Delta G = +129.4\ KJ/mol} \qquad \mathbf{(11)}$$

Reaction 11 is the desired reaction for causticizing (other reactions that are possible have higher ΔG and are not shown due to space available). It is clearly thermodynamically favored. Reaction (11) will proceed at a standard emf of -0.335 volts.

Literature search: No references to direct electrolytical causticizing of a kraft molten salt smelt were discovered in the patent literature and the general published literature. Causticizing of carbonate molten salt smelts (no sulfur compounds) has been described. Causticizing of green liquor by electrolysis has also been described, but suffers from the need to first separate the sulfide entirely from the carbonate (for example U.S. Pat. 2,416,413). Our use of steam at the cathode and a sacrificial carbon anode for kraft smelt electrolysis constitutes an entirely novel approach.
Prior or current funding: this work will be cost shared at 20% through personnel costs by the Institute of Paper Science and Technology and Georgia Tech.

BENEFITS TO THE INDUSTRY

The potential benefits are:

- about 50% energy savings over current kraft causticizing
- reduce deadload (unlimited causticizing efficiency, no chemical equilibrium limitation)
- eliminate non-process element input from lime
- facilitate process control (no large dead times)
- incremental causticizing capacity can be installed
- electrolytical unit with about five square meters of electrode area may suffice for a 1000 tpd kraft mill

Since a very similar process exists on a large scale in aluminum production, the technology transfer would be relatively simple, once a proof-of-concept has been established. This feasibility test is the subject of this work.

SUMMARY OF RESULTS 8-97 TO 1-98:

The electrochemical reactor system for kraft smelt is operating. Several runs ranging from carbonate only (no steam or electricity) to carbonate+sulfide with applied electrical current and steam were performed. Analytical procedures are established (wet chemistry only, no gas analysis of off-gas).

A proposal to the Agenda 2020 Capital Effectiveness group for 2 more years of funding was submitted (starting date Summer 1998). A proposal for electrolysis of kraft ESP dust was submitted to the Georgia Consortium (starting date 7-98, to 7-200).

DELIVERABLES

Evaluate feasibility of electrochemical causticizing with artificial sulfide/carbonate kraft smelt. Final report.

SCHEDULE

Project completion by 8-98.

Highlights of Externally Funded and PhD Projects

DOE FUNDED PROJECT

Sponsor: DOE Agenda 2020, Environmental Performance Task Group

Project Title:	VOC Control in Kraft Mills, Task B: Development of a Membrane Separation Technology
Project Code:	
Project Number:	415702
PAC:	Recovery
Division:	Chemical Recovery and Corrosion
Project Staff	
Faculty/Senior Staff:	P. Pfromm, M. Rezac (GIT)
IPST Staff:	D. Taylor (Senior Technician); I. Christ (MS student)
FY 98-99 Budget:	~$50,000/year, project ends July 1999
Time Allocation	
Faculty/Senior Staff:	P. Pfromm, 1 month/year (Matching)
Support:	IPST MS Student, GIT PhD students, D. Taylor: 12.5%
Supporting Research	
External:	This project is external

RESEARCH LINE/ROADMAP:

PROJECT OBJECTIVE

Show on the laboratory scale that methanol can be selectively removed from wet air streams by membrane permeation.

PROJECT BACKGROUND

Legislative pressure and publicized opinion demand measures to minimize emissions. Only operations that will be able to safely comply with current and future regulations will enjoy long term success. Hazardous Air Pollutants (HAP's) have become a focus for reduction of emissions from pulp and paper mills. Methanol has clearly been identified as the major HAP emitted from pulping and papermaking operations.

We propose to use an emerging technology for separation of methanol from gas and vapor streams to minimize emissions from significant point sources, such as tank vents Ohlrogge and Peinemann, 1990). The removal of methanol through membrane permeation is a continuous, simple, and rugged process. Methanol is recovered as a liquid, and no spent adsorbent is generated. No sludge disposal problem is created, as with biological reactors. In lower concentration ranges, the process is more efficient than condensation. Since the methanol is recovered in liquid form, it can be sold, reused, or easily disposed of. This process is currently being implemented in the petroleum industry for recovery of fuel vapors from tank farms and gas stations. The advantages of methanol recovery by membrane technology are shown in Table 1.

	Methanol recovered	*Regenerate/dispose of adsorbent*	*Sludge generated*	*Startup/shutdown procedure*	*Tolerates feed changes*
Membrane Separation	**yes**	**no**	**no**	**simple**	**yes**
Adsorption	possible	yes	no	yes	limited
Bio Reactor	no	no	yes	complex	no

Table 1: Comparison of alternative control methods for methanol emissions.

BENEFITS TO THE INDUSTRY

- Reduce environmental impact
- Compliance with regulations
- Recover solvent

SUMMARY OF RESULTS 8-97 TO 1-98:

- Engineering approach (steam purge): Exceptional Methanol/Air selectivity confirmed in mixture experiments, complete steam purge experiments.
- Material Science approach (new polymer): New polymer found with very high Methanol/Water selectivity (single component), confirming for mixture experiments.

DELIVERABLES

- Confirm engineering approach (steam purge), system design.
- If MeOH/Water selectivity of new polymer can be confirmed, include this option in design.
- Form laboratory scale high performance composite membranes
- Case studies

SCHEDULE:

Mixture measurements during 1998.

Highlights of Externally Funded and PhD Projects

DOE FUNDED PROJECT

Sponsor: DOE Agenda 2020, Environmental Performance Task Group

Project Title:	Recycling of Bleach Plant Filtrates using Electrodialysis
Project Code:	
Project Number:	4160
PAC:	Recovery
Division:	Chemical Recovery and Corrosion
Project Staff	
Faculty/Senior Staff:	S.-P. Tsai (Argonne National Lab), P. Pfromm
IPST Staff:	D. Taylor (Senior Technician); IPST Research Services
FY 98-99 Budget:	August 97 to August 98: Total $200,000, IPST~$50,000 (3 year project, 1997 to 1999)
Time Allocation	
Faculty/Senior Staff:	P. Pfromm, 1 month
Support:	IPST PhD Student, Analytical Services
Supporting Research	
External:	This project is external

RESEARCH LINE/ROADMAP:

PROJECT OBJECTIVE

The goal of this work is to develop electrodialysis technologies that will enable the pulp mills to tighten the water cycle by using electrodialysis for the selective removal of inorganic NPEs in the bleach plant filtrates for the recovery of filtrates. Electrodialysis is uniquely suited as a selective kidney to remove NPEs from bleach plant effluent, before they reach the recovery cycle. Therefore, the problems caused by accumulation of inorganic NPEs in the pulping cycle and recovery boiler are prevented.

The efforts in this work have been focused on the acidic bleach plant effluent of bleached Kraft pulp mills, because bleached Kraft pulp production is an important segment of the pulp and paper industry and the acidic effluent is where most of the NPEs are present. The major technical hurdles for this process include the membrane selectivity for the NPEs to be removed and the membrane resistance to fouling. In addition to the technical feasibility, the process economics is crucial to the viability of this process.

The objectives of this work are:

•To evaluate the process feasibility, including ion selectivity and organic fouling resistance

•To develop an efficient and economical electrodialysis-based process at the laboratory scale

•To demonstrate the process performance at mill sites

•To transfer the technologies to pulp and paper companies

PROJECT BACKGROUND

Water Reuse in Bleached Kraft Pulp Mills

Water use in the pulp and paper industry is very significant. In recent times, great advances have been made to reduce water use. A few decades ago, water use (and wastewater discharge) of up to 400 m^3 (106,000 gallons) per ton of bleached kraft pulp produced would not have been uncommon. A typical pulp mill produces 1000 tons of pulp per day, resulting in considerable stress to the environment in terms of water consumption and wastewater discharge. Today, the effluent from typical bleached kraft pulp mills ranges from about 30 to 150 m^3 per ton of pulp produced (Mannisto et al., 1995; Bihani, 1996). This is still a very significant water use and the pulp and paper industry has a strong interest in further reduction of water use.

Reduction of water consumption by water recovery and reuse is being actively pursued by the processing industries in general. This, in many cases, has been motivated by the rapidly rising costs of raw water and wastewater disposal. From 1960 to 1995, municipal water costs rose from $0.40 to $3.11 per 1,000 gallon of water and sewer charges rose eight-fold between 1986 and 1995 (Jessen and Kemp, 1996). For plants in certain geographic locations, plant water reuse is needed due to limitations in the availability of fresh water and/or wastewater discharge limits. For pulp mills in particular, the proposed environmental regulations on the discharge of adsorable organic halides (AOX) in bleach plant effluent is an additional driver to tighten the water cycle and reduce the water use and wastewater discharge.

An important segment of the U.S. pulp and paper industry is the bleached kraft pulp production. About 30 million tons of bleached kraft pulp are produced in the U.S. per year. Pollution prevention by recycling of bleach plant effluents from bleached kraft mills is a very important goal for the U.S. pulp and paper industry. It has been proposed that water consumption at a range of 10 to 30 m^3 per ton of pulp is achievable by using various "minimum effluent" technologies.

For the discussions of these technologies, a simple block diagram of bleached Kraft pulp production with considerations for water recycle is shown in Figure 1. Generally speaking, to reduce water use the water from the bleach plant effluent is to be reused in the bleaching and pulping process, while the organic components are to be oxidized to CO_2 in the recovery boiler to reduce the AOX discharge. Essentially, water is countercurrently re-used in the bleach plant for washing of the pulp between bleaching stages, and then finally to wash the pulp that comes directly from the digester (brown stock washing). This scheme will introduce a significant load of unwanted inorganic non-process elements (NPEs) into pulping and bleaching. The ion exchange properties of wood fibers play an important role here. Bleach plant effluents can be divided in the acidic (low pH) effluent and basic (high pH) effluent. Wood pulp contains ion exchange sites. Since the wood pulp is first produced in an alkaline aqueous environment,

multivalent cations (metals, transition metals, earth alkali ions) are retained on the pulp. When the unbleached pulp enters the bleach plant and the pH is shifted to the acidic range for the first time, metals and transition metals (NPEs) are liberated into the bleaching solution by exchange with H^+ ions. This first acidic solution is subsequently separated from the pulp by displacement washing. The acidic bleach plant effluent contains inorganic NPEs and recycling of this effluent has been reported to cause problems such as recovery boiler plugging, corrosion, NPE accumulation in the calcium cycle, increased use of bleaching chemicals, and scaling.

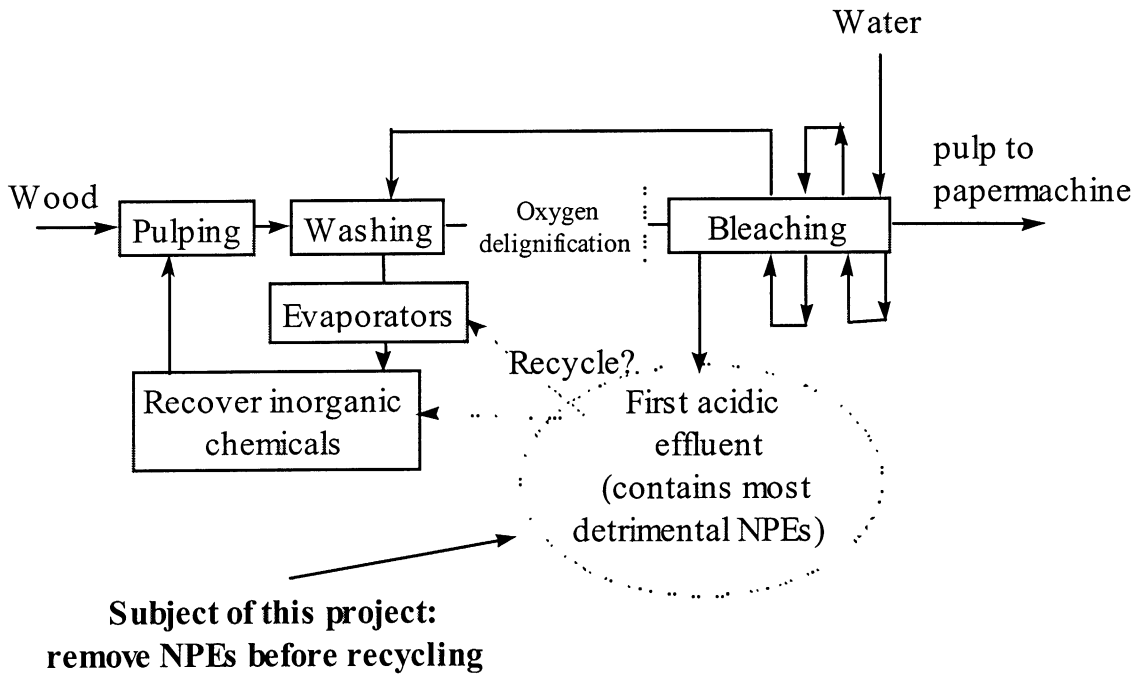

Figure 1: Bleached Kraft pulp production with full countercurrent water use in the bleach plant. Potential oxygen delignification and the extraction of NPEs from pulp in the bleach plant at low pH are shown.

There are generally three concepts of how to achieve recycle of the bleach effluent (Gleadow et al., 1996). Below is a listing of the basic concepts. The mill samples included in our program for this reporting period cover the highlighted recycling concepts:

1. Separate bleach effluent treatment (concentrate by evaporation, burn organics in a separate incinerator, dispose of inorganic ash residue).

This concept is only economical if the evaporator capacity needed is not too large (on the order of a few m^3 of effluent per ton of pulp). It is currently not actively pursued in the U.S.

2. Combine acidic and alkaline bleach effluent, concentrate (by evaporation), and add the concentrate to weak black liquor.

This concept has been put forward by some supplier companies, requirements see under 1.

3.Return alkaline effluent to chemical recovery via brown stock washing, and

3.a.Separately concentrate acidic effluent and add the concentrate to black liquor after NPE removal.

An acidic effluent from a conventional mill is used in our project. It is anticipated to be concentrated by evaporation and then treated by electrodialysis to remove NPEs.

3.b.Use acidic filtrate as weak wash makeup to dissolve smelt.

This has been put forward and tested in Scandinavia. Problems in the chemical recovery cycle result.

3.c.Separate metals from acidic filtrate and reuse it in the bleach plant.

A process is currently marketed by Champion International and US Filter/HPD. A full scale implementation exists at Champion's Canton, NC mill. Acidic effluent from this mill is used in our project.

3.d. Eliminate acidic filtrate by not washing after the first acidic stage.

Electrodialysis Technology

Electrodialysis is a membrane separation technology that uses the permselectivity of ion-exchange membranes and the electric potential driving force to remove, concentrate, or separate ionic species in aqueous streams. The technology was first developed in the 1950's. Currently, successful applications of electrodialysis exist in various processing industries; these applications include:

•Desalination of brackish water

•Production of table salt from sea water

•Chemical, food, and drug processing

•Water and wastewater treatment

•Waste recovery and recycle from industrial wastewater

The scale of commercial systems ranges from vary large (500 million lb/yr) plants for table-salt production to small-scale systems for flavor-extraction in food processing plants.

Electrodialysis separation is achieved by passing the feed and product streams through an electrodialytic stack comprised of alternating cation-exchange and anion-exchange membranes and applying a direct current to a pair of electrodes across the entire set of membranes. Cation exchange membranes are made of a cross-linked polymer with fixed negatively charged function groups, which permit the transport of cations through the membranes while excluding anions

from entering the membranes. Similarly, anion-exchange membranes have fixed positively charged groups, which permit the transport of anions and exclude cations. In the presence of an electric field, cations in the feed (diluate) compartment move towards the cathode, cross through the cation-exchange membrane into the concentrate compartment. Their further movement towards the cathode is blocked by the anion-exchange membrane, resulting in accumulation in the concentrate compartment. Similarly, anions move towards the anode from the feed to the concentrate compartment through the anion-exchange membranes. Most of the non-ionic and weakly ionic species stay in the feed stream, although a small amount can move to the concentrate stream by electro-osmosis. Electrodialysis is, thus, an efficient means of separating the inorganic salts from the non-ionic and weakly ionic organic compounds.

Various kinds of ion-exchange membranes are commercially available from several suppliers. Each of the reputable suppliers (e.g., Tokuyama Corp.) carries more than a dozen different types of membranes. The selection of appropriate membranes are essential to meeting technical and economic objectives for a specific application. Some of the factors that are important to consider when selecting membranes include degree of cross-linking, membrane thickness, and ion selectivity. In general thicker membranes and membranes with a higher degree of cross-linking have better mechanical strength but also higher electrical resistance, whereas thinner membranes and membranes with a lower degree of cross-linking have poorer mechanical strength but lower electrical resistance. Ion selectivity can be an important consideration when it is desired to promote the transport of certain ionic species while minimizing the transport of other ionic species. For example, monovalent-selective anion-exchange membranes can be used to permeate chloride ions while rejecting sulfate ions.

For bleach plant filtrate recycle, electrodialysis can potentially be applied in Concept 3.a and Concept 3.c described earlier. Electrodialysis of bleach plant effluent to remove inorganics, including chloride, has been proposed by Eka Nobel (Gransson et al., 1995). However, an extensive pre-treatment for separation of the organic components before electrodialysis was proposed. This leads to high investment and operating costs. The process proposed here will employ membranes that are intrinsically fouling resistant due to special polymer modifications.

Champion International is currently testing the first installation of their BFR™ process at Canton, NC (Caron and Williams, 1996) to remove metals from the acidic filtrate (Concept 3.c). The metal ion removal sequence requires significant pre-treatment, and is still subject to fouling. Electrodialysis is superior since it requires no regeneration cycles, and can tolerate organic foulants if modified membranes are used. Chloride can be removed by electrodialysis at the same time that metal ions are extracted, which prevents chloride from entering the recovery cycle.

REFERENCES

Bihani, B. G., *Pulp and Paper*, 70(7), 87, 1996.

Jessen, H. M. and Kemp, P. M., Environmental Engineering World, Nov-Dec, 15, 1996.

Mannisto, H., Mannisto, E., and Winter, P., Tappi Journal, 78(1), 65, 1995.

Gleadow, P., Hastings J. B., Schroderus, S., and Warnqvist, B., "Toward Closed-Cycle Kraft: ECF Versus TCF Case Studies", 82nd Annual Meeting, Technical Section, Canadian Pulp and Paper Association (CPPA), page A359, 1996

Gransson, G., Sundblad, B., Landfors J., and Baltsn, H.A., U. S. Patent 5,437,791; 1995

Caron, J. R. and Williams, L. D., "Design and Start-Up of the Bleach-Filtrate Recycle Process", 1996 International Environmental Conference, Proceedings, p. 669 (May 5, 1996; TAPPI Press)

BENEFITS TO THE INDUSTRY

Develop a rugged low-cost technology for simple retrofit to remove NPE's from bleach effluent to be recycled.

SUMMARY OF RESULTS 8-96 TO 1-98:

Detailed results are available as an Annual Report on the project. Please contact P. Pfromm for a copy of the report.

Highlights:

The laboratory runs showed excellent removal of metals and transition metals, and simultaneous selective chloride removal. A new approach to replace unwanted cations with sodium cations was also tested. This approach maintains all anions in the effluent to be recycled, but removes the NPE's. Precipitation issues in the concentrated purge stream are minimized.

Future work will concentrate on the effluent from a bleached kraft mill with full ClO2 substitution, to obtain long term laboratory runs. These runs should confirm that no significant fouling is observed.

Highlights of Externally Funded and PhD Projects

Miscellaneous Projects 1997/98

1. Xerographic Toners for Textiles Printing. Cooperation with C. Carr, GIT School of Textiles and Fiber Engineering, $18,000/year from National Textiles Center to P. Pfromm. Polymers for textiles xerography are being developed.
2. Xerographic Toners from Soybeans. Cooperation with C. Carr, GIT School of Textiles and Fiber Engineering, J. Waterhouse (IPST) and Y. Deng (IPST). Polymers from soybeans are formulated and tested for xerography of paper.

Highlights of Externally Funded and PhD Projects

IPST PhD PROJECT

Project Title:	Removal of Inorganics from Closed-Cycle Papermachine White Water
Project Code:	
Project Number:	
PAC:	Recovery
Division:	Chemical Recovery and Corrosion
Project Staff	
Faculty/Senior Staff:	P. Pfromm
IPST Staff:	Eric Watkins, PhD Candidate (Graduation 1998/99)
FY 98-99 Budget:	N/A

HIGHLIGHTS

Interaction of ion exchange resins with organic foulants (sulfonated lignin, wet end resins) is being investigated. Fouling of electrodialysis membranes is being characterized by frequency spectroscopy. Fouling mechanisms (adsorption, ionic interaction) are the target of this work.

Highlights of Externally Funded and PhD Projects

IPST PhD PROJECT

Project Title: Behavior of Polymeric Toner in Recycling
Project Code:
Project Number:
PAC: Recovery
Division: Chemical Recovery and Corrosion
Project Staff
Faculty/Senior Staff: P. Pfromm
IPST Staff: J. Panek, PhD Candidate (Graduation 1998)
FY 98-99 Budget: N/A

HIGHLIGHTS

Theoretical and experimental behavior of a polymeric composite to model toner layers on paper is being investigated. The dependence of the particle size distribution of toner particles in recycling as a function of material properties and pulping conditions is then predicted.

Highlights of Externally Funded and PhD Projects

IPST MS PROJECT

Project Title:	Removal of potassium from green liquor by ion exchange
Project Code:	
Project Number:	
PAC:	Recovery
Division:	Chemical Recovery and Corrosion
Project Staff	
Faculty/Senior Staff:	P. Pfromm
IPST Staff:	D. Englehart, MS Candidate (Graduation Spring 1998)
FY 98-99 Budget:	N/A

HIGHLIGHTS

Commercial ion exchange resins are tested for their potassium selectivity in green liquor. Full scale application estimates are being developed. Use of ion exchange for potassium control appears feasible and economically attractive.

INSTITUTE OF PAPER SCIENCE AND TECHNOLOGY

ATLANTA, GEORGIA 30318

DUES-FUNDED PROJECT SUMMARY

Project Title: Fundamentals of Dregs Removal
Project Code:
Project Number: F01707
PAC: Chemical Recovery
Division: Chemical Recovery and Corrosion
Project Staff
Faculty: Jeff Empie
Staff: Maribeth Amundsen, Garry Heedick; Analytical
FY 98-99 Budget: $96,000
Time Allocation
Faculty: J. Empie - 2 mo.
Support: M. Amundsen - 4 mo.
M. Ellis - 2 mo.
G. Heedick - 1 mo.
Analytical - 3 mo.
Supporting Research
M.S. Student: John Clark
Ph.D. Student: Brian Campbell

RESEARCH LINE/ROADMAP: Environmental Performance

PROJECT OBJECTIVE: Determine the effect of elevated levels of non-process elements (NPE's) on the composition and settling/filtration rate of green liquor dregs.

PROJECT BACKGROUND: With the enactment of the Cluster Rule, there is a strong push from the environmental sector to close up our pulp and paper mills, minimizing emissions of liquid, solid, and gaseous pollutants, along with usage of fresh water. As moves are made to bring this about, a related problem emerges in the form of non-process elements (NPE's) building up in the liquor streams because opportunities for purge are diminished while input sources remain fixed. Mass balance constraints dictate that concentrations of these unwanted NPE's must increase.

It is evident that one of the key unit operations in the liquor cycle for controlling NPE build-up is dregs removal. An increase in production rate or a reduction in the purge rate of green liquor dregs, brought about by a change in physical/chemical properties, will increase the levels of Mg and Mn in the lime cycle and increase the levels of Al, Fe, and Si in both the liquor and lime cycles. Hence, a detailed study of the effect

of increased levels of NPE's on dregs removal, and therefore purge of NPE's, has been undertaken.

Because actual mill smelt composition varies from shift to shift, as well as within a given shift, this study works with a known, representative, synthetic smelt composition (including dregs), and adds an incremental amount of specified non-process element chemicals. These are heated to typical smelt bed temperatures and held in a nitrogen atmosphere for a period of time to allow the chemicals to equilibrate. The cooled reaction products are then added to hot synthetic weak wash to form a synthetic green liquor.

The insolubles represent the dregs for the simulated process. Their settling and filtration rates will be determined at normal process temperature; the insolubles will be sampled for chemical analysis. Comparisons can then be made with the base condition of synthetic smelt vs. that treated at the same conditions with specific levels of NPE's added.

To ultimately validate the results, the procedure will then be repeated starting with an actual kraft smelt and holding it at 800°C for equilibration. After the treated smelt is dissolved in weak wash, the dregs can be separated and their properties compared with green liquor dregs from the same mill.

A one-liter stirred batch reactor designed to carry out these reactions at smelt bed temperatures in the laboratory has been fabricated. All parts which are contacted by molten smelt have been made out of alumina to avoid corrosion phenomena and contamination of the reaction products.

An apparatus has been built to determine the settling and permeability characteristics of the dregs produced in the lab runs and suspended in synthetic weak wash at 90°C.

SUMMARY OF RESULTS: A literature survey of dregs composition, along with analyses of four actual mill dregs samples, have identified an "average"dregs composition. Carbon content showed the most variation, with values ranging from under 2% to 35%. This has led to an experimental strategy based upon two laboratory smelt compositions featuring low and high carbon content, 2% and 20%.

Five successful smelting runs with low carbon content have been carried out in the alumina reactor. Using the same starting chemical compositions used in these runs, chemical equilibrium calculations have been completed, indicating the compositional changes to be expected when these chemicals are subjected to smelting conditions. The ultimate chemical forms of the NPE's chosen for this study are predicted to be as $Ca(OH)_2$, $Mg(OH)_2$, MnS, SiO_2, $NaAlO_2$, and FeS. Analysis of the reaction products awaits the green liquor formation and settling test results.

Partition coefficients between dregs and clarified green liquor for two earlier shakedown runs showed Ca, Fe, Mg, and Mn to favor the dregs, while Na and Si stayed with the green liquor; Al was distributed more evenly between the two phases.

GOALS FOR FY 98-99:

* Complete the formation of synthetic smelts spiked with NPE's.
* Complete settling/filterability rate determinations of the dregs produced.
* Obtain chemical/physical analyses of the green liquor and dregs products.
* Complete parallel experiments using smelt and green liquor samples from a kraft mill.
* Perform thermodynamic equilibrium calculations for comparison with experimental data.
* Write final report.

DELIVERABLES:

* Laboratory equipment to generate the data needed to meet the objective.
* Determination of changes in removal rates of dregs with elevated levels of NPE's relative to present operation.
* Identification of problematic NPE's upon mill closure.

SCHEDULE:

* Settling column operational (3/1/98)
* Mill smelt and green liquor samples obtained (5/1/98)
* Smelt formation runs completed (8/1/98)
* Settling/filtration rate determinations completed (10/1/98)
* Data analysis completed (12/31/98)
* Final report completed (2/28/99)

Fundamentals of Dregs Removal

(Project F01707)

Annual PAC Report, March 1998

IPST Goal: Improve dregs separation from green liquor in support of facilitating closed-mill operations

Objective: Determine the effect of elevated levels of non-process elements (NPE's) on the composition and settling rate of green liquor dregs.

SUMMARY:

It is evident that one of the key unit operations in the liquor cycle for controlling NPE build-up is dregs removal. An increase in production rate or a reduction in the purge rate of green liquor dregs, brought about by a change in physical/chemical properties, will increase the levels of Mg and Mn in the lime cycle and increase the levels of Al, Fe, and Si in both the liquor and lime cycles. Hence, a detailed study of the effect of increased levels of NPE's on dregs removal, and therefore purge of NPE's, has been undertaken.

Because actual mill smelt composition varies from shift to shift, as well as within a given shift, this study works with a known, representative, synthetic smelt composition (including dregs), and adds a fixed amount of specified non-process element chemicals. These are heated to typical smelt bed temperatures and held in a nitrogen atmosphere for a period of time to allow the chemicals to equilibrate. A one-liter stirred batch reactor has been designed to carry out these reactions at smelt bed temperatures in the laboratory. All parts which are contacted by molten smelt have been fabricated out of alumina to avoid corrosion phenomena and contamination of the reaction products.

The cooled reaction products are then added to hot synthetic weak wash to form a synthetic green liquor. The insolubles represent the dregs for the simulated process. A laboratory settling/permeability apparatus has been fabricated to determine dregs settling and filtration properties at normal process temperature; the insolubles will be sampled for chemical analysis. Comparisons can then be made with the base condition of synthetic smelt vs. that treated at the same conditions with specific levels of NPE's added.

To ultimately validate the results, the procedure will then be repeated starting with an actual kraft smelt and holding it at 800°C for equilibration. After the treated smelt is dissolved in weak wash, the dregs can be separated and their properties compared with green liquor dregs obtained from the same mill.

A literature survey of dregs composition, along with analyses of four actual mill dregs samples, have identified an "average" dregs composition. Carbon content showed the most variation, with values ranging from under 2% to 35%. This has led to an experimental strategy based upon two laboratory smelt compositions featuring low and high carbon content, 2% and 20%.

Five successful smelting runs with low carbon content have been carried out in the alumina reactor. Using the same starting chemical compositions employed in these runs, chemical equilibrium calculations have been completed, indicating the compositional changes to be expected when these chemicals are subjected to smelting conditions. The ultimate chemical forms of the NPE's chosen for this study are predicted to end up as $Ca(OH)_2$, $Mg(OH)_2$, MnS, SiO_2, $NaAlO_2$, and FeS. Analysis of the reaction products awaits the green liquor formation and settling test results.

Partition coefficients between dregs and clarified green liquor for two earlier shakedown runs showed Ca, Fe, Mg, and Mn to favor the dregs, while Na and Si stayed with the green liquor; Al was distributed more evenly between the two phases.

INTRODUCTION:

With the enactment of the Cluster Rule, there is a strong push from the environmental sector to close up our pulp and paper mills, minimizing emissions of liquid, solid, and gaseous pollutants, along with usage of fresh water. As moves are made to bring this about, a related problem emerges in the form of non-process elements building up in the liquor streams because opportunities for purge are diminished while input sources remain fixed. Mass balance constraints dictate that concentrations of these unwanted NPE's must increase.

Serious consequences of this build up are felt throughout the pulping liquor recovery cycle of both kraft and soda mills. Unwanted silica and alumina compounds, chlorides, and various metal salts cause operating problems in excessive scale formation on metal surfaces, increased corrosion rates, and reduced effectiveness of the pulping chemicals (1). The latter factor can lower pulp production rate below nameplate capacity, as well as require more energy to produce a pound of product.

Concurrent with the push toward closed-cycle mills is the shift from chlorine based bleaching sequences to non-chlorine based. Examples are oxygen, ozone, and peroxide. For these chemicals to be effective, small amounts of transition metals in the pulping liquors must be avoided (2). Hence, the combination of chlorine-free bleaching with closed-cycle mill operation raises the priority level of how to purge NPE's to the highest level.

At present, the unwanted insoluble materials, called dregs, are continuously purged from the green liquor in the kraft liquor cycle by sedimentation or filtration. The dregs sediments or filter cakes are then landfilled or processed in the mill effluent system. In addition to the NPE's listed above, the dregs contain about 2-30% carbon, giving the

material the appearance of a coal slag (3). As kraft pulp mills are forced to effect tighter closure, they can expect the compositional change in their dregs flow to adversely impact their ability to separate and remove the dregs. Dregs physical properties, including density, porosity, and carbon content, will have impact here. In addition, there is concern that trace metals not now detected will rise to levels above present detection limits.

For kraft pulping the elements Na and S are the principal process elements. The non-process elements include Cl, Al, Si, K, Fe, Cu, Mn, Mg, P, and V. These enter the pulping process with the wood, water, other processing chemicals, and make-up chemicals. They can increase in concentration unless purge mechanisms are provided; presently, these purges are mill solid, liquid, and gaseous effluent streams. Tighter "mill closure" implies a reduction in these effluent discharges in order to decrease both water use and the environmental impact of the pulp manufacturing process.

Although the NPE's tend to be present in low levels, they may have a disproportionate effect on the operation of the mill. Some NPE's (viz. Al, Fe, Mg) are sparingly soluble in green liquor, but more soluble in white liquor. If they are not removed with the dregs, they can carry through to the digester and subsequently cause fouling in the evaporators. Aluminum can trigger evaporator scaling when its concentration exceeds 50-100 mg/L in the white liquor. Aluminum can be precipitated from green liquor by the addition of magnesium to form hydrotalcite. Since there is some Mg naturally in the liquor cycle, entering with bleach plant effluent and make-up lime, some Al is being removed by this mechanism in present mill caustic plants.

Magnesium causes problems when it is allowed to accumulate in the lime mud because it calcines in the lime kiln, consuming fuel. The magnesium hydrates in the slaker, but it has no causticizing power, making it a heat consuming dead load. Magnesium also causes serious problems in the settling and filtration of lime mud. The finely divided particles of magnesium hydroxide in the dregs cause poor settling rates and a tendency to plug filter cakes. Therefore, it is important to minimize Mg input and control its build-up throughout the caustic plant.

Fe, Cu, and Mn are other trace elements which can cause problems. The only outlet for these elements is the dregs system. Iron build-up is believed to be a cause of dusting from the lime kiln. The concentration of manganese in the lime cycle is quite low because green liquor clarification is effective in removing Mn.

Some NPE's (viz. Si, P) are soluble in green liquor, but less so in white liquor. Hence, if these are not removed from the green liquor, they can accumulate in the lime mud circuit, lowering lime availability and increasing kiln fuel cost. In the presence of lime, phosphorous is precipitated as apatite, $Ca_5OH(PO_4)_3$. In the lime kiln, apatite converts to calcium phosphate, $Ca_3(PO_4)_2$. Some, but probably not all, of the calcium phosphate converts back to apatite in the causticizing process. P does not precipitate in the green liquor circuit, even when lime is added as a settling or filtration aid. Therefore, its build-up can only be controlled by a purge of lime mud, which is best done at the

dregs filter. The recommended bleed is in line with the amount of mud precoat required for optimum operation of the dregs filter.

It is evident that one of the key unit operations in the liquor cycle for controlling NPE build-up is dregs removal. A reduction in the purge rate of green liquor dregs will increase the levels of Mg and Mn in the lime cycle and increase the levels of Al, Fe, and Si in both the liquor and lime cycles. Hence, a detailed study of the effect of increased levels of NPE's on dregs removal, and therefore purge of NPE's, is crucial.

One other NPE that needs to be addressed is chloride. Its removal is difficult because it is soluble and remains with the aqueous liquor streams. Three methods have been practiced commercially in recent years. In the recovery boiler flue gas, SO_2 can react with NaCl, H_2O, and O_2 to form Na_2SO_4 and HCl gas. The HCl can be either scrubbed out of the flue gas by known methods or allowed to escape to the atmosphere. An alternative method for chloride removal is to purge NaCl by leaching precipitator dust. This method has been developed by Champion International, however it appears cumbersome and expensive. Chloride can also be removed by white liquor evaporation-crystallization. This was practiced as part of the closed mill operation at Thunder Bay, Ontario. It has since been discontinued.

EXPERIMENTAL:

Smelt Formation

A one-liter stirred batch reactor has been designed and installed to carry out the smelt formation reactions in the laboratory. All parts which are contacted by molten smelt have been fabricated out of alumina to avoid corrosion phenomena and contamination of the reaction products (c.f. Fig. 1).

The synthetic smelt chemicals (including dregs), along with the specified non-process element chemicals, are added to the alumina reactor. These are heated to typical recovery boiler smelt bed temperatures and held in a nitrogen atmosphere for a period of time to allow the chemicals to equilibrate. The cooled reaction products are then added to a hot synthetic weak wash (2.5% NaOH) to form a synthetic green liquor. Settling and filtration rates of the insolubles are determined; these are then filtered out and washed with hot water.

These washed insolubles represent the dregs for the simulated process and are sampled for chemical and physical property analyses. The physical properties of interest are density, porosity, and particle size distribution. Comparisons are then to be made with the base condition of synthetic smelt treated at the same conditions with no NPE's added.

Smelt, green liquor, and dregs samples will be analyzed for trace metals using a nitric acid, hydrogen peroxide, and hydrochloric acid digestion procedure, followed by

analysis by ICP spectroscopy. Silicon analysis for the solid smelt and dregs samples requires preparation by a caustic fusion procedure.

Comparisons are also to be made with actual kraft smelt obtained from a nearby mill and subjected to the same laboratory test procedures. These will validate the test results with synthetic smelts and green liquors.

Chemical analysis of samples of green liquor clarifier underflows obtained from four member company mills, along with available published data on dregs composition (1-4,7,8,10,11), have been used to establish the baseline starting composition (assuming 95% reduction efficiency) for the study; namely:

Component	Wt.%
Na_2CO_3	74
Na_2S	20
Na_2SO_4	2
NaCl	2
Dregs	2

and the baseline starting dregs components:

Component	Wt.% A	Wt.% B
$CaCO_3$	65	51
Fe_2O_3	3.5	2.5
$Mg(OH)_2$	12.5	10
MnO_2	6	5.5
SiO_2	10	10
Al_2O_3	1	1
C	2	20
	100	100

The starting dregs compositions listed are changed from what was reported last year. In both cases, the initial SiO_2 has been raised by a factor of ten because partitioning between the green liquor and dregs was found to favor the green liquor by more than what has been reported in the literature. To make up for the increase in SiO_2 charged, the $CaCO_3$ charged was adjusted downward as this is in great excess to begin with. The carbon content of composition B was lowered to 20% because of a very practical reality - at 35%, the lab smelts could not be removed from the crucibles without breaking them. This seemed very acceptable in light of the 35% number from mill sampling data being somewhat suspect due to poor sampling technique.

Dregs Separation

Because dregs removal technology is no longer limited to clarification, with the advent of developing crossflow filtration, separability of dregs from green liquor must be

characterized for both sedimentation and filtration. The apparatus and procedure detailed below will be used to determine the settling and permeability characteristics of the dregs produced in the lab runs and suspended in synthetic weak wash (c.f. Fig. 2).

The sedimentation column consists of a graduated plexiglas tube (5 cm. ID, 50 cm. height) enclosed in a 30 cm. O.D. transparent air bath controlled at 90°C. The filter base is connected to a vacuum flask outside the air bath. A constant vacuum is maintained by manually setting an air bleed rate into the line ahead of the vacuum pump. A maximum vacuum of about 30 kPa is set by the vapor pressure of water at process temperature (viz., 70 kPa at 90°C).

To prepare the bed for permeability measurements, green liquor is allowed to flow by gravity through the settled solids. The frictional drag of the flowing liquid compacts the cake particles. A constant liquid head is maintained during the compaction stage by feeding hot weak wash to the column to replace the liquid exiting the cake. When the thickness of the compacted cake is constant, the flows are shut off and the cake thickness and height of liquor in the column are measured. From the liquor height in the column, the fluid pressure under which the cake is compressed can be calculated. Because cake thickness is generally less than 1 mm and grows very slowly with time, a cathetometer has been installed to accurately measure this variable.

Cake permeability is determined by the pressure-decline permeability method which yields bed permeability compressed at a fixed fluid pressure (6). This is done by opening the stopcock in the outflow line and measuring the liquid meniscus as a function of time, using the graduated scale on the side of the column. These measurements yield the permeability of the cake compressed at a fixed fluid pressure. Varying degrees of compression can be obtained by varying the level of vacuum on the system while maintaining a constant level of fluid in the column.

The bed permeability, K, is calculated from Darcy's Law, knowing the volumetric flow rate, Q, through a cake of thickness L and cross-sectional area A:

$$Q = \frac{KA\Delta P}{\eta_f L}$$

where ΔP is the fluid pressure drop across the bed and η_f is the viscosity of the fluid.

The apparatus was tested without difficulty using fine $CaCO_3$ particles in H_2O. Subsequent tests with green liquor and dregs showed that the settling rate determinations were not going to be easy. Locating the interface of the settling dregs with the naked eye is complicated by the nearly opaque appearance of the green liquor. A 3 amp laser was procured to assist with this activity. Shining the laser downward through the liquor in the column, the depth of penetration of the light beam identifies the line of demarcation between the settling solids and the supernatant liquid. The laser can also be used to locate at what height the cake is building. By shining the laser through the side of the column

and slowly moving downward, the light penetrates about the same distance radially until the surface of the cake is encountered, at which point there is no penetration.

As the dregs settle, the clarified green liquor exhibits noticeable convection currents, as evidenced by small dregs particles moving upward in some zones and downward in others. This is attributed to the settling solids displacing liquid which can't leave the filter cake fast enough to maintain a uniform downflow. To make sure that thermal convection currents were not the cause, the temperature profile of the liquor in the heated column was checked axially and found to be uniform. Although the settling rate of the dregs is very slow and takes hours, when left to run overnight, they do settle out completely and leave a clear green liquor.

RESULTS:

Smelt Formation

Five runs using the A composition (i.e. 2% Carbon) with 2% dregs in the smelt have been successfully completed, each where 500 g. of laboratory chemicals were weighed, mixed, charged to the alumina reactor, and held at 800°C for one hour. After cooling down to room temperature, the smelt products were removed under nitrogen. The smelt from Run 009 has been dissolved in synthetic weak wash, and filtered by conventional means with a Buchner funnel. Similar treatment of the other smelts has awaited successful shakedown of the settling/permeability apparatus. Table 1 shows the starting compositions of the chemicals charged to the smelter.

Theoretical chemical equilibrium calculations have been undertaken using Outokumpu HSC Chemistry for Windows (by license) for comparison with the experimental results. This software package computes chemical reaction equilibria for specified input chemicals and temperature using an extensive thermochemical database and minimization of Gibbs free energy. A serious limitation to the results generated is in the number of compounds considered. The user specifies which compounds are to be considered and only those will be in the calculation. One serious omission is Pirssonite ($Na_2Ca(CO_3)_2$) which is known to be present in scale deposits in green liquor processing equipment. Nonetheless, the calculations should reflect what forms the majority of the input chemicals should ultimately assume. Chemical species showing less than 0.001 grams were arbitrarily ruled to not be present. Results are shown in Tables 2-6; these are summarized below:

Chemical	Change in Smelt Chemicals
Na_2CO_3	0.3-1.3% Gain (except for high Mg)
Na_2S	2-5% Decrease
NaCl	No Change
NaOH	Formed
$CaCO_3$	10-30% Decrease
Fe_2O_3	FeS, FeS_2, FeO Formed
$Mg(OH)_2$	MgO, $MgCO_3$ Formed
MnO_2	MnS, MnO Formed
SiO_2	No Change
Al_2O_3	$NaAlO_2$ Formed
C	30-100% Decrease (except for high Mg)
S	Formed (except for high Mn)

It is interesting to note in the high Mg case, Na_2CO_3 is predicted to be decreased and carbon formed, somehow. In the high Al case, not all of the Al_2O_3 is converted to the aluminate. In the high Mn case, no FeS_2, $MgCO_3$, or sulfur are formed.

Green Liquor Formation

The equilibrium smelt compositions were then hypothetically combined at 90°C with a synthetic weak wash containing 2.5% NaOH to form an equilibrium green liquor composition, again using the HSC software. Only chemical and no phase equilibrium calculations were undertaken; note that the same limitations identified with the smelt calculations also apply here. Results are presented in Tables 7-11; these are summarized below:

Chemical	Change from Smelt to Green Liquor Solids
Na_2CO_3	1-3.5% Gain
Na_2S	Variable
NaCl	No Change
NaOH	3-20% Decrease
$CaCO_3$	Converted to $Ca(OH)_2$
Fe_2O_3	None. All Fe as FeS
$Mg(OH)_2$	Increased (only form for Mg)
MnO_2	No Change (only form is as MnS)
SiO_2	No Change
Al_2O_3	None (except for high Al case)
C	Eliminated
S	Eliminated

Net Chemical Changes

The righthand section of Tables 2-11 summarizes the qualitative chemical changes that take place during combined smelting and dissolution - increased, decreased, stayed the same, was eliminated, or was created. The net hypothetical chemical changes in going from the starting materials through smelt formation to the final green liquor are summed up quantitatively in the last column of numbers in Tables 7-11 (i.e. Solids Out - In). Results are summarized below:

Chemical	Change
Na_2CO_3	2-3% Gain
Na_2S	No Change (5% decrease for high Mn)
NaCl	No Change
NaOH	2-10% Decrease
$CaCO_3$	Converted to $Ca(OH)_2$
Fe_2O_3	Converted to FeS
$Mg(OH)_2$	No Change
MnO_2	Converted to MnS
SiO_2	No Change
Al_2O_3	Converted to $NaAlO_2$
C	Eliminated

The limitations in these calculated results should be reemphasized. It is expected that, in reality, $NaAlO_2$ would undergo hydrolysis back to Al_2O_3 and NaOH. Sodium silicates should ultimately be formed, along with certain double salts such as Pirssonite. It should also be noted that if no NaOH were present in the weak wash used to make the green liquor, the ultimate equilibrium form of Ca would be as CaS.

Two smelts (Run 009 and Run 019) produced in the laboratory reactor were actually dissolved in a synthetic weak wash (2.5g. NaOH in 100g. H_2O) at 90°C. The insoluble fractions (i.e. dregs) were separated, washed, and dried. The metals content of both the clarified green liquor and the dregs have been determined by ICP. The exact chemical form of the dregs metals is not known, however based on the thermodynamic predictions presented above, the metal content of the dregs formed, expressed as the equilibrium NPE metal compound, can be calculated. The results for the two runs are presented in Tables 12 and 13.

The agreement between the experimentally determined weight fractions (in the assumed thermodynamic chemical form) and the HSC equilibrium predictions is quite striking. Only two chemical species show any disparity, namely SiO_2 and carbon. The SiO_2 is easily explained by solubility considerations; we've assumed it to be a part of the dregs (hence insoluble) whereas in reality it is somewhat soluble in green liquor. The green liquor analysis did show a significant presence of silicon, the chemical form of which was not determined. The difference in carbon values may be partly due to

analytical accuracy (determined by difference between Total Carbon and Carbonate Carbon). It should also be noted that there were significant amounts of sodium and sulfur in the experimental dregs samples. About one-fourth of the sulfur would be as FeS. The sodium could exist in many forms, including sulfide, sulfate, thiosulfate, carbonate, and other salts.

One quantity of interest is how the NPE's in the product smelt partition themselves between the clarified green liquor and the dregs fraction. Partition coefficients (K_{DG}), defined as the ratio of the amount of metal element in the dregs fraction to the corresponding metal amount in the green liquor fraction, were determined for Runs (009) and (019), based upon the metals analysis and the total mass of green liquor solids and dregs. Results are summarized below. Mass balance closures were variable, with Si showing a significant gain in both runs. There are two analytical procedures for Si, with both having uncertainties. The results shown are based on using a caustic digestion procedure where some contamination is suspected. The alternative acid digestion procedure gave lower Si values, but there is a question of all the sample being solubilized.

NPE Partition Coefficients
(Run 009)

Metal	In Clarified GL	In Dregs (g.)	Coeff. (K_{DG})	Mass Bal. Closure (%)
Ca	0.053	2.161	41	75
Fe	0.003	0.201	67	83
Mg	0.014	0.390	28	78
Mn	0.0004	0.308	770	81
Al	0.053	0.026	0.49	149
Si	0.120	0.003	0.02	262
Na	248.7	2.307	0.01	109

NPE Partition Coefficients
(Run 019)

Metal	In Clarified GL	In Dregs (g.)	Coeff. (K_{DG})	Mass Bal. Closure (%)
Ca	0.042	1.142	27	52
Fe	0.002	0.088	44	64
Mg	0.010	0.189	19	60
Mn	0.001	0.147	147	58
Al	0.007	0.045	6	98
Si	0.467	0.004	0.01	1002
Na	281.0	1.971	0.01	123

From these results, it is evident that, not too surprisingly, Ca, Fe, Mg, and Mn will be predominantly in the dregs, while Na and Si will stay in the clarified green liquor; Al will be distributed somewhat evenly between the two phases.

CONCLUSIONS:

1. A literature survey of dregs composition, along with analyses of four actual mill dregs samples, have identified an "average" dregs composition. Carbon content showed the most variation, with values ranging from under 2% to 35%. This has led to an experimental strategy based upon two laboratory smelt compositions featuring low and high carbon content, namely 2% and 20%.

2. A laboratory smelt formation procedure and the equipment needed have been established to simulate recovery boiler smelt bed conditions. The smelts are then dissolved in a hot synthetic weak wash and settling/filtration rates are determined in a heated settling column. Chemical equilibrium calculations have indicated the compositional changes to be expected when the initial compositions, based upon purchased chemicals, are subjected to smelting conditions, followed by dissolution to make green liquor. The ultimate chemical forms of the NPE's chosen for this study are predicted to be as $Ca(OH)_2$, $Mg(OH)_2$, MnS, SiO_2, $NaAlO_2$, and FeS; in reality other forms may exist.

3. Partition coefficients between dregs and clarified green liquor show Ca, Fe, Mg, and Mn to favor the dregs, while Na and Si stay with the green liquor; Al is distributed more evenly between the two phases.

4. Initial work with the heated dregs settling column has identified a number of experimental difficulties associated with identifying interfaces in a nearly opaque environment. Experimental techniques are under development.

FUTURE ACTIVITY:

Generation of synthetic smelts with 2% and 20% carbon in the dregs fraction will be completed, using purchased chemicals and equilibrated at 800°C under N_2 for 60 minutes. These will be dissolved in hot synthetic weak wash and the settling/filtration rates determined. Chemical and physical properties of the dregs produced will be determined. For comparison and validation reasons, kraft smelt from a mill will be subjected to the same procedures and results compared with a green liquor sample from the same mill. A sampling probe, based on a prototype used by Temple-Inland, has been designed and is being fabricated for sampling smelt from a spout.

The runs with increased levels of NPE's pose a difficult question as to what concentrations should be investigated. Existing liquor cycle models can not yet predict NPE buildup levels. Until such capability is possible, in each run, one NPE chemical will be added at ten times its base case amount to determine the effect of the elevated level of that particular NPE on dregs removal properties. One additional run will be made with all NPE'added to test for possible interactions. The cations to be included are: Al, Si, Fe, Ca, Mn, and Mg.

LITERATURE CITED:

1. Erickson, L.D. and Holman, K.L., AIChE Forest Products Symposium 1, 21-30 (1986).
2. Brunner, F.L. and Pulliam, T.L., TAPPI J. 76(7), 65-74 (1993).
3. Angevine, P., unpublished paper, 1993.
4. Kietaanniemi, O. and Virkola, N., TAPPI J. 65(7), 89-92 (1982).
5. Green, R.P. and Hough, G., Chemical Recovery in the Alkaline Pulping Processe TAPPI Press, Atlanta, GA, 1992.
6. Dorris, G.M., 1992 Intl. Chem. Recov. Conf. Proc., 121-141 (1992).
7. Engdahl, H. and Tormikoski, P., Paperi ja Puu 76(5), 326-329 (1994).
8. Wimby, M., Gustafsson, T., and Larsson, P., 1995 Intl. Chem. Recov. Conf. Proc., A299-A303 (1995).
9. Empie, H.J. and Amundsen, M., IPST Progress Report (F01707), June, 1997.
10. Campbell, A.J., Pulp & Paper Can.82(4), 78-87 (1981).
11. Kiiskila, E. and Lindberg, H., 1995 Intl. Chem. Recov. Conf. Proc., B159-B163 (1995).

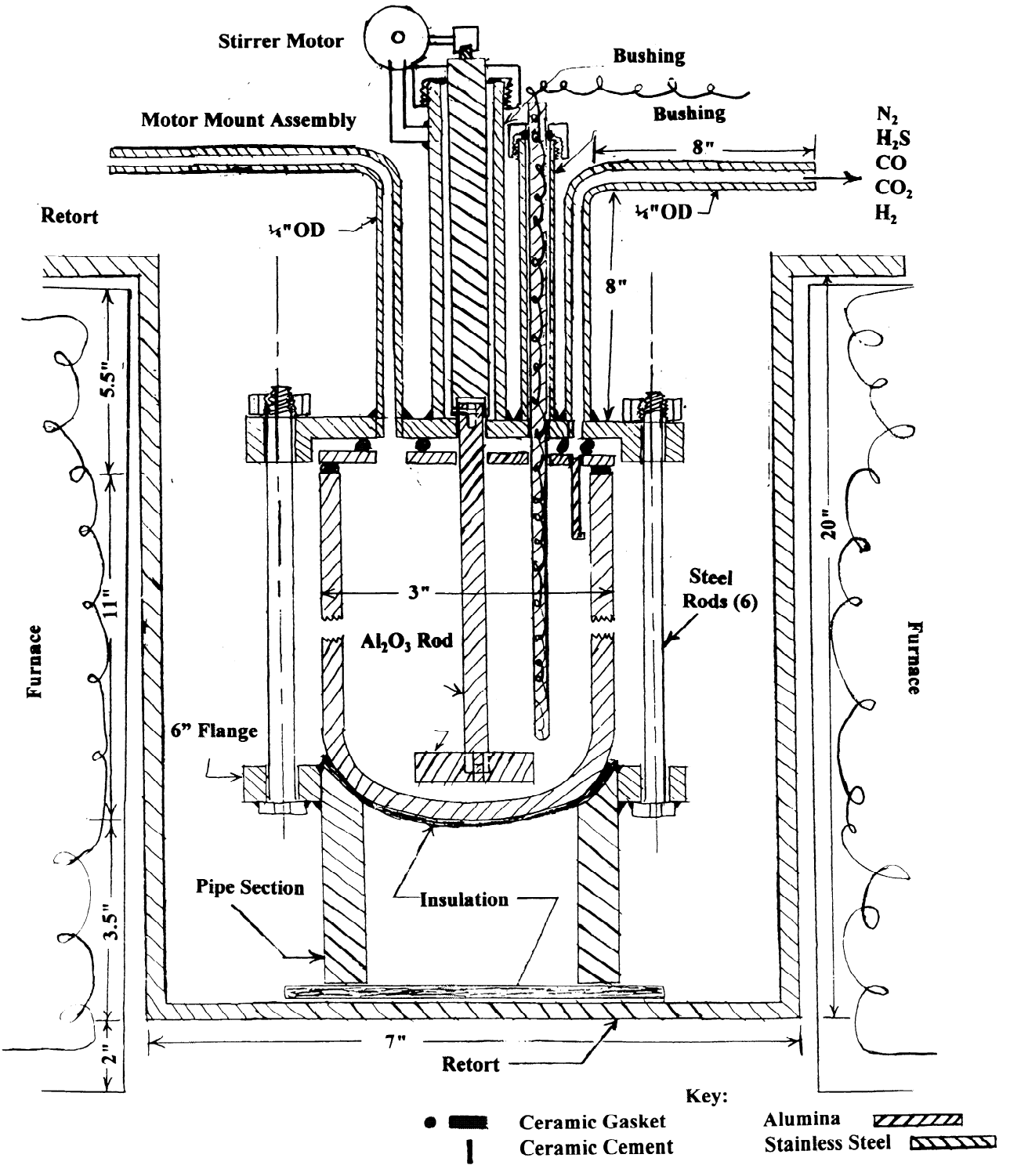

Fig.1 - Laboratory Smelt Reactor

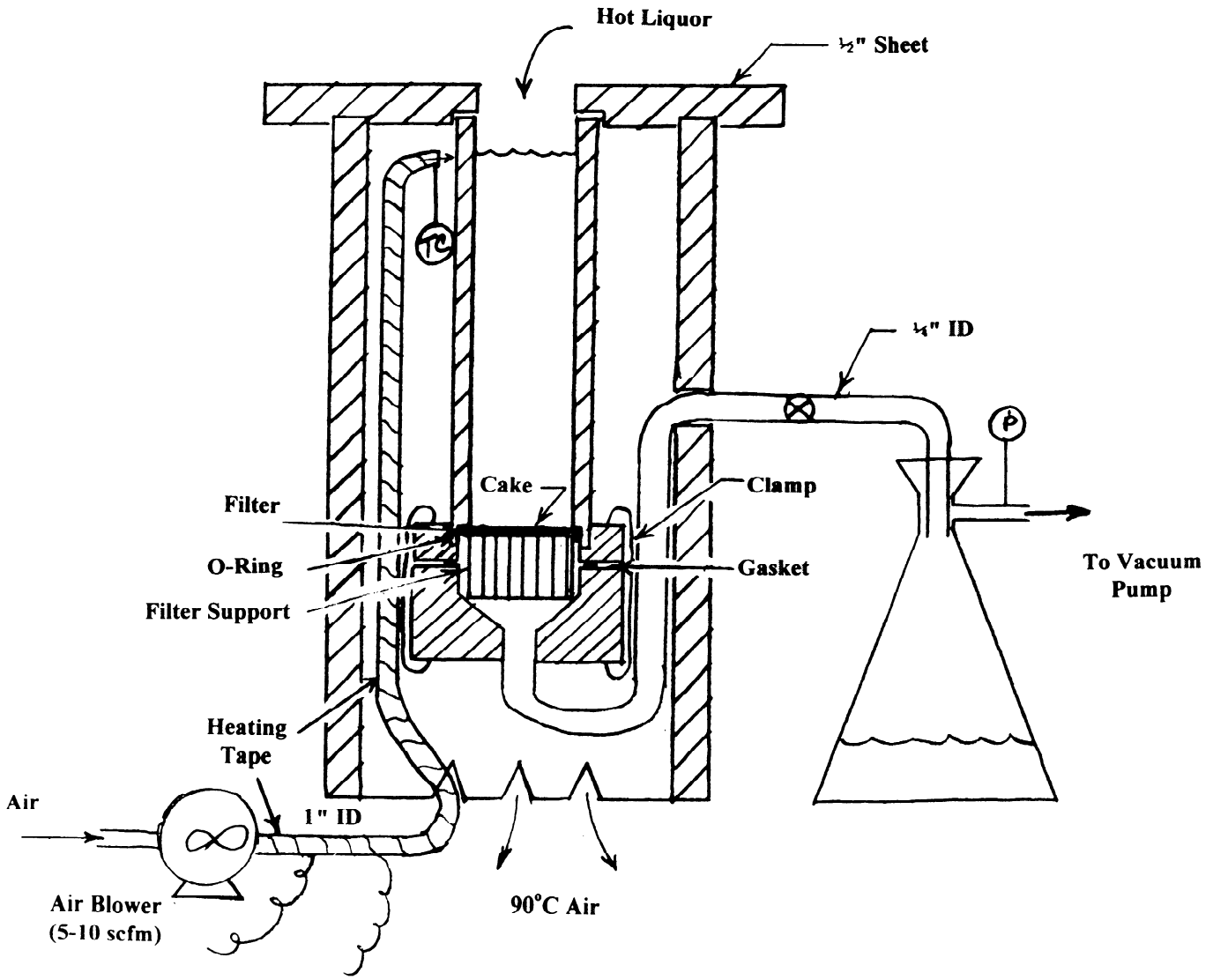

Fig. 2 - Sedimentation/Permeability Apparatus

Table 1 - Laboratory Smelt Formation Runs
Composition A

Species	Wt. %				
	Run 009	Run 040	Run 049	Run 053	Run 057
Na_2CO_3	70.6	70.6	69.0	69.8	70.5
Na_2S	23.5	23.5	22.93	23.26	23.5
Na_2SO_4	1.95	1.95	1.91	1.93	1.95
NaCl	1.95	1.95	1.91	1.93	1.95
$CaCO_3$	1.48	1.3	1.3	1.3	1.3
Fe_2O_3	0.07	0.07	0.07	0.07	0.07
$Mg(OH)_2$	0.25	0.25	**2.5**	0.25	0.25
MnO_2	0.12	0.12	0.12	**1.2**	0.12
SiO_2	0.02	0.20	0.20	0.20	0.20
Al_2O_3	0.02	0.02	0.02	0.02	**0.20**
C	0.04	0.04	0.04	0.04	0.04
	100.00	100.00	100.00	100.00	100.00

Table 2 - Smelt Formation at 800°C
(Base Case with 2% Carbon in Dregs)

SPECIES	Smelt In	Smelt In	Smelt Out	Smelt Out-In		L A	B	S	M E	L T
Run 009	g.	wt.fr.	g.	g.		Incr.	Decr.	Same	Elim.	Create
H2O	0	0			H2O					
Na2CO3	353	0.705986	354.56	1.56	Na2CO3	x				
NaHCO3	0	0	0.22	0.22	NaHCO3					x
Na2S	117.5	0.234995	115.1	-2.4	Na2S		x			
Na2SO3	0	0	0.08	0.08	Na2SO3					x
Na2SO4	9.75	0.0195	8.85	-0.9	Na2SO4		x			
NaCl	9.75	0.0195	9.75	0	NaCl			x		
NaOH	0	0	1.53	1.53	NaOH					x
CaCO3	7.4	0.0148	6.5	-0.9	CaCO3		x			
Fe2O3	0.36	0.00072	0	-0.36	Fe2O3				x	
Mg(OH)2	1.25	0.0025	0.044	-1.206	Mg(OH)2		x			
MnO2	0.6	0.0012	0	-0.6	MnO2				x	
SiO2	0.1	0.0002	0.1	0	SiO2			x		
Al2O3	0.1	0.0002	0	-0.1	Al2O3				x	
C	0.2	0.0004	0.1	-0.1	C		x			
S		0	0.436	0.436	S					x
Ca(OH)2		0	0.016	0.016	Ca(OH)2					x
MgO		0	0.808	0.808	MgO					x
NaAlO2		0	0.157	0.157	NaAlO2					x
FeS		0	0.177	0.177	FeS					x
FeS2		0	0.279	0.279	FeS2					x
MnS		0	0.584	0.584	MnS					x
CaS		0	0.622	0.622	CaS					x
FeO		0	0.012	0.012	FeO					x
MnO		0	0.013	0.013	MnO					x
MgCO3		0	0.03	0.03	MgCO3					x
TOTAL	500.01	1	499.968	-0.042						

Table 3 - Smelt Formation at 800°C (New Base Case with High SiO_2)

SPECIES	Smelt In	Smelt In	Smelt Out	Smelt Out-In	Run 040	L A	B	S	M E	L T
Run 040	g.	wt.fr.	g.	g.		Incr.	Decr.	Same	Elim.	Create
H2O	0	0			H2O					
Na2CO3	353.05	0.706111	354.36	1.31	Na2CO3	x				
NaHCO3	0	0	0.22	0.22	NaHCO3					x
Na2S	117.45	0.234904	115.22	-2.23	Na2S		x			
Na2SO3	0	0	0.08	0.08	Na2SO3					x
Na2SO4	9.749	0.019498	8.85	-0.899	Na2SO4		x			
NaCl	9.76	0.01952	9.75	-0.01	NaCl			x		
NaOH	0	0	1.54	1.54	NaOH					x
CaCO3	6.483	0.012966	5.76	-0.723	CaCO3		x			
Fe2O3	0.348	0.000696	0	-0.348	Fe2O3				x	
Mg(OH)2	1.251	0.002502	0.045	-1.206	Mg(OH)2		x			
MnO2	0.597	0.001194	0	-0.597	MnO2				x	
SiO2	1.002	0.002004	1	-0.002	SiO2			x		
Al2O3	0.102	0.000204	0	-0.102	Al2O3				x	
C	0.2	0.0004	0.1	-0.1	C		x			
S		0	0.44	0.44	S					x
Ca(OH)2		0	0.01	0.01	Ca(OH)2					x
MgO		0	0.81	0.81	MgO					x
NaAlO2		0	0.16	0.16	NaAlO2					x
FeS		0	0.17	0.17	FeS					x
FeS2		0	0.27	0.27	FeS2					x
MnS		0	0.58	0.58	MnS					x
CaS		0	0.5	0.5	CaS					x
FeO		0	0.01	0.01	FeO					x
MnO		0	0.015	0.015	MnO					x
MgCO3		0	0.03	0.03	MgCO3					x
TOTAL	499.992	1	499.92	-0.072						

Table 4 - Smelt Formation at 800°C (Mg Content 10X)

SPECIES Run 049	Smelt In g.	Smelt In wt.fr.	Smelt Out g.	Smelt Out-In g.	Run 049	L A Incr.	B Decr.	S Same	M E Elim.	L T Create
H2O	0	0			H2O					
Na2CO3	344.8	0.689683	342.27	-2.53	Na2CO3		x			
NaHCO3	0	0	1.11	1.11	NaHCO3					x
Na2S	114.787	0.229602	108.72	-6.067	Na2S		x			
Na2SO3	0	0	0.08	0.08	Na2SO3					x
Na2SO4	9.55	0.019102	8.95	-0.6	Na2SO4		x			
NaCl	9.55	0.019102	9.55	0	NaCl			x		
NaOH	0	0	7.78	7.78	NaOH					x
CaCO3	6.501	0.013004	5.43	-1.071	CaCO3		x			
Fe2O3	0.351	0.000702	0	-0.351	Fe2O3				x	
Mg(OH)2	12.5	0.025003	6.14	-6.36	Mg(OH)2		x			
MnO2	0.601	0.001202	0	-0.601	MnO2				x	
SiO2	0.999	0.001998	0.999	0	SiO2			x		
Al2O3	0.101	0.000202	0	-0.101	Al2O3				x	
C	0.2	0.0004	0.44	0.24	C	x				
S		0	1.95	1.95	S					x
Ca(OH)2		0	0.34	0.34	Ca(OH)2					x
MgO		0	4.24	4.24	MgO					x
NaAlO2		0	0.16	0.16	NaAlO2					x
FeS		0	0.17	0.17	FeS					x
FeS2		0	0.27	0.27	FeS2					x
MnS		0	0.58	0.58	MnS					x
CaS		0	0.43	0.43	CaS					x
FeO		0	0.01	0.01	FeO					x
MnO		0	0.015	0.015	MnO					x
MgCO3		0	0.16	0.16	MgCO3					x
TOTAL	499.94	1	499.794	-0.146						

Table 5 - Smelt Formation at 800°C (Mn Content 10X)

SPECIES Run 053	Smelt In g.	Smelt In wt.fr.	Smelt Out g.	Smlt Out-In g.	Run 053	L A Inc.	B Dec.	S Same	M E Elim.	L T Create
H2O	0	0			H2O					
Na2CO3	349	0.698134	353.17	4.17	Na2CO3	x				
NaHCO3	0	0	0.003	0.003	NaHCO3					x
Na2S	116.2	0.232445	110.67	-5.53	Na2S		x			
Na2SO3	0	0	0.09	0.09	Na2SO3					x
Na2SO4	9.652	0.019308	10.91	1.258	Na2SO4	x				
NaCl	9.652	0.019308	9.652	0	NaCl			x		
NaOH	0	0	1.698	1.698	NaOH					x
CaCO3	6.494	0.01299	4.345	-2.149	CaCO3		x			
Fe2O3	0.353	0.000706	0	-0.353	Fe2O3				x	
Mg(OH)2	1.251	0.002502	0	-1.251	Mg(OH)2				x	
MnO2	5.999	0.012	0	-5.999	MnO2				x	
SiO2	1.002	0.002004	1.002	0	SiO2			x		
Al2O3	0.101	0.000202	0	-0.101	Al2O3				x	
C	0.2	0.0004	0	-0.2	C				x	
S		0	0	0	S					
Ca(OH)2		0	0.013	0.013	Ca(OH)2					x
MgO		0	0.856	0.856	MgO					x
NaAlO2		0	0.16	0.16	NaAlO2					x
FeS		0	0.122	0.122	FeS					x
CaO		0	0.234	0.234	CaO					x
MnS		0	3.64	3.64	MnS					x
CaS		0	1.232	1.232	CaS					x
FeO		0	0.2	0.2	FeO					x
MnO		0	1.93	1.93	MnO					x
MgCO3		0	0	0	MgCO3					
TOTAL	499.904	1	499.927	0.023						

Table 6 - Smelt Formation at 800°C (Al Content 10X)

SPECIES	Smelt In	Smelt In	Smelt Out	Smelt Out-In	Run 057	L A	B	S	M E	L T
Run 057	g.	wt.fr.	g.	g.		Incr.	Decr.	Same	Elim.	Create
H2O	0	0			H2O					
Na2CO3	352.3	0.704584	353.38	1.08	Na2CO3	x				
NaHCO3	0	0	0.217	0.217	NaHCO3					x
Na2S	117.3	0.234595	114.66	-2.64	Na2S		x			
Na2SO3	0	0	0.08	0.08	Na2SO3					x
Na2SO4	9.746	0.019492	8.87	-0.876	Na2SO4		x			
NaCl	9.75	0.0195	9.75	0	NaCl			x		
NaOH	0	0	1.543	1.543	NaOH					x
CaCO3	6.5	0.013	5.77	-0.73	CaCO3		x			
Fe2O3	0.347	0.000694	0	-0.347	Fe2O3				x	
Mg(OH)2	1.257	0.002514	0.046	-1.211	Mg(OH)2		x			
MnO2	0.602	0.001204	0	-0.602	MnO2				x	
SiO2	1.006	0.002012	1.005	-0.001	SiO2			x		
Al2O3	1.001	0.002002	0.16	-0.841	Al2O3		x			
C	0.202	0.000404	0.135	-0.067	C		x			
S		0	0.591	0.591	S					x
Ca(OH)2		0	0.014	0.014	Ca(OH)2					x
MgO		0	0.813	0.813	MgO					x
NaAlO2		0	1.35	1.35	NaAlO2					x
FeS		0	0.17	0.17	FeS					x
FeS2		0	0.268	0.268	FeS2					x
MnS		0	0.584	0.584	MnS					x
CaS		0	0.499	0.499	CaS					x
FeO		0	0.013	0.013	FeO					x
MnO		0	0.015	0.015	MnO					x
MgCO3		0	0.03	0.03	MgCO3					x
TOTAL	500.011	1	499.963	-0.048						

Table 7 - Equilibrium Green Liquor
(Base Case with 2% Carbon in Dregs)

SPECIES	Raw GL In	GL Out	GL Out	GLS Out-In	Solids Out-In		G R E E N		L I Q U	
Run 009	g.	g.	wt.fr.(dry)	g.	g.		Incr.	Decr.	Same	Elim.
H2O	2435.4	2435.4				H2O				
Na2CO3	354.56	362.67	0.64494	8.11	9.67	Na2CO3	x			
NaHCO3	0.22	0	0	-0.22	0	NaHCO3				x
Na2S	115.1	116.98	0.208027	1.88	-0.52	Na2S	x			
Na2SO3	0.08		0	-0.08	0	Na2SO3				x
Na2SO4	8.85	8.89	0.015809	0.04	-0.86	Na2SO4	x			
NaCl	9.75	9.75	0.017339	0	0	NaCl			x	
NaOH	64.03	56.1	0.099763	-7.93	-6.4	NaOH		x		
CaCO3	6.5	0	0	-6.5	-7.4	CaCO3				x
Fe2O3	0	0	0	0	-0.36	Fe2O3			x	
Mg(OH)2	0.044	1.23	0.002187	1.186	-0.02	Mg(OH)2	x			
MnO2	0	0	0	0	-0.6	MnO2			x	
SiO2	0.1	0.1	0.000178	0	0	SiO2			x	
Al2O3	0	0	0	0	-0.1	Al2O3			x	
C	0.1	0	0	-0.1	-0.2	C				x
S	0.436	0	0	-0.436		S				x
Ca(OH)2	0.016	5.46	0.00971	5.444	5.46	Ca(OH)2	x			
MgO	0.808	0	0	-0.808	0	MgO				x
NaAlO2	0.157	0.157	0.000279	0	0.157	NaAlO2			x	
FeS	0.177	0.394	0.000701	0.217	0.394	FeS	x			
FeS2	0.279	0	0	-0.279	0	FeS2				x
MnS	0.584	0.6	0.001067	0.016	0.6	MnS	x			
CaS	0.622	0	0	-0.622	0	CaS				x
FeO	0.012	0	0	-0.012	0	FeO				x
MnO	0.013	0	0	-0.013	0	MnO				x
MgCO3	0.03	0	0	-0.03	0	MgCO3				x
TOTAL	2997.868	2997.731		-0.137	-0.179					

Table 8 - Equilibrium Green Liquor (New Base Case with High SiO_2)

SPECIES	Raw GL In	GL Out	GL Out	GLS Out-In	Slds Out-In	Run 040	G R E E N L I Q U				
Run 040	g	g	wt.fr.(dry)	g	g		Inc.		Dec.	Same	Elim.
H2O	2435.4	2435.4				H2O					
Na2CO3	354.36	361.65	0.643294	7.29	8.6	Na2CO3	x				
NaHCO3	0.22	0	0	-0.22	0	NaHCO3					x
Na2S	115.22	116.92	0.207974	1.7	-0.53	Na2S	x				
Na2SO3	0.08		0	-0.08	0	Na2SO3					x
Na2SO4	8.85	8.89	0.015813	0.04	-0.859	Na2SO4	x				
NaCl	9.75	9.75	0.017343	0	-0.01	NaCl				x	
NaOH	64.04	56.82	0.10107	-7.22	-5.68	NaOH			x		
CaCO3	5.76	0	0	-5.76	-6.483	CaCO3					x
Fe2O3	0	0	0	0	-0.348	Fe2O3				x	
Mg(OH)2	0.045	1.237	0.0022	1.192	-0.014	Mg(OH)2	x				
MnO2	0	0	0	0	-0.597	MnO2				x	
SiO2	1	1	0.001779	0	-0.002	SiO2				x	
Al2O3	0	0	0	0	-0.102	Al2O3				x	
C	0.1	0	0	-0.1	-0.2	C					x
S	0.44	0	0	-0.44		S					x
Ca(OH)2	0.01	4.78	0.008503	4.77	4.78	Ca(OH)2	x				
MgO	0.81	0	0	-0.81	0	MgO					x
NaAlO2	0.16	0.16	0.000285	0	0.16	NaAlO2				x	
FeS	0.17	0.38	0.000676	0.21	0.38	FeS	x				
FeS2	0.27	0	0	-0.27	0	FeS2					x
MnS	0.58	0.598	0.001064	0.018	0.598	MnS	x				
CaS	0.5	0	0	-0.5	0	CaS					x
FeO	0.01	0	0	-0.01	0	FeO					x
MnO	0.015	0	0	-0.015	0	MnO					x
MgCO3	0.03	0	0	-0.03	0	MgCO3					x
TOTAL	2997.82	2997.585		-0.235	-0.307						

Table 9 - Equilibrium Green Liquor (Mg Content 10X)

SPECIES	Raw GL In	GL Out	GL Out	GLS Out-In	Slds Out-In	Run 049	G R E E N	L I Q U
Run 049	g.	g.	wt.fr.(dry)	g.	g.		Incr. / Decr. / Same / Elim.	
H2O	2435.4	2435.4				H2O		
Na2CO3	342.27	353.54	0.628986	11.27	8.74	Na2CO3	x	
NaHCO3	1.11	0	0	-1.11	0	NaHCO3		x
Na2S	108.72	114.24	0.203245	5.52	-0.547	Na2S	x	
Na2SO3	0.08		0	-0.08	0	Na2SO3		x
Na2SO4	8.95	8.66	0.015407	-0.29	-0.89	Na2SO4	Decr.	
NaCl	9.55	9.55	0.01699	0	0	NaCl	Same	
NaOH	70.28	56.83	0.101107	-13.45	-5.67	NaOH	Decr.	
CaCO3	5.43	0	0	-5.43	-6.501	CaCO3		x
Fe2O3	0	0	0	0	-0.351	Fe2O3	Same	
Mg(OH)2	6.14	12.32	0.021919	6.18	-0.18	Mg(OH)2	x	
MnO2	0	0	0	0	-0.601	MnO2	Same	
SiO2	0.999	0.999	0.001777	0	0	SiO2	Same	
Al2O3	0	0	0	0	-0.101	Al2O3	Same	
C	0.44	0	0	-0.44	-0.2	C		x
S	1.95	0	0	-1.95		S		x
Ca(OH)2	0.34	4.8	0.00854	4.46	4.8	Ca(OH)2		x
MgO	4.24	0	0	-4.24	0	MgO		x
NaAlO2	0.16	0.16	0.000285	0	0.16	NaAlO2	Same	
FeS	0.17	0.38	0.000676	0.21	0.38	FeS	x	
FeS2	0.27	0	0	-0.27	0	FeS2		x
MnS	0.58	0.6	0.001067	0.02	0.6	MnS	Same	
CaS	0.43	0	0	-0.43	0	CaS	x	
FeO	0.01	0	0	-0.01	0	FeO		x
MnO	0.015	0	0	-0.015	0	MnO		x
MgCO3	0.16	0	0	-0.16	0	MgCO3		x
TOTAL	2997.694	2997.479		-0.215	-0.361			
Dry Basis	562.294	562.079	1	-0.215				

Table 10 - Green Liquor Formation (High Mn Content)

SPECIES	Raw GL In	GL Out	GL Out	GLS Out-In	Slds Out-In	Run 053	G R E E N	L I Q U
Run 053	g	g	wt.fr.(dry)	g	g		Inc. Dec.	Same Elim.
H2O	2435.4	2434.3				H2O		
Na2CO3	353.17	357.81	0.63505	4.64	8.81	Na2CO3	x	
NaHCO3	0.003	0	0	-0.003	0	NaHCO3		x
Na2S	110.67	109.61	0.194539	-1.06	-6.59	Na2S	x	
Na2SO3	0.09		0	-0.09	0	Na2SO3		x
Na2SO4	10.91	10.99	0.019505	0.08	1.338	Na2SO4	x	
NaCl	9.652	9.652	0.017131	0	0	NaCl		x
NaOH	64.198	61.79	0.109666	-2.408	-0.71	NaOH	x	
CaCO3	4.345	0	0	-4.345	-6.494	CaCO3		x
Fe2O3	0	0	0	0	-0.353	Fe2O3		x
Mg(OH)2	0	1.232	0.002187	1.232	-0.019	Mg(OH)2	x	
MnO2	0	0	0	0	-5.999	MnO2		x
SiO2	1.002	1.002	0.001778	0	0	SiO2		x
Al2O3	0	0	0	0	-0.101	Al2O3		x
C	0	0	0	0	-0.2	C		x
S	0	0	0	0		S		
Ca(OH)2	0.013	4.793	0.008507	4.78	4.793	Ca(OH)2	x	
MgO	0.856	0	0	-0.856	0	MgO		x
NaAlO2	0.16	0.16	0.000284	0	0.16	NaAlO2		x
FeS	0.122	0.385	0.000683	0.263	0.385	FeS	x	
CaO	0.234	0	0	-0.234	0	CaO		x
MnS	3.64	6.007	0.010661	2.367	6.007	MnS	x	
CaS	1.232	0.005	8.87E-06	-1.227	0.005	CaS	x	
FeO	0.2	0	0	-0.2	0	FeO		x
MnO	1.93	0	0	-1.93	0	MnO		x
MgCO3	0	0	0	0	0	MgCO3		
TOTAL	2997.827	2997.736		1.009	-0.068			

Table 11 - Green Liquor Formation (High Al Content)

SPECIES	Raw GL In	GL Out	GL Out	GLS Out-In	Solids Out-In		G R E E N		L I Q U	
Run 057	g.	g.	wt.fr.(dry)	g.	g.	Run 057	Incr.	Decr.	Same	Elim.
H2O	2435.4	2433.6				H2O				
Na2CO3	353.38	361.03	0.642222	7.65	8.73	Na2CO3	x			
NaHCO3	0.217	0	0	-0.217	0	NaHCO3				x
Na2S	114.66	116.77	0.207717	2.11	-0.53	Na2S	x			
Na2SO3	0.08	0	0	-0.08	0	Na2SO3				x
Na2SO4	8.87	8.87	0.015778	0	-0.876	Na2SO4			x	
NaCl	9.75	9.75	0.017344	0	0	NaCl			x	
NaOH	64.04	56.1	0.099794	-7.94	-6.4	NaOH		x		
CaCO3	5.77	0	0	-5.77	-6.5	CaCO3				x
Fe2O3	0	0	0	0	-0.347	Fe2O3			x	
Mg(OH)2	0.046	1.24	0.002206	1.194	-0.017	Mg(OH)2	x			
MnO2	0	0	0	0	-0.602	MnO2			x	
SiO2	1.005	1.005	0.001788	0	-0.001	SiO2			x	
Al2O3	0.16	0	0	-0.16	-1.001	Al2O3				x
C	0.135	0	0	-0.135	-0.202	C				x
S	0.591	0	0	-0.591		S				x
Ca(OH)2	0.014	4.8	0.008539	4.786	4.8	Ca(OH)2			x	
MgO	0.813	0	0	-0.813	0	MgO				x
NaAlO2	1.35	1.608	0.00286	0.258	1.608	NaAlO2	x			
FeS	0.17	0.383	0.000681	0.213	0.383	FeS	x			
FeS2	0.268	0	0	-0.268	0	FeS2				x
MnS	0.584	0.602	0.001071	0.018	0.602	MnS	x			
CaS	0.499	0	0	-0.499	0	CaS				x
FeO	0.013	0	0	-0.013	0	FeO				x
MnO	0.015	0	0	-0.015	0	MnO				x
MgCO3	0.03	0	0	-0.03	0	MgCO3				x
TOTAL	2997.86	2995.758		-0.302	-2.15					
Dry Basis	562.46	562.158	1	-0.302						

Table 12 - Predicted Dregs Composition of NPE's (Run 009)

Element Expressed As	Amt. Charged (g.)	Dregs Compound (mg./kg.)	Wt.Fr.	HSC Equil. Dregs (g.)	(Wt. Fr.) .
$CaCO_3$	7.40	-	-	0	0
$Ca(OH)_2$	0	273,800	0.68	5.46	0.69
$Mg(OH)_2$	1.25	39,400	0.10	1.23	0.15
MnO_2	0.60	-	-	0	0
MnS	0	33,400	0.08	0.60	0.08
SiO_2	0.10	400	0.001	0.10	0.01
Al_2O_3	0.10	-	-	0	0
$NaAlO_2$	0	5,300	0.015	0.16	0.02
Fe_2O_3	0.35	-	-	0	0
FeS	0	21,700	0.05	0.39	0.05
C	0.20	30,000	0.075	0	0 .
	10.00	404,000	1.00	7.94	1.00

Table 13 - Predicted Dregs Composition of NPE's (Run 019)

Element Expressed As	Amt. Charged (g.)	Dregs Compound (mg./kg.)	Wt.Fr.	HSC Equil. Dregs (g.)	(Wt. Fr.) .
$CaCO_3$	4.90	-	-	0	0
$Ca(OH)_2$	0	182,200	0.62	3.61	0.51
$Mg(OH)_2$	0.80	39,400	0.13	0.79	0.11
MnO_2	0.40	-	-	0	0
MnS	0	20,100	0.07	0.40	0.06
SiO_2	0.10	700	0.002	0.10	0.01
Al_2O_3	0.10	-	-	0	0
$NaAlO_2$	0	11,800	0.04	0.16	0.02
Fe_2O_3	0.20	-	-	0	0
FeS	0	11,900	0.04	0.22	0.03
C	3.50	28,000	0.10	1.81	0.26 .
	10.00	294,100	1.00	7.94	1.00

DUES-FUNDED PROJECT SUMMARY

Project Title:	VOC in Kraft Mills
Project Code:	
Project Number:	F01708
PAC:	Recovery
Division:	Chemical Recovery and Corrosion Division
Project Staff	
Faculty/Senior Staff:	Junyong Zhu
Staff:	Garry Heedick
FY 98-99 Budget:	$35,000
Allocated as Matching Funds:	$42,000
Time Allocation	
Faculty/Senior Staff:	Junyong Zhu: 25%
Support:	Garry Heedick: 40%
Supporting Research	
M.S. Students:	Jeffrey Colson
Ph.D. Students:	
External:	Xinsheng Chai (Post Doctor supported by DOE)

RESEARCH LINE/ROADMAP: Environmental Performance: 5. Reduce emissions of the entire pulp and paper manufacturing process to meet Tier 3 Cluster Rule criteria while maintaining global competitiveness.

PROJECT OBJECTIVE:

Develop a VOC database of concentrations and vapor-liquid phase equilibrium on various kraft mill streams.

PROJECT BACKGROUND:

The release of VOC into air is an environmental concern. Many VOCs are on the list of hazardous air pollutants (HAPs). The cluster role now requires to control VOCs in many kraft mill processes. The present study will provide database for the control of VOC as well as for computer models to predict VOC emissions in kraft mills.

SUMMARY OF RESULTS:

- Developed measurement techniques to determine VOC concentration and Henry's constants in kraft mill streams.
- Developed an experimental protocol using the techniques reported.
- Conducted VOC measurements in kraft mill streams.
- Obtained empirical correlations of methanol Henry's constant in black liquors.
- Conducted a full air and stream sampling

GOALS FOR FY 98-99:

- Develop understanding and quantify VOC formation during pulping.
- Develop understanding and quantify VOC formation during the evaporation of black liquors.
- Quantify the concentration of sulfur compounds in kraft mill streams.
- Develop understanding the role of resin and fatty acids in kraft mill streams on the Henry's constant of VOCs.
- Another full mill sampling of VOC in both air and streams.

DELIVERABLES:

- Develop an experimental apparatus for black liquor evaporation study
- A report on the understanding and quantifying VOC formation in pulping
- A report on the understanding and quantifying VOC formation in black liquor evaporation

SCHEDULE (Attach Timeline):

- Black liquor evaporation apparatus: months 1-2
- Report on VOC formation in pulping: month 1-3
- Report on VOC formation in evaporation: month 9-12
- Report on mill sampling: month 6-9

INSTITUTE OF PAPER SCIENCE AND TECHNOLOGY

Atlanta, Georgia

Volatile Organic Compounds (VOC) in Kraft Mill Streams -

Part II:

Protocol Development to Measure the Contents and Henry's Constants of VOC's in Kraft Mill Streams

Part III:

Vapor-Liquid Equilibrium Partitioning of Methanol in Black Liquors

Project F01708

Report 2 and 3

to the

MEMBER COMPANIES OF THE INSTITUTE OF PAPER SCIENCE AND TECHNOLOGY

January 1998

Volatile Organic Compounds (VOCs) in Kraft Mill Streams - Part II: Protocol Development to Measure the Contents and Henry's Constants of VOC's in Kraft Mill Streams

J.Y. Zhu, X.S. Chai, and B. Dhasmana
Institute of Paper Science and Technology
500 10th Street, N.W.
Atlanta, GA 30318, USA
(404) 894-5310 (404) 894-4778 (Fax)

ABSTRACT

VOC emission in kraft mills has been an environmental concern. The VOC content and the vapor-liquid phase equilibrium are the two factors that dictate VOC emission. The present report document the measurement protocol to develop a database that describes the contents and the VLE behaviors of VOC's in various kraft mill streams using a commercial headspace gas chromatographic system with the methods described in Part I of this report. The methods are indirect, rapid, automated, and do not require modification of the sample matrix. Validation experiments with VOC-water mixtures indicate that the methods are accurate. Preliminary results of various mill streams are also obtained using the developed protocol.

INTRODUCTION

The new toxic and permit provisions of the 1990 clean air amendments require information on emissions of volatile organic compounds (VOC's) from pulp and paper mill sources. Many VOC's are now on the list of hazardous air pollutants. Several studies on VOC emissions at kraft mills have been conducted. Venketesh et al. [1] reported a millwide VOC prediction using a process simulation technique. The National Council of the Paper Industry for Air and Stream Improvement (NCASI) conducted a series of studies on VOC emissions at kraft mills. NCASI's studies [2] indicated that the VOC content and the thermodynamic vapor-liquid phase equilibrium behavior of VOC's are two of the key factors that affect the release of VOC's during mill operations. Therefore, a database that quantifies the contents and the VLE behaviors of VOC's in kraft mill streams is very important for understanding VOC emissions and emission predictions using computer simulation models [3]. Unfortunately, limited experimental techniques are available for the determination of the contents and VLE behaviors of VOC's in kraft mill streams due to their corrosive nature.

Recently, Gunshefki and Cloutier [4] developed a method for measuring methanol contents in black liquor. However, the method involves a series of sample pretreatment. It is, therefore, very complicated, time-consuming, and less accurate. There are many methods available to study vapor-liquid phase equilibrium [5-7]; however, most available methods are complicated to implement and involve calibration. Much research on vapor-liquid phase equilibrium has been conducted using headspace (HS) GC systems [8-12] that provide direct vapor phase analysis. However, traditional HSGC methods require the direct

analysis of solute content in the sample stream, not suitable for mill stream VLE studies. Furthermore, most of the existing indirect HSGC methods have either practical difficulties to implement or complicated calibration procedures.

In this study, we report on the development of indirect methods for rapid, automated, and precise determination of the contents and the vapor-liquid phase equilibrium partitioning of VOC's in kraft mill streams using a commercial headspace gas chromatography system. The detail protocols for these measurements and the applications for the mill samples are also presented.

METHODOLOGY

Quantification of VOC Contents

The method is schematically described in Fig. 1. The method has been discussed in our previous study [13]. We use two sample vials filled with the same volume of sample solution. We then add a small amount of concentrated solution of known concentration into one of the vials. After a phase equilibrium is established within each vial, we conduct headspace GC analysis for each sample vial. Because of a very low concentration, the solute VLE partitioning coefficients in these two vials agree with Henry's Law, i.e.,

$$H_c = \frac{C_g^1}{C_1} = \frac{C_g^2}{C_2} \qquad (1)$$

where C_i and C_g^i are the solute concentrations in the liquid and vapor phases at equilibrium in vial i, respectively.

The amount of solutes in the vapor phase at equilibrium state in these two vials can be described as:

$$C_g^1 V_g^0 = C_0 V_l^0 - C_1 V_l^0, \qquad (2)$$

and

$$C_g^2 V_g^0 = C_0 V_l^0 + C_s V_s - C_2 V_l^0, \qquad (3)$$

where C_0 and C_s are the concentrations of the solute in the sample and in the standard solution, respectively. The V_l^0, V_s, and V_g^0 are the volumes of the sample, standard solution, and headspace, respectively.

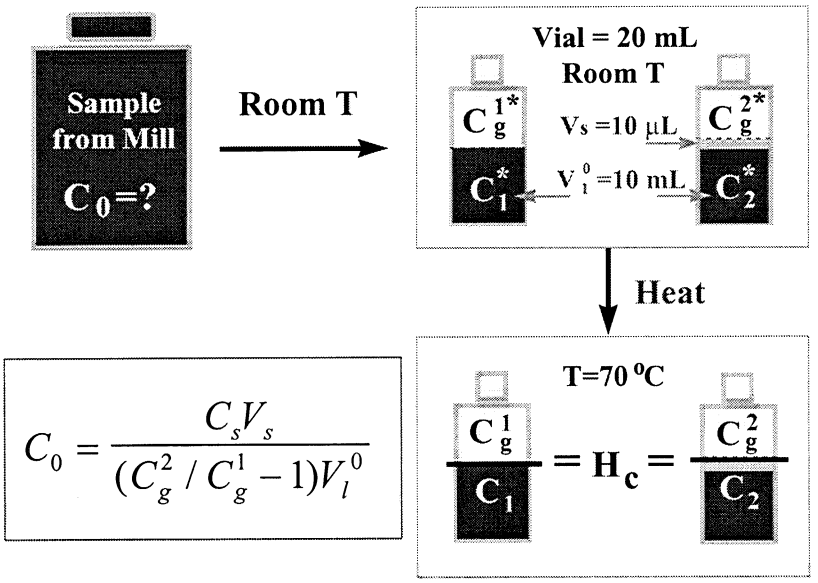

$$C_0 = \frac{C_s V_s}{(C_g^2 / C_g^1 - 1) V_l^0}$$

Fig. 1. Schematic diagram describing the present indirect HSGC method for VOC content measurements.

We can derive the initial solute concentration in the sample solution from Eqns. (2) and (3),

$$C_0 = \frac{C_s V_s}{(C_g^2 / C_g^1 - 1)V_l^0}, \qquad (4)$$

where we assume that the total volume of the solution in the vials remains the same because of $V_l^0 >> V_s$.

The ratio of the solute concentration in the vapor, C_g^2 / C_g^1, is proportional to the ratio of the peak areas, A_2 and A_1, measured from GC analysis. Thus, we can rewrite Eqn. (4) as,

$$C_0 = \frac{C_s V_s}{(A_2 / A_1 - 1)V_l^0}. \qquad (5)$$

Determination of VOC Henry's Constant

The indirect HSGC method for measuring VLE Henry's constant is schematically shown in Fig. 2. The method has been discussed in great detail in our previous study [14]. We used two vials filled with the same sample solution but significant volume difference. We then conducted headspace GC analysis for each vial when the phase equilibrium was established within the vials. Because the two vials contain the same dilute solution, the solute VLE partitioning coefficients in these two vials agree with Henry's Law as shown in Eqn. (1). We can express the total moles, M, of the solute in these two vials as follows,

$$M_1 = C_l^0 V_l^1 = C_l^1 V_l^1 + C_g^1 V_g^1 = C_g^1 \left[\left(V_l^1 / H_c \right) + V_g^1 \right], \qquad (6)$$

and

$$M_2 = C_l^0 V_l^2 = C_l^2 V_l^2 + C_g^2 V_g^2 = C_g^2 \left[\left(V_l^2 / H_c \right) + V_g^2 \right], \qquad (7)$$

where C_g is the concentration of solute in the vapor phase, and V_g is the vapor volume in the vial.

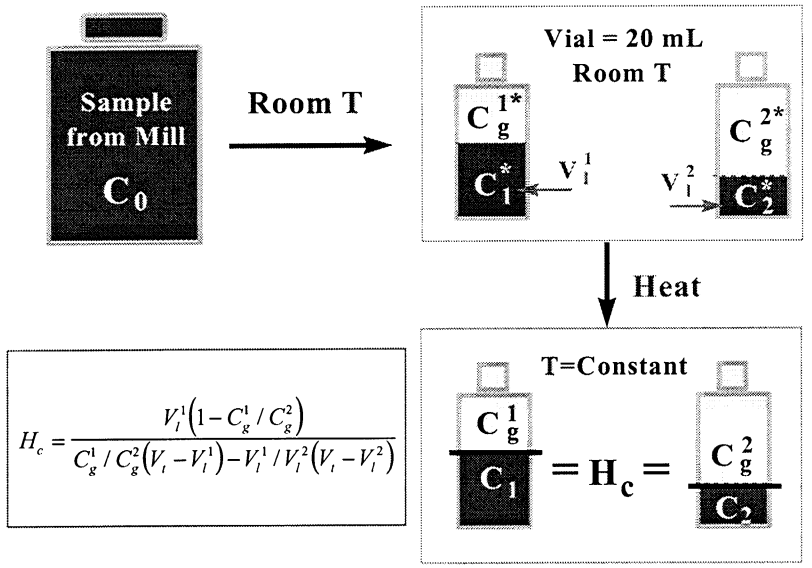

Fig. 2. Schematic diagram describing the present indirect HSGC method for VLE partitioning Henry's constant measurements.

We can derive the dimensionless Henry's constant H_c from Eqns. (6) and (7),

$$H_c = \frac{V_l^1\left(1 - C_g^1 / C_g^2\right)}{C_g^1 / C_g^2\left(V_t - V_l^1\right) - V_l^1 / V_l^2\left(V_t - V_l^2\right)} = \frac{V_l^1\left(1 - A_1 / A_2\right)}{A_1 / A_2\left(V_t - V_l^1\right) - V_l^1 / V_l^2\left(V_t - V_l^2\right)} \quad (8)$$

MEASUREMENT PROTOCOLS

I. Liquid VOC Content Measurement.

This measurement protocol is used to simultaneously determine liquid contents of methanol, MEK, and acetone in sample solution.

Apparatus

1. A gas chromatograph, HP 6890 (Hewlett-Packard) equipped with a single or dual column instrument with flame ionization detector (FID). A HP-5 capillary column (Hewlett-Packard) operated at 30°C with an injection port temperature of 250°C and a detector temperature of 250°C is used for species separation. GC conditions: helium carrier

gas flow rate: 3.8 ml/min, and hydrogen gas and compress air flow rates for the FID: 35 and 400 ml/min, respectively.

2. An automatic Headspace Sampler, HP-7694 (Hewlett-Packard). Headspace conditions: thermo equilibration time 25 min with gentle shaking, injection time: 1.0 min, vial pressurization time: 0.3-0.5 min, and sample loop fill time: 0.2 min. In headspace sampling, the solid, liquid, or gaseous sample is placed in a vial and sealed by a septum with a crimper. The sampling operation is controlled by a personal computer and automated.

3. Miscellaneous: volumetric flask, pipettes, 10 μl microsyringe, 20-ml vials.

Reagents

Standard mix solvent of methanol, acetone, and MEK. Preparation: Add about 9 ml of methanol into a 10-ml dried volumetric flask. Pipette 0.1 ml of MEK and 0.1 ml of Acetone into the volumetric flask, respectively, then fill methanol to the mark of 10 ml of the flask. The volume of the headspace in the volumetric flask should be as small as possible to avoid the vaporization of the solutes from the solvent. The concentrations of methanol, acetone, and MEK are 24.5, 0.135, and 0.111 mole/L, respectively.

Procedure

1. Pipette 10 ml of sample solution into three 20-ml vials, then close the vials.
2. Pipette 10 ml of sample solution into another three 20-ml vials. Add 10 μl of standard solvent by microsyringe into each vial, then close the vial.
3. Put the vials into the headspace Sampler for equilibration and then measure by the GC.
4. Triplicate run the samples in step 1, determine the peak areas at retention times of 2.24, 2.50, and 3.23 min for methanol, acetone, and MEK, respectively. Then calculate the average peak areas $\overline{A}_{1,MeOH}$, $\overline{A}_{1,acetone}$, and $\overline{A}_{1,MEK}$.

5. Triplicate run the samples in step 2, determine the peak areas at retention times of 2.24, 2.50, and 3.23 min for methanol, acetone, and MEK, respectively. Then calculate the average peak areas $\overline{A}_{2,MeOH}$, $\overline{A}_{2,acetone}$ and $\overline{A}_{2,MEK}$.

Calculation

Use the following equation to calculate the concentrations:

$$C_{0,i} = \frac{C_{s,i}V_s}{(\overline{A}_{2,i} / \overline{A}_{1,i} - 1)V_l^0}$$

where $C_{0,i}, C_{s,i}$ and V_l^0, V_s are i component concentrations and the volumes of the original testing sample and the standard solution in mole/L, respectively; $\overline{A}_{1,i}$ and $\overline{A}_{2,i}$ are the averaged GC peak areas of component i in the vapor phase measured before and after standard addition, respectively.

II. VLE Measurement.

This protocol is used to determine Henry's constant of VOC's in the sample solution.

Apparatus

The system and operating conditions of gas chromatography are the same as that mentioned in *Protocol I.* The operating conditions of the headspace Sampler are also the same as above, except the time of equilibration will be determined by the sample volume used in the experiment. The suggested sample volumes (*a* and *b*) and equilibrium time in the headspace Sampler are listed in Table I.

Procedure

1. Pipette *a* ml of sample solution into three 20-ml vials, then close the vials.
2. Pipette *b* ml of sample solution into another three 20-ml vials, then close the vials.
3. Put the vials into the Headspace Sampler for equilibration and then measure by the GC.
4. Triplicate run the samples in step 1, determine the peak area at the retention time of the solute as indictated in *Protocol I.* Then calculate the average peak areas $\overline{A}_{1,i}$.
5. Triplicate run the samples in step 2, determine the peak areas at the retention time of the solute. Then calculate the average peak areas $\overline{A}_{2,i}$.

Table I. Suggested sample volumes and equilibration time in headspace sampler.

Henry's constant	V_1, ml	V_2, ml	Equilibration time*, min.
0.001	0.1	0.01	5
0.01	1	0.1	15
0.1	10	1	25
1	10	5	25
10	10	7	25
100	10	9	25

*For the samples with humic matters or particles, HSGC analysis should be conducted immediately after adding sample solution into the vial.

Calculation

Use the following equation to calculate results:

$$H_c = \frac{V_1\left(1-\overline{A}_{1,i}/\overline{A}_{2,i}\right)}{\overline{A}_{1,i}/\overline{A}_{2,i}\left(V_t-V_1\right)-V_1/V_2\left(V_t-V_2\right)}$$

where H_c is the Henry's law constant (dimensionless). $\overline{A}_{1,i}$, $\overline{A}_{2,i}$ and V_1, V_2 are the average GC peak area of the *i* component measured and the sample volume (in ml) in vial 1 and 2, respectively.

APPLICATIONS

Measurement of Liquid VOC Contents in Mill Streams.

Methanol, acetone, and MEK are the major VOC species with lower boiling points in most mill streams. Traditional methods to measure these VOC's use organic solvents to extract them from the aqueous phase. These methods are time-consuming and less accurate due to a low concentration of these species in mill streams. With the present method (Protocol I), we can measure methanol, acetone, and MEK in various mill streams simultaneously. The measurements are rapid, automated, and accurate as demonstrated in a previous study [13]. Some results of VOC contents in various streams of a kraft mill are shown in Table II.

Measurement of Methanol Henry's Constant in Black Liquors.

It is known that 90 % of VOC's in mill streams is methanol. It is therefore important to understand methanol's thermodynamic behavior in these mill streams. The measurement of methanol Henry's constant in mill streams is also very difficult because it is very small. We can use the present method (Protocols II) to measure the Henry's constant of methanol in mill streams with a reasonable accuracy.

Both softwood and hardwood black liquor samples from a mill were used in this study. Fig. 3 shows the effect of temperature on the methanol Henry's constant in black liquors along with the data obtained in the methanol-water mixture. The results indicate that the logarithm of Henry's constant in the two black liquor samples decreases linearly with the inverse of temperature. The variation in the measured Henry's constant among these three types of samples is very significant. We believe that the significant variations in the composition, ionic strength, solid contents, etc., among these samples, may cause the large

variation in the Henry's constant. We will conduct a detailed study to understand the effect of various parameters on the Henry's constant in the future.

CONCLUSIONS

The present study reported on the methods and protocols to measure the contents and the vapor-liquid phase equilibrium partitioning coefficients of VOC's in mill streams using a commercial headspace gas chromatography system. Both methods are rapid, automated, accurate, and do not require calibration and modification of the sample matrix and can also be easily applied to various industrial and environmental streams. Preliminary measurements of VOC content and Henry's constant of methanol in kraft mill streams using the methods developed were conducted.

Table II. VOC contents measured in various streams from a pulp mill.

Sample Location Description	Label	MeOH (ppm)	Acetone (ppb)	MEK (ppb)
1st stage showers, 2nd stage filtrate	No. 1 Washer	209.5	494	406
	No. 2 Washer	275.0	484	394
2nd stage showers, 1st stage filtrate	No. 1 Washer	149.8	980	439
	No. 2 Washer	312.7	852	511
3rd stage showers	No. 1 Washer	122.6	683	452
	No. 2 Washer	203.8	715	526
side combined condensate (blow recovery)	No. 1 Washer	178.6	1327	592
	No. 2 Washer	382.6	1113	774
1st stage filtrate	No. 2 Washer	349.0	520	270
3rd stage filtrate	No. 1 Washer	332.2	930	564
combined weak black liquor to recovery		292.4	670	315
evaporator seal tank condensate	No. 2 (M24-	93.1	762	665
	No. 2 (24-0529)	673.1	4138	425
evaporator clean condensate	No. 3	2.0	-	31
	No. 3 (24-0509)	1.7	-	231
evaporator	No. 2	27.1	-	218
evaporator seal tank	No. 1 (M24-	3954.4	11	2706
combined condensate of hotwell	No. 3	659.1	16067	7826
paper-machine condensate	No. 1	3.3	-	59
	No. 2 & No. 3	3.5	-	124
top headbox	No. 1	57.4	323	108
	No. 2	55.3	260	129
base headbox	No. 1	88.8	433	167
	No. 2	64.9	315	158
headbox	No. 3	46.8	-	-
wire pit	No. 1	86.5	375	141
	No. 2	91.8	508	129
	No. 3	90.9	-	-
water reclaim sump	No. 1	13.0	192	62
vacuum dump	No. 2	20.6	-	-
side hill screen drain off	No. 3	65.7	-	-

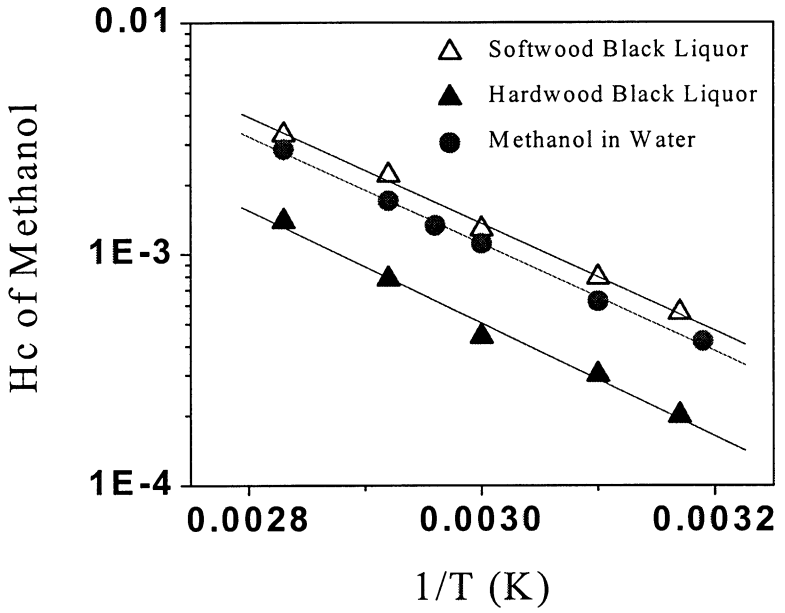

Fig. 3. Measured methanol Henry's constant in two black liquor samples.

ACKNOWLEDGEMENT

This research was supported by the United States Department of Energy (Grant No. DE-FC07-96ID13438) and the State of Georgia (Grant No. PP97-EN5).

REFERENCES

1. Venketesh, V., Lapp, W., and Parr, J., 1996 TAPPI International Environmental Conference and Exhibit 31 (1996).
2. Jain, A., TAPPI Minimum Effluent Mills Symposium (1996).
3. Gu, Y., Edwards, L.L., Haynes, J., and Euhus, L.E., (1997), Application of modular computer simulation to aid development of pulp and paper mill closure technology: VOC Prediction. Accepted for Publication by *Tappi J.*
4. Gunshefki, M. and Cloutier, S., NCASI Technical Memo (1994).
5. Mackay, D. and Shiu, W.Y., *J. Phys. Chem. Ref. Data,* 10 (1981) 1175.
6. Turner, L.H., Chiew, Y.C., Ahlert, R.C., and Kosson, D.S., *AIChE J.,* 42 (1996) 1772.
7. Sherman, S.R., Trampe, D.B., Bush, D.M., Schiller, M., Eckert, C.A., Dallas, A.J., Li, J., and Carr, P.W., *Ind. Eng. Chem. Res.,* 35 (1996) 1044.
8. Ioffe, B.V. and Vitenbery, A.G., "Head-Space Analysis and Related Methods in Gas Chromatography," John Wiley & Sons, Inc., New York, (1984).
9. Hussam, A. and Carr, P.W., *Anal. Chem.*, 57 (1985) 793.
10. Kolb, B., Welter, C., and Bichler, C., Chromatographia 34 (1992) 235.
11. Jones, W., Egoville, M.J., Strolle, E.O., and Dellamonien, E.S., *J. Chromatogr.* 455(1988) 45.
12. Lincoff, A.H. and Gossett, J.M., In Gas Transfer at Water Surfaces, Brutsaert, W. and Jirka, G.H., Eds. Reidel: Dordrecht, Holland, p.17, (1984).
13. Chai, X.-S., Dhasmana, B., and Zhu, J.Y., J. Pulp & Paper Sci., **24**(2) (1998), (in press)
14. Chai, X.-S. and Zhu, J.Y., accepted for publication by *J. Chromatogr. A.,* (1998),

Volatile Organic Compounds (VOCs) in Kraft Mill Streams -

Part III: Vapor-Liquid Phase Equilibrium Partitioning of Methanol in Black Liquors

J.Y. Zhu* and X.S. Chai
Institute of Paper Science and Technology
500 10th Street, N.W.
Atlanta, GA 30318

ABSTRACT

In Part III of this report, we report on the behaviors of methanol vapor-liquid partitioning in various weak black liquor samples. We used six samples from four kraft mills and five samples collected from our laboratory batch pulping processes under known pulping conditions. The samples have a good representation of black liquors yielded from hardwood and softwood, kraft and soda pulping processes. We found that temperature and total solids content are the two major factors that affect the Henry's constant of methanol in black liquor samples. Linear regression analysis indicates that the methanol Henry's constant in black liquors increases exponentially with the inverse of temperature in Kelvin and decreases linearly with the total solids content.

Application:

Analysis of VOC content and VLE partitioning in mill and environmental streams.

Keywords:

VOC, Henry's law, vapor-liquid partitioning, headspace, GC, black liquor, mill streams.

INTRODUCTION

The vapor-liquid phase equilibrium partitioning is one of the key factors that dictates VOC emission at Kraft mills as we discussed in Part I of this study. The VLE partitioning approach has been used in computer models to describe the VOC emission in various mill processes [1, 2]. This type of computer model can provide a predictive tool for mills to qualitatively determine VOC emissions when processes change. Unfortunately, few studies have been conducted on the VLE behavior of VOC's in mill streams. The understanding of the subject is very limited. A previous study by NCASI [3] indicated that using existing VLE data obtained in VOC-water mixtures overpredict VOC emission. Therefore, it is important to develop a VLE database of VOC's in Kraft mill streams that can be used as an input of computer models for accurate prediction of VOC emissions.

As we discussed in Part I of this study, the VOC contents in various Kraft mill streams are very low; therefore, Henry's Law best describes the VLE partitioning behavior of VOC's. Because methanol is the major species that accounts for more than 90% of the VOC emission in Kraft mills [4] and black liquor is one of the most difficult stream to analysis, we focus our research on the measurements of Henry's constant of methanol in various black liquor samples using the method and protocol developed in Parts I and II of this study. The objective of this part of the study is to understand the major factors that affect the VLE partitioning of methanol in various black liquor samples. Black liquor has a very complex composition, which contains dissolved lignin and other humic material; therefore, the understanding of the effects of various composition parameters on the VLE partitioning behavior of methanol in black liquor is not trivial and deserves detailed study in the future.

EXPERIMENTAL

Black Liquors

Weak black liquor samples collected during various pulping stages of five pulping processes in our laboratory were used to understand the effect of pulping processes on the Henry's constant of methanol in black liquors. These black liquor samples are obtained under known pulping conditions such as wood species, sulfidity, active alkali concentration, etc. Six other black liquor samples from four kraft mills (mills A, B, C, and D) were also used for the present study. These samples have a good representation of black liquors yielded from different wood species and pulping processes.

Apparatus and Operation

All measurements were carried out using an HP-7694 Automatic Headspace Sampler and Model HP-6890 capillary gas chromatograph (Hewlett-Packard). The GC conditions were described in Parts I and II of this study. The basic principles of the headspace sampler can be found in Chai et al. [5]. The measurement procedure was as follows: pipette 0.05 and 10 mL of sample solution into two 20 mL vials, then close the vials and put into the oven of the Headspace Sampler. The vial is gently shaken for a certain length of time until VLE phase equilibrium within the vial is achieved according to our previous study [6]. The vial is then pressurized by helium to create a pressure head to fill the sample loop. The vapor in the sample loop is finally injected into the GC column and analyzed. The peak areas of the GC analysis were recorded by a personal computer for the calculation of Henry's constant using Eqn. (8) in Part II of this study.

RESULTS AND DISCUSIONS

The total solids content of all the black liquors used in this study is below 20%. Therefore, we treat them as aqueous solutions, which is a good assumption for weak black liquors in most mill processes except in evaporators. Black liquor has a very complex composition, which contains both inorganic and organic species. For volatile organic compounds, methanol is a dominating species in black liquors; however, in sulfide-involved kraft pulping process, an organic sulfur compound, dimethyl sulfide (DMS), and α-pinene in the softwood pulping are also significant. The effects of multicomponents on methanol VLE partition are very complicated. In this study, we only examine the effects of several important parameters, *i.e.,* temperature, ionic strength, and solids content, on the Henry's constant of methanol in black liquors. We leave the work of understanding the effects of various composition parameters on methanol Henry's constant in black liquor for future investigations.

Measurement Uncertainty

Precision analysis of the present measurement method [6] indicated that the potential measurement error of the present method was less than 10% for the experimental parameters used. Measurement uncertainty can occur in applying the present method to black liquor samples due to the inhomogeneous nature of black liquors. It is difficult to obtain uniform and representative samples during experiments. We determined the actual experimental uncertainty by analyzing the Henry's constants of methanol in the soda hardwood liquor obtained in our laboratory from 11 replica measurements. We found the maximum error for single measurement is about 15% as shown in Fig. 1. However, the relative standard deviation was 8.8%, within the error margin from our precision analysis [6]. We conducted triplicate experiments and averaged

the measurements; therefore, the actual measurement uncertainty of the data presented in the paper is less than 8.8%.

Effect of Temperature

From basic thermodynamics, we know that the VLE partitioning behavior of any solute is strongly dependent on temperature. The operating temperature of weak black liquor in Kraft mills varies significantly. We measured the Henry's constants of five black liquors from four different kraft mills in a temperature range of 40-70°C. Our measurement results indicate that the Henry's constant of methanol in all the black liquors examined increases exponentially with temperature. We found that the Logarithm of Henry's constant of methanol in all the black liquors fits to a linear line with the inverse of temperature in Kelvin very well as shown in Fig. 2. This linear relationship in Eqn. (1) agrees with the basic thermodynamic theory very well, i.e, the Henry's constant is related to the partial molar excess enthalpy, which is a function of temperature.

For comparison purposes, we also plotted the Henry's constants of methanol in a water mixture in Fig. 2. The results show that the overall slope of the data of all the five black liquor samples is very close to the slope of the methanol-water mixture data. Because of the limited data points in each individual data set of the black liquor samples and the data scattering caused by the measurement uncertainty, linear regression analysis shows that there are some variations among the slopes of each individual data set as listed in Table I. The slopes of the data of the black liquor samples are slightly lower than that of the methanol-water mixture solution. However, the relative standard deviation of the slopes of all the six data sets is only 15%. More data and black liquor samples are required to further validate this argument.

$$Log_{10}(H_c) = \frac{a}{T} + b \qquad (1)$$

Figure 2 shows there is a significant variation in the intercepts among the linear lines. The variations in the compositions of the black liquors such as the solids contents, the wood species, the pulping conditions, and other parameters could contribute to the differences in the Henry's constants. The data also show that the Henry's constants of methanol in most of the black liquor samples are smaller than those in the methanol-water mixture under the same temperature. This behavior can be explained as due to the multicomposition of black liquors, in particular the dissolved solids, which could have a strong affinity to organic compound molecules [7]. The results in Fig. 2 indicate that using the Henry's constants of methanol in water mixture for VOC computer models could overpredict mill VOC emissions.

Effect of Ionic Strength

Black liquor contains a large quantity lot of inorganic salts. The inorganic salts cause a variation of ionic strength among various black liquors. Basic thermodynamic principles indicate that ionic strength has an adverse effect on the solubility of most solutes. Therefore, it is important to understand the effect of ionic strength on the methanol Henry's constant. We added different amounts of potassium chloride into several methanol-water mixtures to obtain the solutions with different ionic strengths. We then measured the methanol Henry's constants in these solutions. We found that the Henry's constant increases with the increase of ionic strength as shown in Fig. 3. We analyzed the sodium and potassium contents in all of the five liquors from mills A, B, and C and found that the ionic strength calculated based on the measured sodium and potassium varies from 0.89-1.5 mol/L. The variation of ionic strength among these five liquors only accounts for 10% of the variation in Henry's constant according to Fig. 3,

indicating that ionic strength is not a major factor that contributes to the significant variation of Henry's constant in the different black liquors shown in Fig. 2.

Effect of pH

We took the similar approach to study the effect of pH on the Henry's constant of methanol. A different amount of sodium hydroxide was added into several methanol-water mixtures. Measurements show that the effect of pH on the measured methanol constant is not significant after correction of ionic strength.

Effect of Total Solids Content

To explain the significant variation in Henry's constant in different black liquors as shown in Fig. 2, we measured methanol Henry's constant in 11 black liquor samples at three different temperatures. Six samples were obtained from four kraft mills of unknown pulping conditions, and the other five samples were collected from our laboratory under known pulping conditions. These 11 samples represent black liquors yielded from hardwood and softwood, kraft and soda pulping processes. We found from our measurements that the methanol Henry's constants in these black liquors correlate with the total solids content well, even though the black liquors are completely different in terms of wood species, pulping conditions, etc. As shown in Fig. 4, the Henry's constant of methanol decreases linearly with the increase of solids content in the sample. As we discussed previously, the measurement errors of our experiments are less than 8.8% with triplicate averaging; therefore, the scattering of the data in Fig. 4 is partly due to measurement uncertainty and partly due to the real variation in Henry's constant caused by the variation in the composition matrix of black liquors and other parameters such as ionic strength that affect Henry's constant.

Linear regression analysis indicates that there is not much difference among the slopes of the three sets of data presented in Fig. 4 with the consideration of the data scattering. We use the following equation to express this relation,

$$H_c = cS + d\,, \tag{2}$$

where S is the total solids content of the liquor. Constants c and d are listed in Table II for the plots shown in Fig. 4. The standard deviation of the three slopes listed in Table II is less than 15%.

By combining Eqns. (1) and (2), we can correlate methanol Henry's constant in black liquors using the following equation,

$$H_c = m \cdot \exp(\frac{A}{T}) + B \cdot S + C\,. \tag{3}$$

More data are required for linear regression analysis to obtain good empirical correlation of Henry's constant of methanol in various black liquors.

Several significant VOC's such as α-pinene from softwood and sulfur compounds from kraft cooking will not be formed in a soda hardwood pulping process; therefore, the effect of these major species can be eliminated in the study of the methanol Henry's constant in soda hardwood black liquors. To obtain a better understanding of the effect of total solids content on methanol Henry's constant, we measured Henry's constants of several black liquor samples collected from a soda pulping process of a hardwood at various pulping stages in our laboratory. The total solids content in the cooking liquors included both inorganic and organic compounds. The inorganic chemicals were mainly alkali and various sodium and potassium salts. Their effects on methanol Henry's constant should be similar to those of potassium chloride as shown

in Fig. 3. The chemical in the starting cooking liquor was sodium hydroxide that was consumed to form other salts during pulping. The total solids content increase in the process was mainly caused by dissolved lignin from wood chips. As shown in Fig. 5, the methanol Henry's constant decreases linearly with time (or solids content as shown) as the pulping process proceeds. It should be clarified that the methanol Henry's constants shown in Fig. 5 are all measured at a liquor temperature of 70°C. Fig. 5 indicates that the methanol Henry's constant in black liquors decreases with the increase of dissolved lignin in the liquor. The data scatter is mainly due to experimental uncertainty and nonrepresentative sample collection in the experiments. The effect of dissolved lignin, mainly humic materials, on methanol Henry's constant is rather complicated, and the understanding on the subject is very limited [7]. It is unclear whether the decrease of Henry's constant is very slow when the solids content is very low. Further study on the subject is required.

SUMMARY

We conducted measurements of Henry's constant of methanol in various black liquors using the HSGC method that we developed. The results indicate that the Henry's constant of methanol in black liquor is mainly affected by temperature and the total solids content. Linear regression analysis indicates that the methanol Henry's constant in black liquors increases exponentially with the inverse of temperature in Kelvin and decreases linearly with the total solids content. More experimental data are required to better correlate Henry's constant of methanol in various black liquors with major parameters such as temperature and solids content.

ACKNOWLEDGEMENT

This research was supported by the United States Department of Energy (Grant No. DE-FC07-96ID13438).

REFERENCES

1. Gu, Y., Edwards, L., Haynes, J., and Euhus, L., Tappi J., 82(2):173 (1998).
2. Venketesh, V., Lapp, W., and Parr, J., Tappi J., 81(2):171 (1997).
3. NCASI, Technical Bulletin No. 678, (1994).
4. Jain, A., TAPPI Minimum Effluent Mills Symposium (1996).
5. Chai, X.-S., Dhasmana, B., and Zhu, J.Y., J. Pulp & Paper Sci., 24(2):50, (1998).
6. Chai, X.-S. and Zhu, J.Y., J. Chromatogr. A., 799(1-2):207, (1998).
7. Anderson, M.A., Environ. Sci. Tech., 26:2186 (1992).

List of Figures

List of Tables

Fig. 1

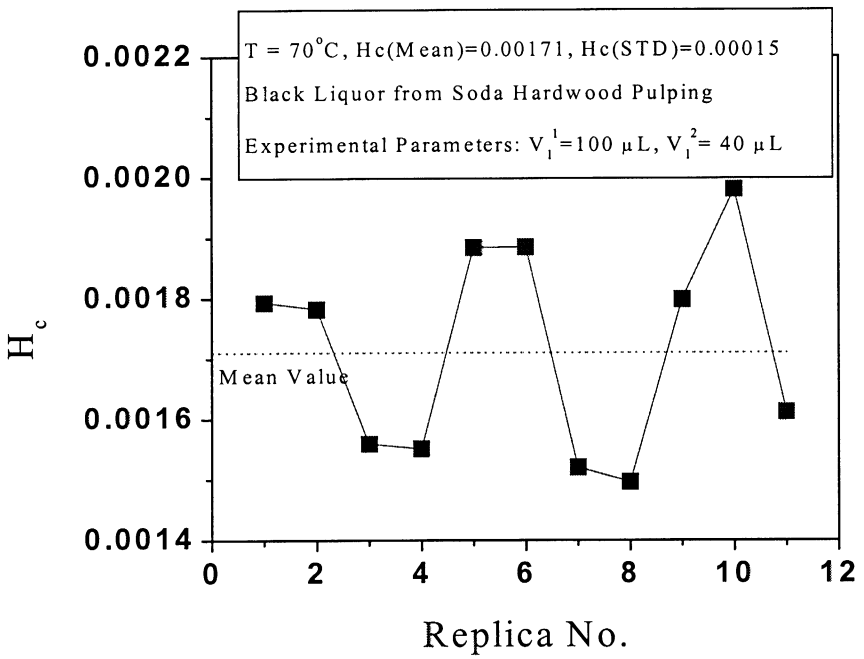

Fig. 2

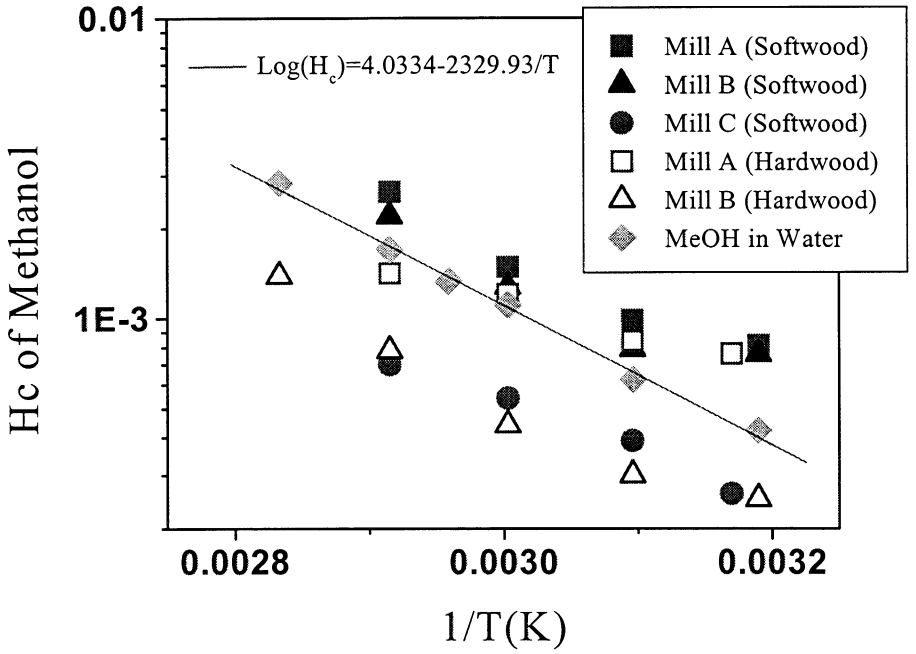

Fig. 3

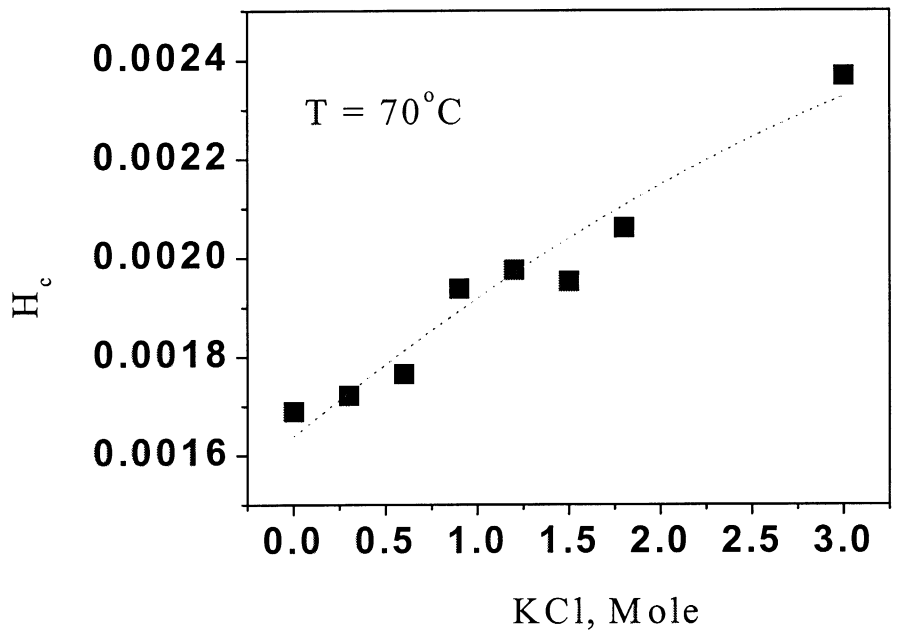

Fig. 4

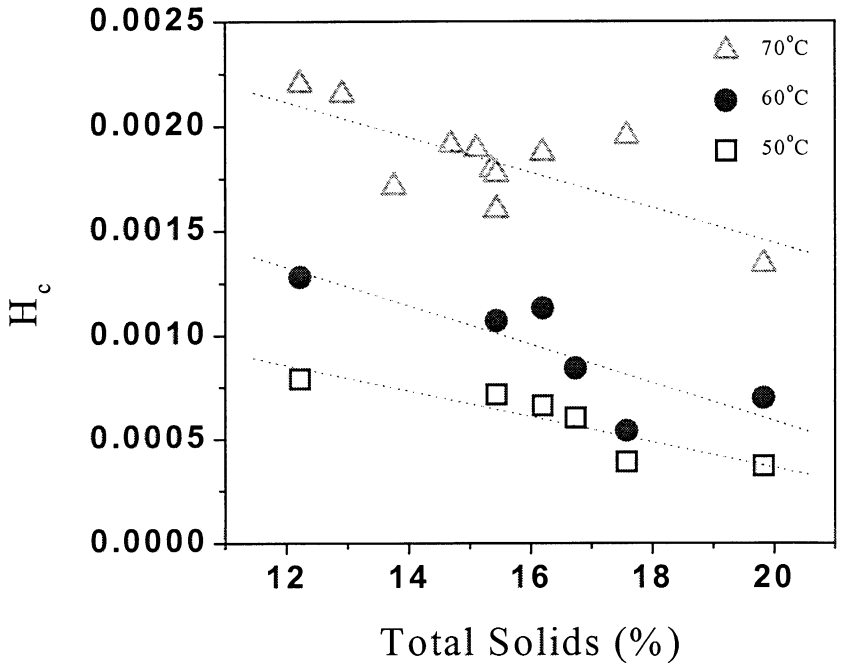

Fig. 5

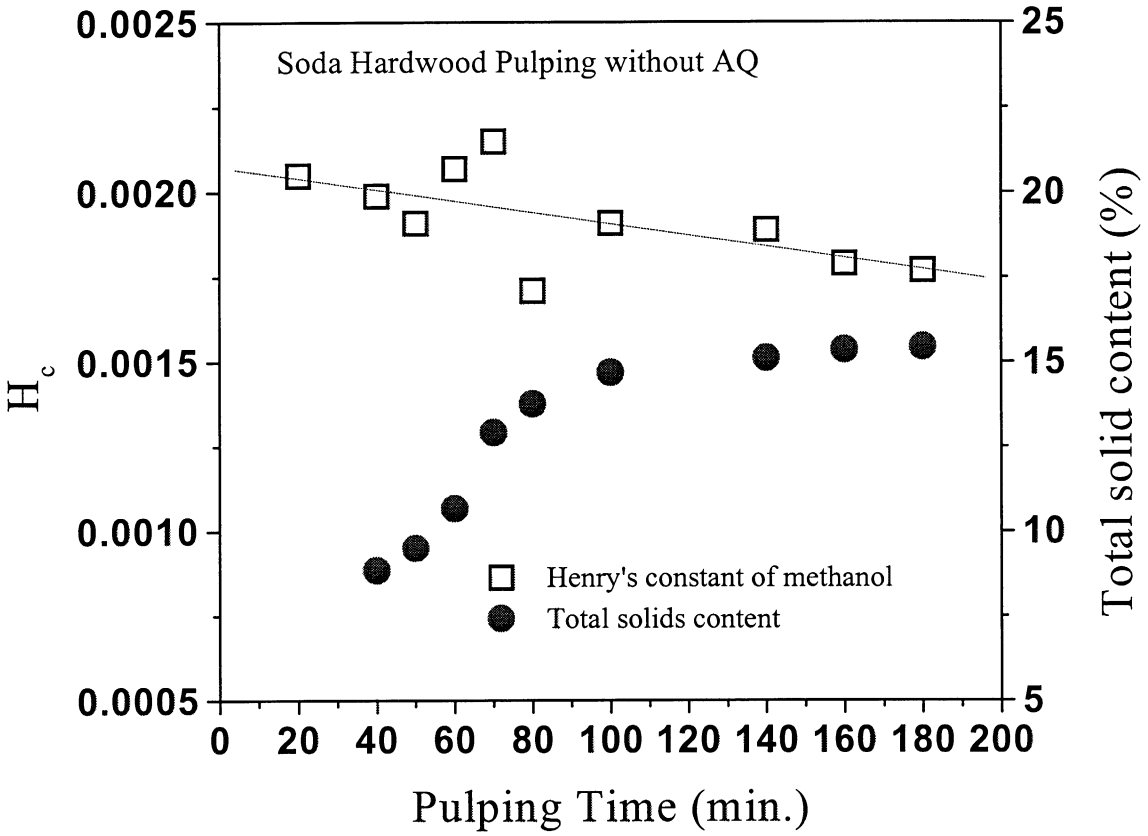

Table I: List of fitting parameters of Eqn. (1) for various samples.

Sample	Intercept: b	Slope: a
Mill A, Softwood	2.8356	-1871.83
Mill B, Softwood	2.3504	-1735.11
Mill C, Softwood	1.6990	-1658.92
Mill A, Hardwood	0.4845	-1140.67
Mill B, Hardwood	3.0757	-2116.45
Methanol-Water Mixture*	3.4957	-2147.23
MEAN	-	**-1778.37**
STD	-	**266.8**
RELATIVE STD	-	**15.0%**

* The values are from Part I of this study

Table II: List of fitting parameters of Eqn. (2) at different temperatures.

Temperature	Intercept: d	Slope: cxE10^5
50°C	0.0016	-6.1765
60°C	0.0024	-9.2325
70°C	0.0031	-8.3825
MEAN	-	**-7.9305**
STD	-	**1.1693**
RELATIVE STD	-	**14.7%**

DUES-FUNDED PROJECT SUMMARY

Project Title:	Gasification of Black Liquor
Project Code:	
Project Number:	F028
PAC:	Chemical recovery
Division:	Chemical Recovery and Corrosion
Project Staff	
Faculty/Senior Staff:	Kristiina Iisa
Staff:	Qun Jing
FY 98-99 Budget:	$40,000
Allocated as Matching Funds:	None
Time Allocation	
Faculty/Senior Staff:	K. Iisa 14 %
Support:	Q. Jing 17 %
Supporting Research	
M.S. Students:	Steve Horenziak: Fate of Sulfur During Black Liquor Gasification
Ph.D. Students:	
External:	
Exploratory:	Seed grant with Dr. Agrawal from Georgia Institute of Technology for destruction of tar from low temperature gasification
RESEARCH LINE/ROADMAP:	- Improved Capital Effectiveness. 8. Develop technologies to allow cost-effective expansion of kraft-pulp-equivalent fiber capacity by 30 % without adding Tomlinson recovery boilers. - Energy performance. 10. Reduce net energy consumption per ton by 30 % compared to '97 levels.

PROJECT OBJECTIVE:
The objective of the project is to study the kinetics of inorganic species transformation during black liquor gasification. The chemical species of interest are sodium, nitrogen, chlorine and sulfur, and their split between the gas phase, fume and solid residue will be determined as well as their chemical form.

PROJECT BACKGROUND:
Black liquor gasification is being developed as a replacement for traditional recovery boilers. There are several open questions related to the transformation of different elements during gasification. The separation of sulfur and sodium by conversion of sulfur into the gas phase is essential for the development of new pulping methods. Whether chlorine will be evolved as hydrogen chloride or alkali chlorides will affect the purge of chlorine from the recovery cycle as well as HCl emissions. The formation of NOx precursors (NH_3) or retention of nitrogen in the smelt residue will have an impact on nitrogen oxides emissions. The rates of fume formation are essential for the operation of gasifiers and gas turbines.

SUMMARY OF RESULTS:
Preliminary CO_2 gasification experiments have been made at 500-1100 °C with one liquor in a laminar entrained-flow reactor. The reproducibility of the runs was good: the average variation in duplicate runs was 6 % for char yield and 7 % for fume yield. At a given condition the char yields and fume yields are constant above a threshold liquor feed rate. No measurements of the chemical components have been made yet. A pressurized entrained-flow reactor for the study of gasification under pressurized conditions has been ordered from Risoe National Laboratory in Denmark. The maximum operation pressure of the pressurized reactor is 80 bar and maximum temperature 1500C. The expected delivery time is June 1998.

GOALS FOR FY 98-99:
FY98: Study of CO_2 gasification: effect of temperature, time and CO_2 concentration.
FY99: Study of H_2O and combined CO_2/H_2O gasification: effect of temperature, time, CO_2 and H_2O concentrations.

DELIVERABLES:
Impact of gasification conditions on a) fume formation, b) NO formation, and c) chlorine purge and HCl emissions.

SCHEDULE (Attach Timeline):